Title
Mechanisms of Rickettsia parkeri invasion of host cells and early actin-based motility

Author
Reed, Shawna

Publication Date
2012

Peer reviewed|Thesis/dissertation

Mechanisms of *Rickettsia parkeri* invasion of host cells and early actin-based motility

By

Shawna Reed

A dissertation submitted in partial satisfaction of the

requirements for the degree of

Doctor of Philosophy

in

Microbiology

in the

Graduate Division

of the

University of California, Berkeley

Committee in charge:

Professor Matthew D. Welch, Chair

Professor David G. Drubin

Professor Daniel Portnoy

Professor Kathleen R. Ryan

Fall 2012

Mechanisms of *Rickettsia parkeri* invasion of host cells and early actin-based motility

By
Shawna Reed

ABSTRACT

Mechanisms of *Rickettsia parkeri* invasion of host cells and early actin-based motility
by
Shawna Reed

Doctor of Philosophy in Microbiology
University of California, Berkeley

Professor Matthew D. Welch, Chair

Rickettsiae are obligate intracellular pathogens that are transmitted to humans by arthropod vectors and cause diseases such as spotted fever and typhus. Spotted fever group (SFG) *Rickettsia* hijack the host actin cytoskeleton to invade, move within, and spread between eukaryotic host cells during their obligate intracellular life cycle. *Rickettsia* express two bacterial proteins that can activate actin polymerization: RickA activates the host actin-nucleating Arp2/3 complex while Sca2 directly nucleates actin filaments. In this thesis, I aimed to resolve which host proteins were required for invasion and intracellular motility, and to determine how the bacterial proteins RickA and Sca2 contribute to these processes.

Although rickettsiae require the host cell actin cytoskeleton for invasion, the cytoskeletal proteins that mediate this process have not been completely described. To identify the host factors important during cell invasion by *Rickettsia parkeri*, a member of the SFG, I performed an RNAi screen targeting 105 proteins in *Drosophila melanogaster* S2R+ cells. The screen identified 34 proteins important for invasion, including a signal transduction pathway involving Abl tyrosine kinase, the RhoGEF Vav, the GTPases Rac1, Rac2, and Cdc42, the WAVE nucleation promoting factor (NPF) complex and the Arp2/3 complex. In mammalian cells, including HMEC-1 endothelial cells, the natural targets of *R. parkeri*, the Arp2/3 complex was also crucial for invasion, while requirements for WAVE2 as well as Rho GTPases depended on the particular cell type. I propose that *R. parkeri* invades S2R+ arthropod cells through a primary pathway leading to actin nucleation, whereas invasion of mammalian endothelial cells occurs via redundant pathways that may involve the activity of host and bacterial proteins. Our results reveal a key role for the WAVE and Arp2/3 complexes, as well as a higher degree of variation than previously appreciated in actin nucleation pathways activated during *Rickettsia* invasion.

Most pathogens undergo actin-based motility during a single phase of their life cycle, using the force of actin "tails" to push into neighboring cells without accessing the extracellular milieu. In contrast, I found that *R. parkeri* undergo two phases of motility, early and late, during the infectious cycle. Early actin tails are formed between 15 and 60 minutes after infection, have a distinctive short and curved appearance, are decorated with Arp2/3 complex proteins Arp3 and ARPC5, and are associated with polar localization of the *Rickettsia* Arp2/3 NPF, RickA. Late actin tails, as previously described (Haglund *et al*. 2010, Serio *et al*. 2010) are long, composed of

helical bundles of actin, and associated with polar localization of the *Rickettsia* formin-like actin nucleator, Sca2. Early motility is Arp2/3-dependent and is significantly slower, and less efficient when compared to late motility. Finally, isolation of *R. parkeri* strains with transposon insertions in either the *rickA* or *sca2* genes revealed that RickA is required for robust early actin tail formation, while Sca2 is required for late actin tail formation and efficient cell-to-cell spread. Thus, *Rickettsia* appear to be unique in their ability to promote two temporally and mechanistically distinct phases of actin-based motility during infection. Continued investigation of invasion and actin-based motility may shed light on the pathogenesis of *Rickettsia*, the function of actin in the host cell, and the purpose of actin tail formation during intracellular infection.

DEDICATION

To my grandmother, Mrs. Martha Rice Reed, and to my husband, John W. Nixon III, both of whom gave me the strength to persevere.

TABLE OF CONTENTS

LIST OF FIGURES AND TABLES

ABBREVIATIONS

ATP – Adenosine triphosphate
AG – Ancestral Group *Rickettsia*
TG – Typhus Group *Rickettsia*
TRG – Transitional Group *Rickettsia*
SFG – Spotted Fever Group *Rickettsia*
G-actin – Monomeric actin
F-actin – Filamentous actin
WH2 – actin-monomer binding motif
T3SS – Bacterial type III secretion system
T4SS – Bacterial type IV secretion system
PLA2 – *Rickettsia* phospholipase A2
PLD – *Rickettsia* phospholipase D
tlyA – *Rickettsia* hemolysin A
tlyC – *Rickettsia* hemolysin C
ER – Endoplasmic Reticulum
RER – Rough Endoplasmic Reticulum
NPF – Nucleation Promoting Factor for Arp2/3 complex
WCA – Arp2/3 activating domain with WH2, Central and Acidic motifs
HMEC-1 – Human Microvascular Endothelial Cells
dsRNA – double-stranded RNA
RNAi – RNA interference
PAK1-PBD-mCherry - p21-binding domain of p21-activated kinase fused to mCherry
FLC – Fibroblast-like cell line (mouse embryonic origin)
DMSO – Dimethyl sulfoxide
EB – *Chlamydia* Elementary Body
RB – *Chlamydia* Reticulate Body

ACKNOWLEDGEMENTS

In this scientific endeavor, I have been lucky enough to be supported intellectually, scientifically, and emotionally by many friends, family, and colleagues.

I will begin by thanking and acknowledging those whose work at the lab bench contributed to the data presented here. Alisa Serio, a postdoctoral fellow in the Welch Lab, assisted in the design and execution of the RNAi screen described in Chapter 2, which was modeled after her own successful experiments. Emma Abernathy, an excellent rotation student also from the Microbiology Graduate Group, kick-started the research discussed in Chapter 3 by performing the first timecourse included in Figure 3.1. Another hard-working rotation student, Matthew Shurtleff, performed the TEM1-RickA secretion assay presented in Figure 4.2. Viviana Risca, a Molecular and Cell Biology graduate student, kindly wrote a MATLAB program to perform the calculations of average cosine($\Delta\theta$) presented in Figure 3.2. John Nixon, my husband, assisted me by re-organizing the same data before analysis and by counting quite a few actin tails. Finally, I am incredibly indebted to Becky Lamason, also a postdoctoral fellow, for performing a screen of small-plaque mutants in *R. parkeri*, then isolating and sequencing the mutant strains described in Figure 3.5. Becky and Julie Choe, a graduate student in the Welch Lab, have assisted invaluably with labor-intensive *Rickettsia* preparations and mutagenesis.

I must also thank current and former members of the Welch lab, including Alisa, Julie, Becky, Cat Haglund, Ken Campellone, Taro Ohkawa, Robert Jeng, Erin Benanti, Steve Duleh, Elif Nur Firat-Kiralar, Anosha Siripala, Alex Paradez, and Haiming Wu and of course Matthew Welch for intellectual and technical assistance and comments on the work in Chapter 2 before publication. I also must thank our collaborators: T. Clark, S. Dooley, T. Hackstadt and members of the T. Hackstadt lab for assistance with *R. parkeri* transformations; J. Hartman and Cytokinetics for providing the Arp2/3 complex inhibitor CK-548; G. Bokoch, K. Campellone, L. Cooley, T. Hackstadt, U. Munderloh, T. Ohkawa, C. Paddock, J. Pomerantz, D. Portnoy, S. Snapper, T. Takenawa, R. Tjian, O. Weiner, and D. Wood for providing strains, reagents, or protocols.

Of course, I have to thank Matthew Welch. Matt interviewed me for admission to UC Berkeley, and I was immediately struck by his kindness, professionalism, creativity, and intelligence. I am incredibly grateful to Matt for taking me on as a graduate student, encouraging me to forge my own way with my projects, and pushing me to grow and become more independent throughout my time at Berkeley. I'm lucky to have a mentor who is so patient, honest, irreverent, and supportive with a sometimes capricious and anxious student – I hope that I can continue to make Matt proud as I continue my career as an academic scientist. Alisa, Becky, Ken, Robert, Taro and Erin deserve special mention for being co-mentors, always ready and willing to talk through a protocol or idea, ease the pain of failure and celebrate success, and assure me that graduate school would eventually, come to an end and I too could move on to an illustrious post-doc. My thesis committee, David Drubin, Dan Portnoy, and Kathleen Ryan, have been a source of encouragement and helpful suggestions throughout my work.

I came to Berkeley in 2005 with an amazing class of first-year Microbiology and Plant Biology graduate students; the camaraderie and support of the whole class helped me through the

first year and beyond, but especially Kali Lader, Justin Richner, Nhu Nguyen, Adrien Burch, Russell Scott, Kevin Hockett and Tanya Renner. Some of my classmates have become lifelong friends, including Danielle Augustin, Karl Erhard, Kate Williams, and Solomon Stonebloom. Graduate students from classes before and after mine, too many to list here, have contributed to my growth as a scientist and been great friends throughout my graduate experience. In addition to the Welch Lab, the Trilab group (Welch, Heald and Weis labs) have provided social and scientific support as well as a yearly, epic Halloween party and a killer margarita recipe. Finally, the faculty, support staff and postdoctoral fellows of the PMB and MCB departments have provided the academic and logistical support necessary for my success.

My family has been an incredible source of support and love throughout my life. To my parents, John Reed and Carla Oswald Reed, and my siblings, Rachel Spencer-Reed, Alexa Hutchins, and Matthew Reed – thank you for everything. My 'newer' family includes my brother and sisters-in-law, Alyson Spencer-Reed, Jeremy Hutchins, and Shelley Nixon Hitch, and my wonderful parents-in-law, Jack and Brenda Nixon. All of my family members are an unwavering source of love, have incredible faith in me, never judge me on whether my experiments are a success, and think I'm the smartest woman alive even when I feel incredibly ignorant and incompetent (a part of graduate school). I'll especially acknowledge my nieces and nephews – Emerson, Phoebe, Max and Ada – for truly being the 'antidote' to graduate school. I'm lucky to be your Shawna-Mashi. Thank you all for everything – your pride makes me want to be a better woman and a better scientist.

Finally, I have to thank my husband, John Nixon. When someone is lucky enough to have a spouse who is a true partner and best friend, it's hard to put feelings into words. John, thank you for your advice, a bit of scientific assistance, and countless hours in the lab, waiting for me to finish my work - and thank you for leaving home to give me a warm car ride home on late and rainy nights. I'm so grateful to have met you before graduate school – I may not have even applied to Berkeley without your encouragement and I certainly would not have made it through my qualifying exam, writing a paper, or completing my thesis without you. Thank you.

CHAPTER 1

Introduction

Biology of the genus Rickettsia

Rickettsiae are Gram-negative alpha-proteobacteria with an obligate intracellular growth requirement. These bacteria infect both arthropod and mammalian hosts, and virulent species cause spotted fever or typhus diseases when transmitted to humans through the bite of an infected tick, flea, or mite. Bacteria infect capillary and microvascular endothelial cells in small blood vessels of the mammalian host, eventually spreading systemically to multiple organ systems. Lysis of infected cells, along with immune responses of the host, cause vascular leakage, loss of blood volume, edema, organ dysfunction, and (for the spotted-fever group) a characteristic eschar and/or petechial rash (Walker *et al.*, 2008; Paddock *et al.*, 2008).

Rickettsia species are highly adapted to growth within the eukaryotic host cell cytosol – with small genomes ranging from 1 to 2Mb (http://www.patricbrc.org/; Gillespie *et al.*, 2011), specialized metabolism to scavenge ATP, UTP, NAD, proline, and other metabolites from the host, and a range of cytotoxicity from highly pathogenic to nearly endosymbiotic (Hackstadt, 1996; Winkler, 1990). Indeed, the genus is closely related to the insect endosymbionts *Wolbachia* and to the ancestors of mitochondria (Brindefalk *et al.*, 2011; Georgiades *et al*., 2011; Hackstadt, 1996; Thrash *et al.*, 2011). Presumably because of their highly adapted lifestyle, attempts to cultivate *Rickettsia* outside of cultured host cells or embryonated chicken embryos have failed (Hackstadt, 1996; Winkler, 1990).

Species in the genus *Rickettsia* are classified by both genetic relationship and disease etiology (Figure 1) (Azad *et al.*, 1998; Gillespie *et al.*, 2008; Weinert *et al.*, 2009). Species of the Ancestral Group (AG, *R. belii, R. canadensis*) are generally non-pathogenic for mammals (Breitschwerdt *et al.*, 1995) have multiple arthropod hosts, and tend to be less cytotoxic in tissue culture (Philip *et al*., 1983). Species of the Typhus Group (TG) are transmitted by fleas (*R. prowazekii*) or human body lice (*R. typhi*), and are highly pathogenic, spreading from cell to cell in tissue culture only after lysing the infected host cells. Species of the Spotted Fever Group (SFG, *R. rickettsii, R. conorii, R. parkeri*) are transmitted by various species of ticks, range from moderately to severely cytotoxic and pathogenic, and spread from cell to cell *in vitro* by polymerizing actin "tails" on their surface. Finally, Transitional Group species (TRG, *R. felis, R. australis, R. akari)* lay phylogenetically between ancestral and spotted-fever group. *R. felis* is transmitted by cat fleas and causes rare disease in humans (Parola, 2011), while *R. akari* is transmitted by mites and causes rickettsiapox, but few details are known of the pathogenicity and intracellular growth phenotype of TRG species (Azad *et al.*, 1998).

Interestingly, host species specificity, cytotoxicity, amenability to culture, intracellular growth and actin tail phenotypes, and disease severity all appear to be related between *Rickettsia* species (Gillespie *et al*., 2008; Hackstadt, 1996; Kaplan, 1996). Less pathogenic species (e.g. AG/TRG) are generally found in only one species of insect host, are difficult to culture, and rarely cause human disease. More pathogenic species, such as *R. typhi* and *R. rickettsii*, are found in one preferred insect vector (*Xenopsylla* flea and *Dermacentor* tick, respectively) but can be transmitted by others, grow in a wide variety of cultured cells, are highly cytotoxic, and cause severe human disease. Finally, moderately pathogenic species (*R. parkeri, R. africae, R. felis)* are generally restricted to one or a few vector species, grow in a variety of cells with variable phenotype, are moderately to highly cytotoxic and cause moderate human disease. *Rickettsia* generally have preferred vector species but do not co-evolve with their arthropod hosts, and host switching appears to be related to pathogenicity within groups (Weinert *et al.*, 2009).

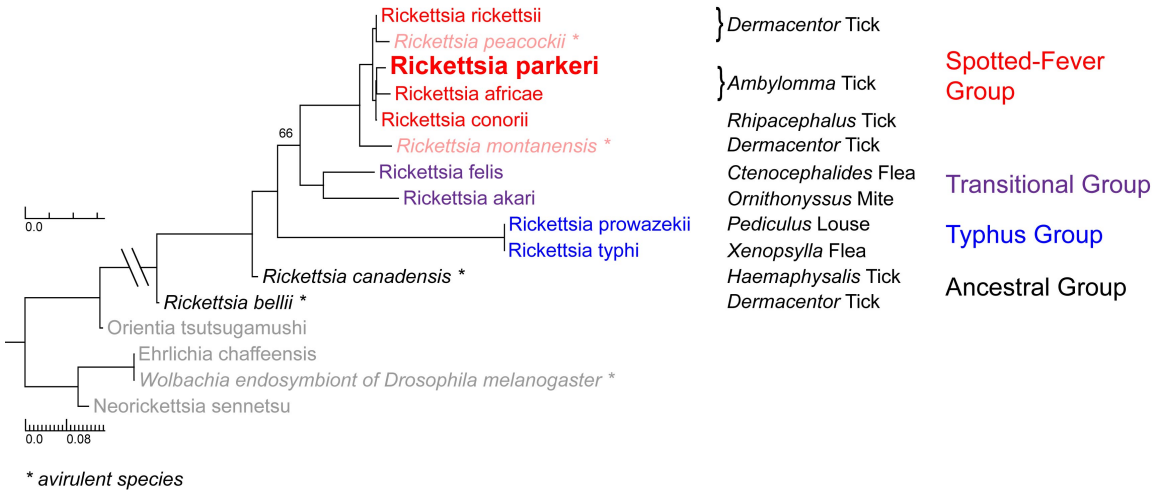

Figure 1.1 Phylogram of selected *Rickettsia* species, with group name (Gillespie *et al*., 2008; Weinert *et al*., 2009), and major arthropod vector (Azad *et al.*, 1998; Kaplan, 1996) indicated. Avirulent species are *italicized* and indicated with an asterisk. Note that genetic distance is condensed for divergent species (in grey) on the lower part of phylogram. Adapted from www.patricbrc.org (Gillespie *et al*., 2011).

Despite a basic understanding of replication kinetics, disease etiology (Hackstadt, 1996; Kaplan, 1996; Walker *et al.*, 2008), metabolism (Winkler, 1990), and many newly sequenced *Rickettsia* genomes (Gillespie *et al*., 2008; Weinert *et al*., 2009), the molecular details of the intracellular life cycle remain unclear. Understanding the molecular interactions between *Rickettsia* and their host cells may reveal how cells are initially infected, as well as how and when cytotoxic effects occur. Moreover, such an understanding may reveal new information about host cell biology. In particular, studying the locally generated and exaggerated activation of cytoskeletal rearrangements by bacteria and viruses informs our understanding of how the host cell regulates these complex processes (Haglund *et al.*, 2011). In addition, symptoms of rickettsial disease arise from vasculitis and capillary damage of unknown etiology (Walker, 1989), but may be caused by lysis of host cells during heavy infection and cell-to-cell spread. Nevertheless, the processes of invasion, spread and host cell lysis remain poorly understood. Using a combination of biochemical and genetic tools to interrogate the bacterium and the host cell, I have worked to elucidate the mechanism of both pathogen invasion and early intracellular actin tail formation by the moderately pathogenic SFG species *Rickettsia parkeri*.

Actin filament nucleation

The eukaryotic actin cytoskeleton is a dynamic network responsible for maintaining cell shape, adhesion, movement, division, and intracellular trafficking. Actin in the host cell exists in monomeric (G-actin) and filamentous (F-actin) forms. Nucleation of a filament begins when three actin monomers come together, favoring association of additional monomers with the fast growing (barbed or (+) end) of the filament over the slower growing (pointed or (-) end). Polymerization of F-actin occurs primarily at the barbed end and is controlled by proteins that nucleate new actin filaments, or elongate, sever, bundle, and cap existing filaments. Nucleation of filaments is a critical step. Although a pool of G-actin exists in the cytosol, spontaneous nucleation is not a favorable reaction. Instead, actin-nucleating proteins, in three functional classes, bring together three or more actin monomers to begin a filament in a regulated manner (Firat-Karalar *et al.*, 2011).

The first class of nucleator to be discovered was the Arp2/3 complex (Goley *et al.*, 2006), a multiprotein complex that binds to the side of existing filaments. The Arp2 and Arp3 subunits of the complex mimic the structure of actin itself, forming the nucleus for a new filament that emerges from the existing filament at a characteristic 70˚ angle. The second class of nucleator, typified by Spire, is termed "tandem-monomer-binding" – with three or more adjacent monomer-binding motifs (WH2) bringing together actin to form a nucleus in varying arrangements (Firat-Karalar *et al.*, 2011). A third class of nucleators are the formin family proteins, such as mDia and Bnl1p, which contain an FH2 domain that recruits two actin monomers to form a nucleus, and an FH1 domain which delivers profilin-bound actin monomers to the growing filament (Firat-Karalar *et al.*, 2011). In uninfected cells, the polymerization of actin filaments after nucleation provides the force for extension of lamellipodia and filopodia from the plasma membrane and for the movement and remodeling of intracellular membrane-bound organelles such as membrane tubules, vesicles, and recycling endosomes (Firat-Karalar *et al.*, 2011). Intracellular bacterial pathogens, including *Rickettsia*, harness actin during host cell invasion and again for actin-based motility within the cytosol by mimicking or activating all three pathways of actin nucleation (Haglund *et al.*, 2011).

Rickettsia *invasion of host cells*

The first step in the life cycle of an intracellular pathogen is inducing its uptake into a host cell. *Rickettsia* invade non-phagocytic endothelial cells in the mammalian host. As with other intracellular pathogens, invasion may occur when host surface receptors bind to bacterial invasins, bacterial secretion systems inject proteins to activate host membrane extension, or a combination of both pathways (Cossart *et al.*, 2004). Receptor-mediated "zipper" invasion occurs when a pathogen binds to a protein on the cell surface, activating downstream actin polymerization pathways to induce localized actin polymerization and membrane extension around the bacterium. "Zipper" invasion is typified by *Yersinia*, for which the Invasin protein binds to b-integrin on the cell surface and activates Rac1, N-WASP, and the Arp2/3 complex (Cossart *et al.*, 2004).

Injection-mediated "trigger" invasion occurs when pathogens use needle-like Type III (T3SS) or Type IV secretion systems (T4SS) to transduce bacterial proteins directly into the host cytosol, activating actin nucleating pathways and inducing dramatic, localized membrane ruffling. *Salmonella* invades by a classic "trigger" pathway, using the Spi1 T3SS to inject several effector proteins in an orchestrated sequence. SopE and SopE2 first activate Rac1 and Cdc42 upstream of N-WASP and Arp2/3, then SopB initiates Rho-Myosin II mediated actin assembly (Hänisch *et al*., 2011), followed by SipC and SipE directly nucleating actin filaments, and finally SptP deactivates the Rho GTPases to tune down actin assembly after macropinocytosis has engulfed the bacteria (SptP) (Cossart *et al.*, 2004; Haglund *et al.*, 2011).

Rickettsia, as obligate intracellular pathogens, must invade host cells in order to replicate. Surprisingly, the molecular mechanisms of *Rickettsia* invasion, including whether invasion occurs via "zipper", "trigger" or hybrid pathways, are not fully understood. For SFG *Rickettsia* species, a large protein family of outer-membrane autotransporters, termed Surface cell antigens (Sca), seem to mediate both adhesion and invasion. rOmpA (Sca0) and Sca1 contribute to adherence (Li *et al.*, 1998), while Sca2 and rOmpB (Sca5) contribute to invasion of host cells (Cardwell *et al.*, 2009; Chan *et al*., 2009; Uchiyama *et al*., 2006). While *Rickettsia* genomes encode a P-type *rvh* Type IV secretion system, it is unclear whether it functions for protein secretion and/or in conjugative DNA transfer, and whether secreted proteins may contribute to invasion or pathogenesis (Gillespie *et al*., 2009). In addition, a host binding partner (Ku70) has only been described for one rickettsial adhesin/invasin (rOmpB). What are the host factors required for actin-dependent invasion by *Rickettsia*? Are the pathways used for invading insect cells, endothelial cells, and other cultured cell lines identical? Does *R. parkeri* invade cells using the same pathway(s) as *R. conorii* and *R. rickettsii?* In Chapter 2 of this thesis, I present a comprehensive analysis of host proteins and pathways contributing to *R. parkeri* invasion in *Drosophila* cells as well as mammalian epithelial (COS-7) and endothelial (HMEC-1) cells.

Escape from the vacuole and intracellular growth

After invasion of host cells, a bacterium remains enclosed in a vacuole derived from the host cell membrane. Many intracellular pathogens remain inside this vacuole (e.g. *Chlamydia*, *Salmonella, Coxiella*), while others escape only after phagosomes acidify (e.g. *Listeria, Shigella*). In contrast, *Rickettsia* appear free in the host cell cytosol only 5-15 min post-infection (Teysseire *et al*., 1995), before acidification is likely to occur, and the mechanism of vacuole escape is poorly understood. Four *Rickettsia* enzymes that are candidates for vacuolar lysis have

been described: phospholipase A2 (PLA2), phospholipase D (PLD), hemolysin A (tlyA) and hemolysin C (tlyC). Inhibition of PLA2 reduces cell invasion (Silverman *et al*., 1992) and plaque formation by *R. rickettsii* (Walker *et al*., 1983), implicating this enzyme in the processes of invasion and/or vacuole escape. PLA2 homologs are also encoded in the *R. typhi, R. prowazekii, R. massiliae,* and *R. bellii* genomes, and the enzyme was found in the host cell cytoplasmic fraction during *R. typhi* infection (Rahman *et al.*, 2010), suggesting that PLA2 may play a role during infection of cells by diverse *Rickettsia*. However, the mechanism of PLA2 secretion into the host cell and its specific function during infection is not well understood.

The *PLD* gene is also widely distributed in all SFG and TG species studied (Renesto *et al*., 2003). *R. prowazekii* express PLD within 30 min of infection, when vacuole escape would occur, and expression of PLD in *Salmonella enterica typhimurium* allows this normally vacuole-bound pathogen to escape into the host cytosol (Whitworth *et al*., 2005). However, directed knockout of the *pld* gene in *R. prowazekii* did not result in a defect in phagosomal escape or intracellular growth (Driskell *et al*., 2009). Interestingly, when introduced into guinea pigs, the *Δpld* mutant was attenuated for virulence and induced protective immunity to wild-type *R. prowazekii*.

Lastly, *Rickettsia* possess two genes encoding hemolysins, *tlyA* and *tlyC*. While *tlyA* remains uncharacterized, TlyC expression is sufficient to confer hemolytic activity on non-hemolytic *E. coli* or *Proteus mirabilis* (Radulovic *et al.*, 1999), and to enhance *S. typhimurium* escape from the phagosome, although to a lesser extent than PLD (Whitworth *et al*., 2005). Taken together, these data suggest that PLD functions in virulence, but redundant factors including TlyC and possibly PLA2 or TlyA may contribute to phagosomal escape (Welch *et al.*, 2012b). Despite the presence of four candidate enzymes, a lack of genetic tools has hampered complete investigations of their activity during *Rickettsia* escape from the internalization vacuole.

Following escape from the phagosome, all *Rickettsia* species replicate freely in the host cell cytosol. The growth kinetics, mechanism of cell-to-cell spread, and affect on the host cell vary between the pathogenic SFG and TG species of *Rickettsia.* For the TG species *R. prowazekii*, exponential growth initiates immediately and continues for 36-48 h, with a doubling time of about 9 h (Wisseman *et al.*, 1975). Replication continues until bacteria completely fill the host cell cytosol, and lysis occurs between 96-120 h post-infection (Silverman *et al*., 1980). The ultrastructure of the host cell remained mostly unchanged during infection, with limited swelling and disruption of mitochondria along with some dissociation of ribosomes from the rough endoplasmic reticulum (RER). Overall, growth of TG species seems to occur with each individual cell acting as a culture vessel, with cell-to-cell spread occurring only via host cell lysis.

The SFG species *R. rickettsii* also initiates replication immediately, with approximately 10-12 h doubling time (Wisseman *et al*., 1976). However, *R. rickettsii* begin to spread to other host cells beginning at 10 h post infection and spreads throughout host cells in culture within 48-72 h. Despite a maximum number of bacteria/cell between 30-50 (Wisseman *et al*., 1976), changes in host cell ultrastructure are more apparent during SFG infection (Silverman *et al.*, 1979; Walker *et al.*, 1977; Walker *et al.*, 1980). At 48 h post-infection, the RER and nuclear membrane become dilated, and after 72 h bacteria are observed within the RER, nuclear envelope, and nucleus. From 72-96 h membrane-bound organelles begin to change, with a less distinct Golgi apparatus, swollen mitochondria, and increasing ER dilation. After 120 h, host cells lose plasma membrane integrity and begin to lyse. While the exact mechanism of host cell

damage is unclear, dilation of the ER, ribosome disassociation, and mitochondrial swelling are signs of cytoplasmic membrane damage, ATP depletion, or oxidative stress. These changes could be caused by increasing bacterial growth depleting ATP (Silverman *et al.*, 1979), enzymatic targeting of membranes by bacterial enzymes, or by host cell response to infection causing a buildup of oxygen radicals (Silverman, 1984). Overall, growth of SFG species appears to occur with the host cell acting as a chemostat, where continuous exit allows cell-to-cell spread and growth of low numbers of bacteria in each cell.

Rickettsia *actin-based motility*

The movement of *Rickettsia* within the host cytosol was first observed in by Schaechter in 1957 using phase contrast timelapse microscopy. However, the nature of *Rickettsia* motility was not understood until nearly forty years later, when both *R. conorii* and *R. rickettsii* were observed to associate with host F-actin (Teysseire *et al.*, 1992) (Heinzen *et al.*, 1993). These actin comet tails are similar to those formed by intracellular *Shigella flexneri* and *Listeria monocytogenes*, which harness the force of host actin polymerization to move within the cytosol (Bernardini *et al.*, 1989) (Tilney *et al.*, 1992).

For *Shigella* and *Listeria*, actin-based motility depends on the activation of the host actin nucleating Arp2/3 complex (Haglund *et al.*, 2011). The Arp2/3 complex is activated by a family of proteins called Nucleation Promoting Factors (NPFs). WASP and N-WASp are the prototypical NPFs, with a variable N-terminus and a C-terminus consisting of a central proline-rich region (P) that interacts with the G-actin binding protein profilin, one or two G-actin binding WH2 motifs (W), and a C-terminal central and acidic region (CA) that binds to Arp2/3 (Campellone *et al.*, 2010). *Listeria* express an NPF-like protein, ActA, on their surface, and use Arp2/3 to nucleate a branched actin network and form an actin tail (Welch *et al.*, 1998). In contrast, *Shigella* express IcsA, an activator of host N-WASp, accomplishing the same goal (Skoble *et al.*, 2000). Both *Listeria* and *Shigella* actin tails are composed of branched actin networks characteristic of Arp2/3 nucleated filaments (Gouin *et al.*, 1999).

Rickettsia actin tails are longer than those of *Listeria* and *Shigella* and are composed of helical bundles of actin filaments (Goldberg, 2001; Gouin *et al*., 1999). *Rickettsia* species express two proteins with similarity to host actin nucleators, RickA and Sca2, which could activate actin-based motility. RickA was identified as a possible Arp2/3 NPF by the presence of a C-terminal WCA domain, but is not homologous to *Listeria* ActA and is thought to have evolved independently. RickA acts *in vitro* as an NPF, activating the Arp2/3 complex to nucleate branched actin networks (Jeng *et al*., 2004). Initially, RickA was thought to be present only in virulent SFG *Rickettsia* that undergo actin-based motility, including *R. rickettsii, R. conorii and R. parkeri,* and was proposed to mediate Arp2/3-dependent intracellular motility (Gouin *et al*., 2004; Jeng *et al*., 2004).

However, a recent expansion of genomic information about the *Rickettsiae* indicates that the *rickA* gene is widespread in both virulent and avirulent species, although it is absent in the typhus group (Table 1). Interestingly, *R. typhi* lacks RickA but still forms short actin tails (Heinzen *et al*., 1993; Teysseire *et al*., 1992), while *R. peacockii* lacks RickA, has a deletion in Sca2 (see below), and forms no actin tails (Baldridge *et al*., 2004). In addition, *Rickettsia* actin tails are formed from linear rather than branched actin filaments (Gouin *et al.*, 1999; Van Kirk *et al.*, 2000), and although one report indicated that expression of an Arp2/3 sequestering WCA domain reduced actin tail formation (Gouin *et al*., 2004), others indicated that there was no effect

(Heinzen, 2003), and that Arp2/3 was absent from the actin tail (Gouin *et al*., 1999; Heinzen, 2003; Serio *et al*., 2010). Therefore, the proposed role for RickA and the Arp2/3 complex during *Rickettsia* actin-based motility was called into question.

Biochemical and genetic evidence points to the *Rickettsia* Sca2 protein, rather than RickA, as the key activator of actin-based motility. Sca2 is an outer-membrane autotransporter protein localized to the bacterial pole, like *Shigella* IcsA (Goldberg *et al*., 1993; Haglund *et al*., 2010). Unlike RickA, Sca2 nucleates linear, unbranched actin filaments *in vitro*, similar to those in *Rickettsia* actin tails, and biochemically mimics formin family proteins (Haglund *et al*., 2010). In addition, *R. rickettsii* with a transposon insertion in the *sca2* gene are unable to make actin tails, have a defect in cell-cell spread, and are less virulent in a guinea pig model of infection (Kleba *et al*., 2010). The profilin-dependent nucleation function of Sca2 (Haglund *et al*., 2010) explains why *R. parkeri* actin-based motility was found to depend on profilin but not Arp2/3 complex in *Drosophila* cells (Serio *et al*., 2010). Finally, Sca2 is widely distributed throughout the genus *Rickettsia*: species with divergent N-terminal passenger domains form unusual actin tails (*R. typhi),* while those with partial or complete deletions of the passenger domain (*R. peacockii, R. canada, R. prowazekii)* do not form actin tails (Table 1). Therefore, Sca2 is the major activator of actin-based motility leading to cell-cell spread of *Rickettsia* species, and is the first example of a formin-like protein activating motility of an intracellular pathogen (Haglund *et al*., 2010).

Why would *Rickettsia* species evolve two actin nucleators? What is the functional role of RickA during invasion and actin-based motility of *Rickettsia*? If RickA and Sca2 are both virulence factors, why are both proteins widespread throughout the genus in both virulent and avirulent species (Table 1)? In chapter 3 of this thesis, I describe a role for RickA in an unusual, temporally limited form of actin-based motility occurring immediately after invasion of host cells, and compare early (RickA-mediated) and late (Sca2-mediated) motility. A complete understanding of the function, regulation, and contribution of each protein to virulence will inform our understanding of the evolution of the *Rickettsiae* as well as the general role of actin-based motility during infection by intracellular pathogens.

Species	Group	Virulence/Disease	RickA (% ID to R. rickettsii)	PWCA domain % ID	Notes	RickA accession	Sca2 (% ID to R. rickettsii)	Passenger domain %ID	Sca2 notes	Sca2 accession	Actin tails?
R. rickettsii "Sheila Smith"	SFG	Severe Rocky Mountain Spotted Fever	100	100		YP_001495006	100	100	*Himar* insertion = no late tails	YP_001494228	yes
R. peacockii "Rustic"	SFG	*avirulent*	-	-	ISRpE1 insertion	-	90.6	89.3	deletions in WH2 and N-terminus	YP_002916397	no
R. africae ESF-5	SFG	African tick-bite fever	89.2	79.1		YP_002845437	84.2	83	DUF2869 insertion	YP_002844823	?
R. parkeri "Portsmouth"	SFG	Eschar-asst Spotted Fever	89.4	78.1	Poly-proline extension	YP_005393149	87.1	85.2	formin-like nucleator	YP_005392373	yes
R. conorii "Malish 7"	SFG	Mediterranean Spotted Fever	90	80.1	Poly-proline extension	NP_360546	89.9	89.8	formin-ike nucleator	NP_359747	yes
R. montanensis "OSU 85-930"	SFG	*avirulent*	73.8	61.5	double WH2, Poly-pro extension	YP_005391347	85.3	84.9	-	YP_005391839	yes
R. felis "URRWXCal2"	TRG	Cat-flea typhus	80.7	67.6	double WH2	YP_246387	41.6	33.4	-	YP_246083	yes
R. akari "Hartford"	TRG	Rickettsialpox	76.7	61.8	double WH2	YP_001493700	26.8	18.6	-	YP_001492962	?
R. prowazekii "Madrid E"	TG	Epidemic Typhus	-	-	absent	-	15.6	3.4	64-aa passenger domain fragment	NP_220474	none
R. typhi "Wilmington"	TG	Murine Typhus	-	-	absent	-	26.7	18.5	N-terminal truncation in passenger domain	YP_067021	short/rare
R. canadensis "McKiel"	AG	*avirulent*	67.8	53.8	double WH2, Poly-pro extension	YP_001492102	55.1	50.1	deletions in N-terminal and PRD domains	YP_005299139	none
R. belii "RML369-C"	AG	*avirulent*	44.5	32.6	15aa truncation at C- terminus	YP_538025	18	10.3	N-terminal truncation, similar to typhi Sca2	YP_538450	yes

Table 1. *Rickettsia* species, RickA and Sca2 genes, and virulence and actin tail phenotypes. RickA and Sca2 genes were downloaded from the genomes of the species and strains indicated (GenBank). Virulence phenotypes from (Hackstadt, 1996; Kaplan, 1996). RickA and Sca2 genes were aligned with *R. rickettsii* Sheila Smith genes using a BLOSUM alignment (Generous) and percent amino acid identity to either the full-length protein or functional domain is indicated. Actin tail phenotypes are from (Baldridge *et al.*, 2004; Gouin *et al.*, 1999; Heinzen *et al.*, 1993; Ogata *et al.*, 2005; Serio *et al.*, 2010; Teysseire *et al.*, 1992) and our unpublished data.

REFERENCES

Azad, A.F. and Beard, C.B. (1998). Rickettsial pathogens and their arthropod vectors. *Emerg Infect Dis* **4,** 179-186.

Baldridge, G.D., Burkhardt, N.Y., Simser, J.A., Kurtti, T.J. and Munderloh, U.G. (2004). Sequence and Expression Analysis of the ompA Gene of Rickettsia peacockii, an Endosymbiont of the Rocky Mountain Wood Tick, Dermacentor andersoni. *Applied and Environmental Microbiology* **70,** 6628-6636.

Bernardini, M.L., Mounier, J., d'Hauteville, H., Coquis-Rondon, M. and Sansonetti, P.J. (1989). Identification of icsA, a plasmid locus of Shigella flexneri that governs bacterial intra- and intercellular spread through interaction with F-actin. *Proceedings of the National Academy of Sciences* **86,** 3867-3871.

Breitschwerdt, E.B., Hegarty, B.C., Davidson, M.G. and Szabados, N.S. (1995). Evaluation of the pathogenic potential of Rickettsia canada and Rickettsia prowazekii organisms in dogs. *J Am Vet Med Assoc* **207,** 58-63.

Brindefalk, B.r., Ettema, T.J.G., Viklund, J., Thollesson, M. and Andersson, S.G.E. (2011). A Phylometagenomic Exploration of Oceanic Alphaproteobacteria Reveals Mitochondrial Relatives Unrelated to the SAR11 Clade. *PLoS ONE* **6,** e24457.

Campellone, K.G. and Welch, M.D. (2010). A nucleator arms race: cellular control of actin assembly. *Nat Rev Mol Cell Biol* **11,** 237-251.

Cardwell, M.M. and Martinez, J.J. (2009). The Sca2 Autotransporter Protein from Rickettsia conorii Is Sufficient To Mediate Adherence to and Invasion of Cultured Mammalian Cells. *Infection and Immunity* **77,** 5272-5280.

Chan, Y.G.Y., Cardwell, M.M., Hermanas, T.M., Uchiyama, T. and Martinez, J.J. (2009). Rickettsial outer-membrane protein B (rOmpB) mediates bacterial invasion through Ku70 in an actin, c-Cbl, clathrin and caveolin 2-dependent manner. *Cellular Microbiology* **11,** 629-644.

Cossart, P. and Sansonetti, P.J. (2004). Bacterial Invasion: The Paradigms of Enteroinvasive Pathogens. *Science* **304,** 242-248.

Driskell, L.O., Yu, X., Zhang, L., Liu, Y., Popov, V.L., Walker, D.H.*, et al.* (2009). Directed Mutagenesis of the Rickettsia prowazekii pld Gene Encoding Phospholipase D. *Infect. Immun.***,** IAI.00395-00309.

Firat-Karalar, E.N. and Welch, M.D. (2011). New mechanisms and functions of actin nucleation. *Current Opinion in Cell Biology* **23,** 4-13.

Georgiades, K., Madoui, M.-A., Le, P., Robert, C. and Raoult, D. (2011). Phylogenomic Analysis of Odyssella thessalonicensis Fortifies the Common Origin of Rickettsiales, Pelagibacter ubique and Reclimonas americana Mitochondrion. *PLoS ONE* **6,** e24857.

Gillespie, J.J., Ammerman, N.C., Dreher-Lesnick, S.M., Rahman, M.S., Worley, M.J., Setubal, J.C.*, et al.* (2009). An Anomalous Type IV Secretion System in Rickettsia Is Evolutionarily Conserved. *PLoS ONE* **4,** e4833.

Gillespie, J.J., Wattam, A.R., Cammer, S.A., Gabbard, J.L., Shukla, M.P., Dalay, O.*, et al.* (2011). PATRIC: the Comprehensive Bacterial Bioinformatics Resource with a Focus on Human Pathogenic Species. *Infection and Immunity* **79,** 4286-4298.

Gillespie, J.J., Williams, K., Shukla, M., Snyder, E.E., Nordberg, E.K., Ceraul, S.M.*, et al.* (2008). Rickettsia Phylogenomics: Unwinding the Intricacies of Obligate Intracellular Life. *PLoS ONE* **3,** e2018.

Goldberg, M.B. (2001). Actin-based motility of intracellular microbial pathogens. *Microbiol Mol Biol Rev* **65,** 595-626, table of contents.
Goldberg, M.B., Bârzu, O., Parsot, C. and Sansonetti, P.J. (1993). Unipolar localization and ATPase activity of IcsA, a Shigella flexneri protein involved in intracellular movement. *Journal of Bacteriology* **175,** 2189-2196.
Goley, E.D. and Welch, M.D. (2006). The ARP2/3 complex: an actin nucleator comes of age. *Nat Rev Mol Cell Biol* **7,** 713-726.
Gouin, E., Egile, C., Dehoux, P., Villiers, V., Adams, J., Gertler, F.*, et al.* (2004). The RickA protein of Rickettsia conorii activates the Arp2/3 complex. *Nature* **427,** 457-461.
Gouin, E., Gantelet, H., Egile, C., Lasa, I., Ohayon, H., Villiers, V.*, et al.* (1999). A comparative study of the actin-based motilities of the pathogenic bacteria Listeria monocytogenes, Shigella flexneri and Rickettsia conorii. *J Cell Sci* **112 (Pt 11),** 1697-1708.
Hackstadt, T. (1996). The Biology of Rickettsiae. *Infectious Agents and Disease* **5,** 127-143.
Haglund, C.M., Choe, J.E., Skau, C.T., Kovar, D.R. and Welch, M.D. (2010). Rickettsia Sca2 is a bacterial formin-like mediator of actin-based motility. *Nat Cell Biol* **12,** 1057-1063.
Haglund, C.M. and Welch, M.D. (2011). Pathogens and polymers: Microbe‚Äìhost interactions illuminate the cytoskeleton. *The Journal of Cell Biology* **195,** 7-17.
Hänisch, J., Kölm, R., Wozniczka, M., Bumann, D., Rottner, K. and Stradal, T.E.B. (2011). Activation of a RhoA/Myosin II-Dependent but Arp2/3 Complex-Independent Pathway Facilitates Salmonella Invasion. *Cell Host & Microbe* **9,** 273-285.
Heinzen, R.A. (2003). Rickettsial actin-based motility: behavior and involvement of cytoskeletal regulators. *Ann N Y Acad Sci* **990,** 535-547.
Heinzen, R.A., Hayes, S.F., Peacock, M.G. and Hackstadt, T. (1993). Directional actin polymerization associated with spotted fever group Rickettsia infection of Vero cells. *Infect Immun* **61,** 1926-1935.
Jeng, R.L., Goley, E.D., D'Alessio, J.A., Chaga, O.Y., Svitkina, T.M., Borisy, G.G.*, et al.* (2004). A Rickettsia WASP-like protein activates the Arp2/3 complex and mediates actin-based motility. *Cell Microbiol* **6,** 761-769.
Kaplan, L.I. (1996). Other spotted fevers. *Clinics in Dermatology* **14,** 259-267.
Kleba, B., Clark, T.R., Lutter, E.I., Ellison, D.W. and Hackstadt, T. (2010). Disruption of the Rickettsia rickettsii Sca2 Autotransporter Inhibits Actin-Based Motility. *Infection and Immunity* **78,** 2240-2247.
Li, H. and Walker, D.H. (1998). rOmpA is a critical protein for the adhesion of Rickettsia rickettsii to host cells. *Microbial Pathogenesis* **24,** 289-298.
Ogata, H., Robert, C., Audic, S., Robineau, S., Blanc, G., Fournier, P.E.*, et al.* (2005). Rickettsia felis, from culture to genome sequencing. *Ann N Y Acad Sci* **1063,** 26-34.
Paddock, C.D., Finley, R.W., Wright, C.S., Robinson, H.N., Schrodt, B.J., Lane, C.C.*, et al.* (2008). Rickettsia parkeri Rickettsiosis and Its Clinical Distinction from Rocky Mountain Spotted Fever. *Clinical Infectious Diseases* **47,** 1188-1196.
Parola, P. (2011). Rickettsia felis: from a rare disease in the USA to a common cause of fever in sub-Saharan Africa. *Clinical Microbiology and Infection* **17,** 996-1000.
Philip, R.N., Casper, E.A., Anacker, R.L., Cory, J., Hayes, S.F., Burgdorfer, W. and Yunker, C.E. (1983). Rickettsia bellii sp. nov.: a Tick-Borne Rickettsia, Widely Distributed in the United States, That Is Distinct from the Spotted Fever and Typhus Biogroups. *International Journal of Systematic Bacteriology* **33,** 94-106.

Radulovic, S., Troyer, J.M., Beier, M.S., Lau, A.O.T. and Azad, A.F. (1999). Identification and Molecular Analysis of the Gene Encoding Rickettsia typhi Hemolysin. *Infect. Immun.* **67,** 6104-6108.

Rahman, M.S., Ammerman, N.C., Sears, K.T., Ceraul, S.M. and Azad, A.F. (2010). Functional Characterization of a Phospholipase A2 Homolog from Rickettsia typhi. *The Journal of Bacteriology* **192,** 3294-3303.

Renesto, P., Dehoux, P., Gouin, E., Touqui, L., Cossart, P. and Raoult, D. (2003). Identification and characterization of a phospholipase D-superfamily gene in rickettsiae. *J Infect Dis* **188,** 1276-1283.

Schaechter M., Bozeman F.M. and Smadel J.E. (1957). Study on the growth of Rickettsiae. II. Morphologic observations of living Rickettsiae in tissue culture cells. *Virology* **3**, 160-172.

Serio, A.W., Jeng, R.L., Haglund, C.M., Reed, S.C. and Welch, M.D. (2010). Defining a Core Set of Actin Cytoskeletal Proteins Critical for Actin-Based Motility of Rickettsia. *Cell Host & Microbe* **7,** 388-398.

Silverman, D.J. (1984). Rickettsia rickettsii-induced cellular injury of human vascular endothelium in vitro. *Infect. Immun.* **44,** 545-553.

Silverman, D.J., Santucci, L.A., Meyers, N. and Sekeyova, Z. (1992). Penetration of host cells by Rickettsia rickettsii appears to be mediated by a phospholipase of rickettsial origin. *Infect Immun* **60,** 2733-2740.

Silverman, D.J. and Wisseman, C.L. (1979). In vitro studies of rickettsia-host cell interactions: ultrastructural changes induced by Rickettsia rickettsii infection of chicken embryo fibroblasts. *Infection and Immunity* **26,** 714-727.

Silverman, D.J., Wisseman, C.L. and Waddell, A. (1980). In Vitro Studies of Rickettsia-Host Cell Interactions: Ultrastructural Study of Rickettsia prowazekii-Infected Chicken Embryo Fibroblasts. *Infection and Immunity* **29,** 778-790.

Skoble, J., Portnoy, D.A. and Welch, M.D. (2000). Three regions within ActA promote Arp2/3 complex-mediated actin nucleation and Listeria monocytogenes motility. *J Cell Biol* **150,** 527-538.

Teysseire, N., Boudier, J.A. and Raoult, D. (1995). Rickettsia conorii entry into Vero cells. *Infect Immun* **63,** 366-374.

Teysseire, N., Chiche-Portiche, C. and Raoult, D. (1992). Intracellular movements of Rickettsia conorii and R. typhi based on actin polymerization. *Res Microbiol* **143,** 821-829.

Thrash, J.C., Boyd, A., Huggett, M.J., Grote, J., Carini, P., Yoder, R.J*., et al.* (2011). Phylogenomic evidence for a common ancestor of mitochondria and the SAR11 clade. *Sci. Rep.* **1**.

Tilney, L.G., DeRosier, D.J. and Tilney, M.S. (1992). How Listeria exploits host cell actin to form its own cytoskeleton. I. Formation of a tail and how that tail might be involved in movement. *J Cell Biol* **118,** 71-81.

Uchiyama, T., Kawano, H. and Kusuhara, Y. (2006). The major outer membrane protein rOmpB of spotted fever group rickettsiae functions in the rickettsial adherence to and invasion of Vero cells. *Microbes and Infection* **8,** 801-809.

Van Kirk, L.S., Hayes, S.F. and Heinzen, R.A. (2000). Ultrastructure of Rickettsia rickettsii actin tails and localization of cytoskeletal proteins. *Infect Immun* **68,** 4706-4713.

Walker, D.H. (1989). Rocky Mountain spotted fever: a disease in need of microbiological concern. *Clin. Microbiol. Rev.* **2,** 227-240.

Walker, D.H. and Cain, B.G. (1980). The rickettsial plaque. Evidence for direct cytopathic effect of Rickettsia rickettsii. *Lab Invest* **43,** 388-396.

Walker, D.H., Firth, W.T., Ballard, J.G. and Hegarty, B.C. (1983). Role of Phospholipase-Associated Penetration Mechanism in Cell Injury by Rickettsia rickettsii. *Infect. Immun.* **40,** 840-842.

Walker, D.H., Harrison, A., Henderson, F. and Murphy, F.A. (1977). Identification of Rickettsia rickettsii in a guinea pig model by immunofluorescent and electron microscopic techniques. *Am J Pathol* **86,** 343-358.

Walker, D.H. and Ismail, N. (2008). Emerging and re-emerging rickettsioses: endothelial cell infection and early disease events. *Nat Rev Microbiol* **6,** 375-386.

Weinert, L.A., Werren, J.H., Aebi, A., Stone, G.N. and Jiggins, F.M. (2009). Evolution and diversity of Rickettsia bacteria. *BMC Biol* **7,** 6.

Welch M.D., Haglund C.M. and Reed, S.C. (2012b) Establishing intracellular infection: escape from the phagosome and intracellular colonization. In *Intracellular Pathogens II: Rickettsiales*, G.H. Palmer, a.A.F. Azad (eds.) 1 edn. Washington DC, ASM Press, In press.

Welch, M.D., Rosenblatt, J., Skoble, J., Portnoy, D.A. and Mitchison, T.J. (1998). Interaction of human Arp2/3 complex and the Listeria monocytogenes ActA protein in actin filament nucleation. *Science* **281,** 105-108.

Whitworth, T., Popov, V.L., Yu, X.-J., Walker, D.H. and Bouyer, D.H. (2005). Expression of the Rickettsia prowazekii pld or tlyC Gene in Salmonella enterica Serovar Typhimurium Mediates Phagosomal Escape. *Infect. Immun.* **73,** 6668-6673.

Winkler, H.H. (1990). Rickettsia Species (As Organisms). *Annual Review of Microbiology* **44,** 131-153.

Wisseman, C.L., Edlinger, E.A., Waddell, A.D. and Jones, M.R. (1976). Infection cycle of Rickettsia rickettsii in chicken embryo and L-929 cells in culture. *Infection and Immunity* **14,** 1052-1064.

Wisseman, C.L. and Waddell, A.D. (1975). In Vitro Studies on Rickettsia-Host Cell Interactions: Intracellular Growth Cycle of Virulent and Attenuated Rickettsia prowazeki in Chicken Embryo Cells in Slide Chamber Cultures. *Infection and Immunity* **11,** 1391-1401.

CHAPTER 2

Rickettsia parkeri *invasion of diverse host cells involves an Arp2/3 complex, WAVE complex and Rho-family GTPase-dependent pathway.*

Note: The information presented in this chapter was included in the publication: Reed S.C., Serio A.W., Welch M.D. (2012). *Rickettsia parkeri* invasion of diverse host cells involves Arp2/3 complex, WAVE/Abi complex, and Rho-family GTPase-dependent pathways. *Cellular Microbiology*, 14: 529-545

INTRODUCTION

Rickettsiae are Gram-negative, obligate intracellular alpha-proteobacteria that infect both mammalian and arthropod hosts. The spotted fever group (SFG) of *Rickettsia* includes *Rickettsia parkeri*, an emerging cause of mild-to-moderate spotted fever disease in North and South America (Paddock *et al.*, 2004). Infection of endothelial cells by *Rickettsia parkeri* and related SFG species such as *Rickettsia rickettsii* and *Rickettsia conorii* results in systemic disease including vascular damage, edema, a characteristic petechial rash, and a necrotic eschar at the inoculation site (Walker *et al.*, 2008).

To gain access to non-phagocytic host cells, rickettsiae must induce their own uptake. For other bacterial pathogens, invasion generally occurs either when bacterial surface proteins bind host cell surface receptors and activate local extension of the host membrane, or when secretion-system mediated injection of bacterial effector proteins induces membrane ruffling and actin polymerization (Cossart *et al.*, 2004). While *Rickettsia* genomes encode a type IV secretion system (T4SS) as well as a number of proteins with eukaryotic-specific sequence motifs that could function as effectors (Gillespie *et al.*, 2009), no effectors have been demonstrated to date. However, a number of *Rickettsia* outer membrane proteins contribute to bacterial adherence and invasion. Both the *R. rickettsii* surface protein rOmpA and the *R. conorii* surface protein Sca1 contribute to adherence (Li *et al.*, 1998; Riley *et al.*, 2010) while the *R. conorii* and *Rickettsia japonica* rOmpB and *R. conorii* Sca2 proteins are functionally important for bacterial entry and their expression in *E. coli* is sufficient to allow invasion of host cells (Cardwell *et al.*, 2009; Chan *et al.*, 2009; Uchiyama *et al.*, 2006). Unfortunately, a lack of robust genetic tools for *Rickettsia* species has hindered analysis of how the T4SS, secreted effectors, and outer membrane proteins might cooperate to mediate host cell invasion.

In addition to bacterial proteins, *Rickettsia* invasion requires the activation of host signaling pathways upstream of actin polymerization. The only known receptor for *Rickettsia* entry is the DNA-dependent protein kinase subunit Ku70, which binds to *R. conorii* rOmpB (Chan *et al.*, 2009; Martinez *et al.*, 2005). Downstream of receptor engagement, *R. conorii* invasion of mammalian cells requires host protein tyrosine kinases, results in the accumulation of tyrosine-phosphorylated proteins around invading bacteria, and also requires phosphoinositide 3-kinase activity (Martinez *et al.*, 2004). In addition, the Rho family GTPase Cdc42 was implicated in invasion (Martinez *et al.*, 2004).

Actin polymerization during invasion could be initiated by formin-family proteins, tandem monomer-binding nucleators, or nucleation promoting factors (NPFs) that act in conjunction with the Arp2/3 complex (Campellone *et al.*, 2010). Based on experiments implicating Cdc42, it was proposed that the host NPF N-WASP was important for *R. conorii* invasion (Martinez *et al.*, 2004). Indeed, the Arp3 subunit of the Arp2/3 complex was observed around invading bacteria and expression of an Arp2/3-activating WCA domain from WAVE1 (also known as WASF1 or Scar1) inhibited *R. conorii* invasion (Martinez *et al.*, 2004). However, a direct role for the Arp2/3 complex has not been demonstrated via depletion or inhibition studies. In addition, it is unclear which NPF proteins act during *Rickettsia* entry, whether additional bacteria or host actin nucleators may be involved, and whether invasion by diverse *Rickettsia* species or of physiologically relevant host cell types utilize the same or different pathways.

To achieve a comprehensive understanding of the host cytoskeletal proteins important for *Rickettsia* invasion, we investigated the invasion of multiple cultured cell lines by the SFG

species *Rickettsia parkeri*, which is genetically similar to *R. rickettsii* and *R. conorii* (Ralph *et al.*, 1990), displays a similar ability to invade cells and form actin tails (Serio *et al.*, 2010), but is less pathogenic and is not a select agent (Paddock *et al.*, 2008). We performed a targeted RNAi-based screen in *Drosophila* S2R+ cells to identify a core group of host cytoskeletal proteins required for this process. We identified 21 proteins including Rho-family GTPases, and the WAVE and Arp2/3 complexes, which played a key role in invasion. During invasion of mammalian cells, including a human endothelial cell line, the requirement for WAVE family proteins and Rho family GTPases was not as stringent as in *Drosophila* cells, but the Arp2/3 complex was critical. Overall, these results suggest a pathway activating actin nucleation around invading rickettsiae and demonstrate that the molecular requirements for invasion vary depending on host cell type.

RESULTS

R. parkeri *invasion of* Drosophila *and mammalian cells is rapid and depends on viable bacteria and host actin*

Invasion of host cells by *Rickettsia* has been reported to occur within 5 min to 2 h post-infection (Martinez *et al.*, 2004; Teysseire *et al.*, 1995; Walker *et al.*, 1978; Walker, 1984). To determine the kinetics of *R. parkeri* invasion, we infected immortalized human microvascular endothelial cells (HMEC-1), African green monkey kidney-derived cells (COS-7), and adherent *Drosophila* embryo-derived hemocyte-like cells (S2R+) with *R. parkeri* and determined the percentage of internalized bacteria at various times post-infection by differential fluorescence staining of internal and external bacteria (Figure 2.1A). In all cell types examined, internalization plateaued between 30-60 min post-infection and was >50% complete by 15 min. Based on the rapid speed of invasion, subsequent experiments were conducted using 15 min infection times.

We next sought to determine whether rapid invasion of S2R+ and HMEC-1 cells was due to generalized phagocytosis by these cells. We compared internalization of live *R. parkeri* versus heat-treated or formaldehyde-fixed bacteria, non-invasive *E. coli* (commercial strain XL-10), and the invasive *Listeria monocytogenes* strain 10403S (Agaisse *et al.*, 2005; Greiffenberg *et al.*, 1998) (Figure 2.1B,C). In S2R+ cells, live *R. parkeri* were internalized more than two-fold more efficiently than nonviable or other bacteria (Figure 2.1B; Appendix 1). In HMEC-1 cells, live *R. parkeri* were internalized at least three-fold more efficiently than nonviable or other bacteria (Figure 2.1C). Therefore, under these experimental conditions, invasion of host cells occurs through an active, *R. parkeri*-specific process.

We also confirmed that *R. parkeri* invasion requires host actin polymerization and tyrosine kinase activity, as is the case for *R. conorii* (Chan *et al.*, 2009; Martinez *et al.*, 2004). Using Lifeact-mCherry as a marker for F-actin, we observed actin accumulation around invading *R. parkeri* in S2R+, HMEC-1, and COS-7 cells (Figure 2.1D, Movies 2.1-2.2 and data not shown). The actin depolymerizing agent latrunculin A reduced *R. parkeri* invasion of both S2R+ and HMEC-1 cells by 3.5 and 5.7-fold, respectively, while the microtubule-disrupting drug nocodazole did not significantly alter invasion (Figure 2.1E,F; Appendix 1; Figure 2.2). In addition, invasion of HMEC-1 cells depended on

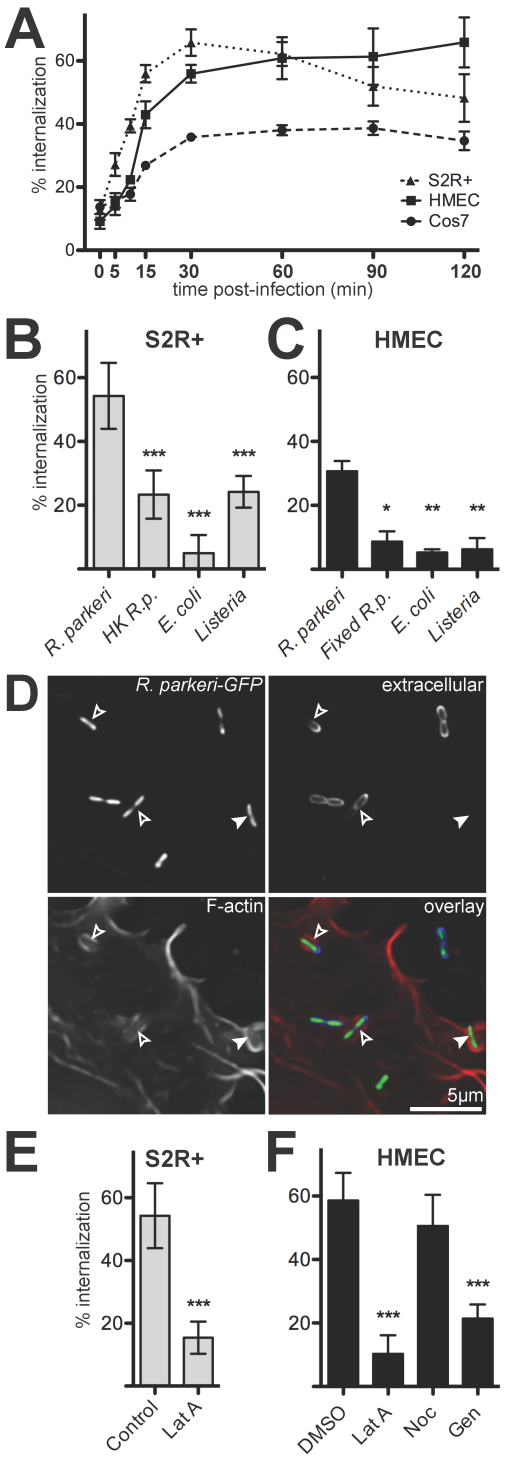

Figure 2.1. *R. parkeri* invade cells quickly in a process dependent on viable bacteria and host actin. (A) Percent of cell-associated *R. parkeri* that were internalized by S2R+ (triangles), HMEC-1 (squares) or COS-7 (circles) cells at various times post-infection (n=3). (B) Percent internalization by S2R+ cells infected for 15 min with live *R. parkeri*, heat-killed *R. parkeri* (HK R.p.), E. coli XL-10 Gold (E. coli), or *L. monocytogenes* 10403S (*Listeria*). (C) Percent internalization by HMEC-1 infected for 15 min with live *R. parkeri*, or formaldehyde-fixed *R. parkeri* (Fixed R.p.), L. monocytogenes, or E. coli. Note: live R.p. in panel C were incubated at

RT while samples were fixed (D) Maximum intensity projection of a deconvolved image of COS-7 cells transfected with pLifeact-mCherry (lower left, red in merge) and infected 48 h later with GFP-expressing *R. parkeri* (GFP, top left, green in merge) for 15 min. Extracellular bacteria were stained with anti-*Rickettsia* antibody without permeabilization (upper right, blue in merge). Open arrowheads; partially internalized bacteria, closed arrowheads; fully internalized bacterium. (E) Internalization by S2R+ cells infected for 15 min with *R. parkeri* and untreated (Control) or treated for 30 min prior to infection with 4 μM latrunculin A (Lat A). (F) Internalization by HMEC-1 cells after 15 min infection; cells were either pretreated with 1% DMSO alone, or treated 30 minutes before infection with 4 μM latrunculin A (LatA), 20 μM nocodazole (Noc) or 250 μM genistein (Gen) in 1% DMSO. For all panels: graphs plot the mean percent internalization for at least three independent experiments. Error bars indicate SEM (A), SD (B-D); * $p<0.05$, ** $p<0.01$, *** $p<0.001$ versus mean of control (*R. parkeri* or DMSO) by unpaired t-test.

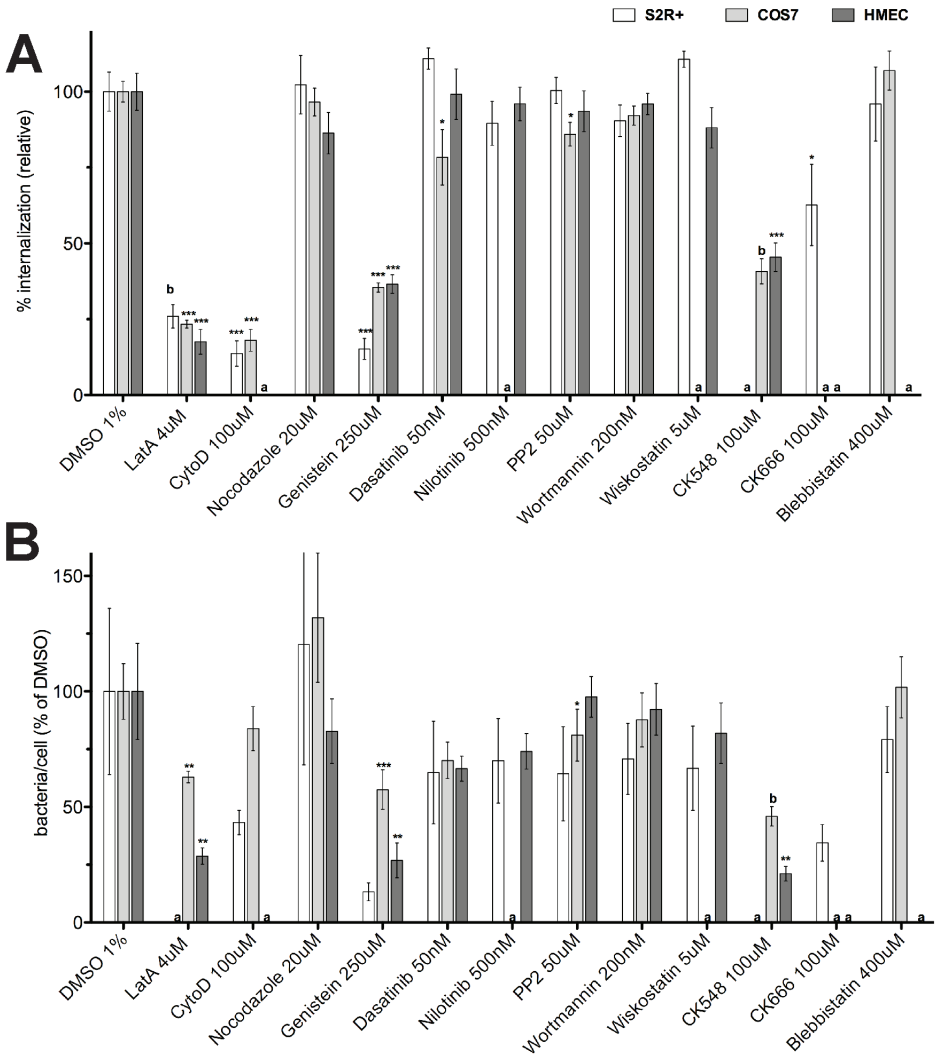

Figure 2.2 – *R. parkeri* adherence to and invasion of host cells does not require microtubules, Myosin II, N-WASP or a single tyrosine kinase family.
(A) Percent internalization and **(B)** average bacteria per host cell after 15 mins of infection by *R. parkeri* in S2R+ (white bars) COS-7 (light grey bars) and HMEC-1 cells (dark grey bars); cells were either pretreated with 1% DMSO alone, or treated 30 min before infection with drugs diluted to the indicated concentrations in 1% DMSO. Data are the mean of two (S2R+) or three (COS-7 and HMEC) independent experiments and were normalized with the average of DMSO-treated control cells set as 100%. (a) indicates a treatment not performed for a particular cell type, (b) indicates that data were normalized to control values not shown in histogram. Abbreviations: LatA, latrunculin A; CytoD, cytochalasin D, Error bars, SEM, * $p<0.05$, ** $p<0.01$ *** $p<0.001$, raw data compared versus matched DMSO controls by unpaired t-test.

tyrosine kinase activity, as genistein significantly reduced internalization (Figure 2.1E). Treatment with latrunculin A and genistein also reduced the total number of bacteria associated with host cells (Figure 2.2B). Treatment of S2R+, HMEC-1 and COS-7 cells with specific inhibitors of Abl (nilotinib), Src/Abl-family (dasatinib), Src/LCK/FYN-family (PP2), and phosphatidylinositol 3-kinases (wortmannin) had little or no effect on invasion or binding, suggesting that entry does not depend on one specific tyrosine kinase signaling pathway (Figure 2.2A-B). Overall, these results demonstrate that *R. parkeri*, like *R. conorii*, rapidly invade a variety of cell types in a manner dependent on host actin polymerization and tyrosine kinase activity.

RNAi screening identifies 21 proteins important for **R. parkeri** *invasion of S2R+ cells*

Because of the essential role of actin in *R. parkeri* invasion, we sought to determine which host proteins direct actin polymerization during this process. To this end, we carried out a screen for invasion using S2R+ cells, which are highly amenable to RNAi-mediated gene silencing and have been used previously to find host factors important for *R. parkeri* motility as well as *L. monocytogenes*, *Chlamydia trachomatis, Pseudomonas aeruginosa,* and *Candida albicans* host cell invasion (Agaisse *et al.*, 2005; Elwell *et al.*, 2008; Pielage *et al.*, 2008; Stroschein-Stevenson *et al.*, 2005; Serio *et al.*, 2010). We targeted 105 genes encoding proteins that regulate, modify, or comprise the actin cytoskeleton, drawing from a list previously screened for involvement in *R. parkeri* actin tail formation (Serio *et al.*, 2010) and *Drosophila* lamellipodia formation (Rogers *et al.*, 2003). S2R+ cells were treated with dsRNA for 4 d, infected with *R. parkeri* for 15 min, fixed and differentially stained for intracellular and extracellular bacteria (Figure 2.3A). We confirmed protein depletion for a subset of targets (Figure 2.3B) and consistently observed changes in cell shape and actin organization that served as a visual confirmation of successful RNA interference during each experiment (Rogers *et al.*, 2003; Zallen *et al.*, 2002).

Twenty-one proteins were identified as having potential functions in *R. parkeri* invasion of host cells based on a statistically significant ($p \leq 0.01$ by students t-test) decrease in the percentage of internalized bacteria compared to untreated control cells (Table 2.1). When data were normalized to matched control cells for each day's experiments, differences remained statistically significant (Table 2.1, Appendix 1).

The 21 proteins could be segregated into five functional classes, including: (1) small G proteins and G protein exchange or activating factors; (2) Arp2/3 complex subunits, NPFs and NPF-binding proteins; (3) phagocytosis-associated myosin motors and adapters; (4) membrane-cytoskeleton linking proteins; and (5) actin filament organizing, bundling and severing proteins.

Individual proteins identified in the screen included Rac1 and Rac2, suggesting an involvement of Rho-family GTPases in *R. parkeri* invasion (silencing Rac1/Rac2 or Rac1/Cdc42 in combination also decreased entry; Table 2.1, Figure 2.3C). Downstream of Rac1 and Rac2, RNAi targeting of the Rac effector and Arp2/3 complex NPF WAVE (*Drosophila* SCAR) as well as subunits of the WAVE complex (Abi, Sra-1, Kette), decreased *R. parkeri* invasion to levels similar to invasion of heat-killed bacteria (Table 2.1, Figure 2.1B, Figure 2.3D). Depletion of subunits of the Arp2/3 complex (ARP2, ARP3, ARPC1, ARPC2, ARPC4, and ARPC5) also significantly reduced invasion (Table 2.1, Figure 2.3D). Targeting of WASP, a second Arp2/3 complex NPF, did not significantly reduce internalization (Appendix 1), although targeting of the WASP- interacting protein WIP did inhibit internalization (Table 2.1, Figure 2.3D).

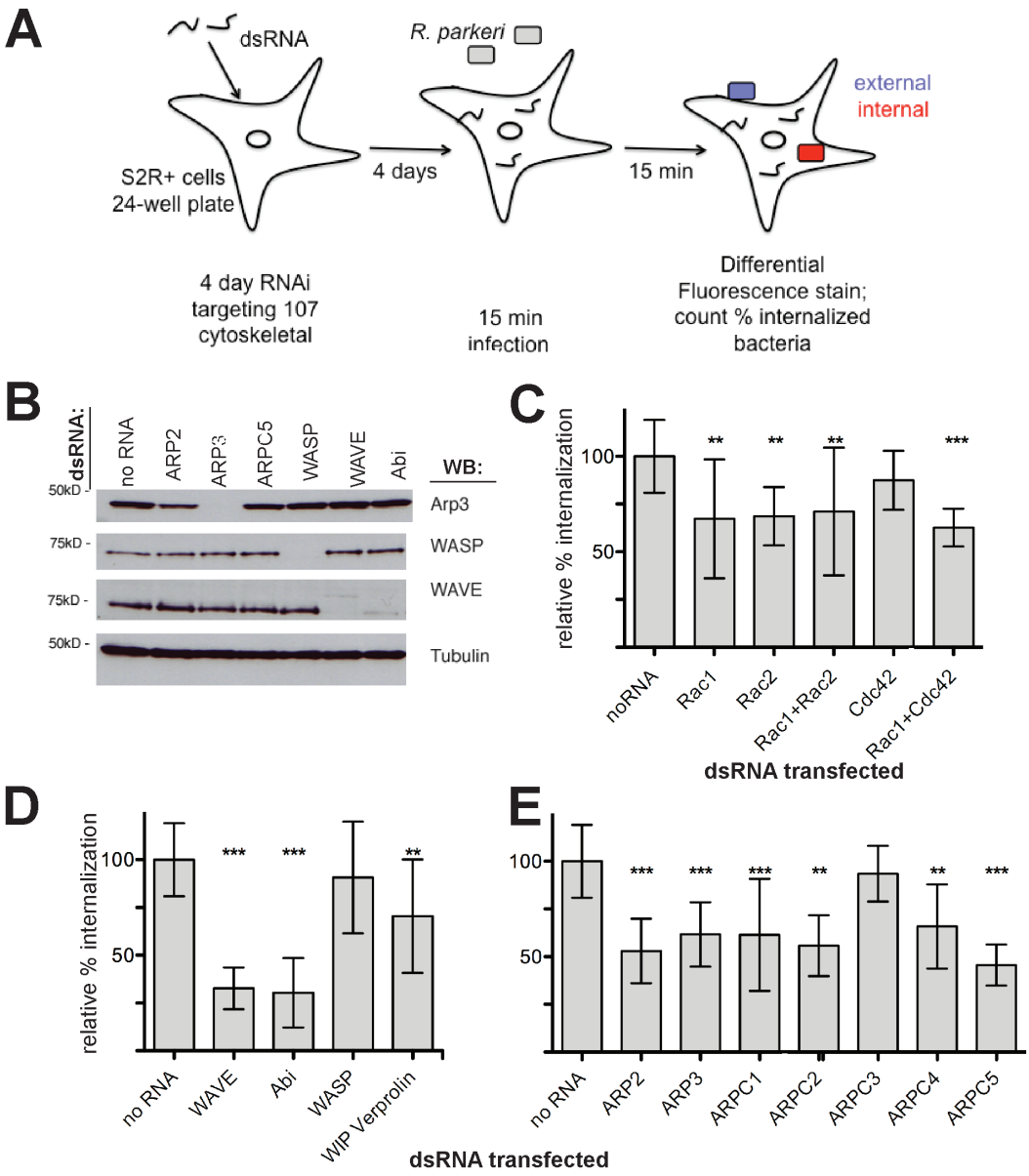

Figure 2.3 RNAi screening in S2R+ cells reveals that Rac, the WAVE complex and the Arp2/3 complex are important for *R. parkeri* invasion. (A) Schematic representation of the RNAi screening approach. All genes targeted are listed in Dataset S1. **(B)** Western blot of S2R+ cell lysates after RNAi targeting the indicated proteins for 4 d. **(C-E)** Subset of the S2R+ RNAi screening results represented as relative % internalization after targeting **(C)** Rho-family GTPases alone or in combination, **(D)** the NPFs WAVE/Scar or WASP and their complex subunits, or **(E)** Arp2/3 complex subunits. Results are normalized to the mean of 2-3 untreated control coverslips for each day's experiment, corresponding to column 5 of Table 2.1. Data represent at least three independent experiments. Error bars represent SD; ** $p<0.01$, *** $p<0.001$ versus untreated controls by unpaired Student's t-test.

Table 2.1 Proteins implicated in *Rickettsia* invasion of S2R+ cells by RNAi screening

Functional group	Protein implicated in invasion	Internalization [a] (%)	p-value[b]	Normalized internalization[c]	Hit shared with other screens[d]
---	untreated control cells	54 ± 10	---	1 ± 0.09	---
Rho family GTPase	Rac1	37 ± 17	0.0021	0.84 ± 0.5	4,5,7,10
	Rac2	37 ± 8	0.002	0.77 ± 0.09	3,4,5,10
	Rac1 + Cdc42	34 ± 5	0.0003	0.68 ± 0.11	---
	Rac1 + Rac2	39 ± 18	0.0031	0.84 ± 0.46	---
Actin filament nucleator	ARP2	29 ± 9	<0.0001	0.59 ± 0.15	2,3,9
	ARP3	34 ± 9	0.0002	0.67 ± 0.07	2,3,4,6,9
	ARPC1 (p41)	33 ± 16	0.0013	0.66 ± 0.25	
	ARPC2 (p34)	30 ± 9	<0.0001	0.63 ± 0.21	2,3
	ARPC4 (p20)	36 ± 12	0.001	0.61 ± 0.22	1,2,3,4,5,6,7,8,10
	ARPC5 (p16)	25 ± 6	<0.0001	0.5 ± 0.04	2,3,4,5,10
Actin nucleation promoting factor	WAVE (SCAR)	18 ± 6	<0.0001	0.38 ± 0.08	1,4,5,6,7,8,9,10
WAVE complex member, regulator	Abi	17 ± 10	<0.0001	0.34 ± 0.18	1,2,3,4,5,7,8
	Kette HEM-protein	31 ± 9	<0.0001	0.57 ± 0.24	1,7,8
	Sra-1	35 ± 6	0.0027	0.55 ± 0.07	1,4,6,7
WASP binding, regulator	WIP verprolin	38 ± 16	0.005	0.78 ± 0.34	
Myosin motor protein	Myosin IA	28 ± 12	<0.0001	0.62 ± 0.37	10
	Myosin II (zipper)	33 ± 6	0.0002	0.72 ± 0.27	1
Endocytic / phagocytic adapter	Hip1R	35 ± 7	0.0005	0.74 ± 0.17	10
Membrane-cytoskeleton linker	MIM homolog	33 ± 8	0.0001	0.69 ± 0.21	9
	Myoblast city	38 ± 4	0.0089	0.87 ± 0.11	7
Actin filament bundling/organizing	α-actinin	34 ± 14	0.0004	0.71 ± 0.19	7,8,10
	Fimbrin	38 ± 6	0.0078	0.86 ± 0.05	7,10
Actin monomer dynamics	Cofilin (twinstar)	40 ± 12	0.0088	0.8 ± 0.09	1,7,10

[a]Percent of *R. parkeri* internalized 15 mins after infection in cells treated with dsRNA targeting the indicated protein(s). The data presented are the mean ± SD of at least three independent experiments. [b]Determined by pairwise comparison with the untreated control using the Student's t-test. $p<0.01$ was considered statistically significant. [c]Data were adjusted with the mean percent internalization of matched untreated control cells (duplicate samples) for each day's experiment set as 1 (100%). [d]RNAi targeting this protein was also found to [1]reduce lamella formation (Rogers *et al*., 2003); [2]*Listeria monocytogenes* and/or [3]*Mycobacterium fortuitum* infection (Agaisse *et al*., 2005); [4]*Candida albicans*, [5]*E. coli* or [6]latex bead phagocytosis (Stroschein-Stevenson *et al*., 2005); [7]*Chlamydia trachomatis* infection (Elwell *et al*., 2008); [8]*Pseudomonas aeruginosa* internalization (Pielage *et al*., 2008); [9]*Rickettsia parkeri* infection, or [10]*R. parkeri* actin tail formation (Serio *et al*., 2010).

Other targets for which RNAi reduced internalization included the myosin motors Myosin 1A and Myosin II, the actin organizing proteins a-actinin and fimbrin, the severing protein cofilin, the membrane-cytoskeleton linker proteins MIM homolog and Myoblast city, and the endocytic/phagocytic adapter protein Hip1R (Table 2.1). In contrast, notable proteins not implicated in internalization included a seventh Arp2/3 complex subunit (ARPC3), three other WAVE-interacting proteins (Drk, HSPC300, Nck), four other Arp2/3 complex regulators (Coronin, Cortactin, Dcarmil, POD-1), six formin actin nucleation and elongation proteins, and the Spire tandem monomer-binding actin nucleator (Appendix 1). Overall, our targeted screen implicated numerous cytoskeletal proteins in actin assembly during *R. parkeri* invasion of *Drosophila* S2R+ cells, and identified a specific actin nucleation pathway involving Rac proteins, the WAVE/Abi NPF complex, and the Arp2/3 complex.

Mammalian Rho-family GTPases are recruited to invading **R. parkeri** *and are important for entry*

We hypothesized that the proteins implicated in *R. parkeri* invasion of *Drosophila* cells might also be utilized during invasion of mammalian cells. To test this, we employed two mammalian cell types, COS-7 and HMEC-1 (Ades *et al.*, 1992), the latter of which are endothelial cells derived from the tissue naturally infected by *Rickettsia* species (Walker *et al.*, 2008). Given the importance of Rho GTPase signaling for *R. parkeri* invasion in S2R+ cells, and the previously-implied role for Cdc42 in *R. conorii* invasion of Vero cells (Martinez *et al.*, 2004), we sought to define the requirement for Rho-family GTPases in mammalian cell invasion.

We first tested whether active GTPases were recruited to sites of invasion. HMEC-1 cells were transfected with a plasmid expressing either eGFP-Rac1, eGFP-Cdc42 (Subauste *et al.*, 2000) or the p21-binding domain (PBD) of p21-activated kinase (PAK) fused to mCherry (PAK1-PBD-mCherry), a marker for active (GTP-bound) Rac1 and Cdc42 (Chenette *et al.*, 2006; Srinivasan *et al.*, 2003;). Both eGFP-Rac1 and eGFP-Cdc42 proteins, but not eGFP-RhoA, were observed around invading, actin-associated *R. parkeri* (Figure 2.4A-B, data not shown). Immunolocalization of Rac1 and Cdc42 was inconclusive due to nonspecific binding of antibodies to bacteria (data not shown). In addition, PAK1-PBD-mCherry was robustly recruited to sites of bacterial invasion 5-15 min after infection (Figure 2.4A, 2.4C), and could be imaged by time-lapse microscopy while invasion was progressing (Movies 2.3, 2.4). The marker was found around bacteria both with and without associated actin, suggesting that recruitment occurs before actin polymerization begins.

To evaluate the function of Rho GTPases during entry, HMEC-1 and COS-7 cells were transfected with siRNAs targeting Rac1, Rac2, or Cdc42 alone or in combination, infected with *R. parkeri*, and the percentage of internalized bacteria was measured. Gene silencing was confirmed for Rac1 and Cdc42 by immunoblotting (Figure 2.4D, Figure 2.5A-B). We were unable to detect significant levels of Rac2 in HMEC-1 cells by either immunoblotting or RT-PCR, suggesting it may not be expressed at appreciable levels in this cell type (Figure 2.4D, data not shown).

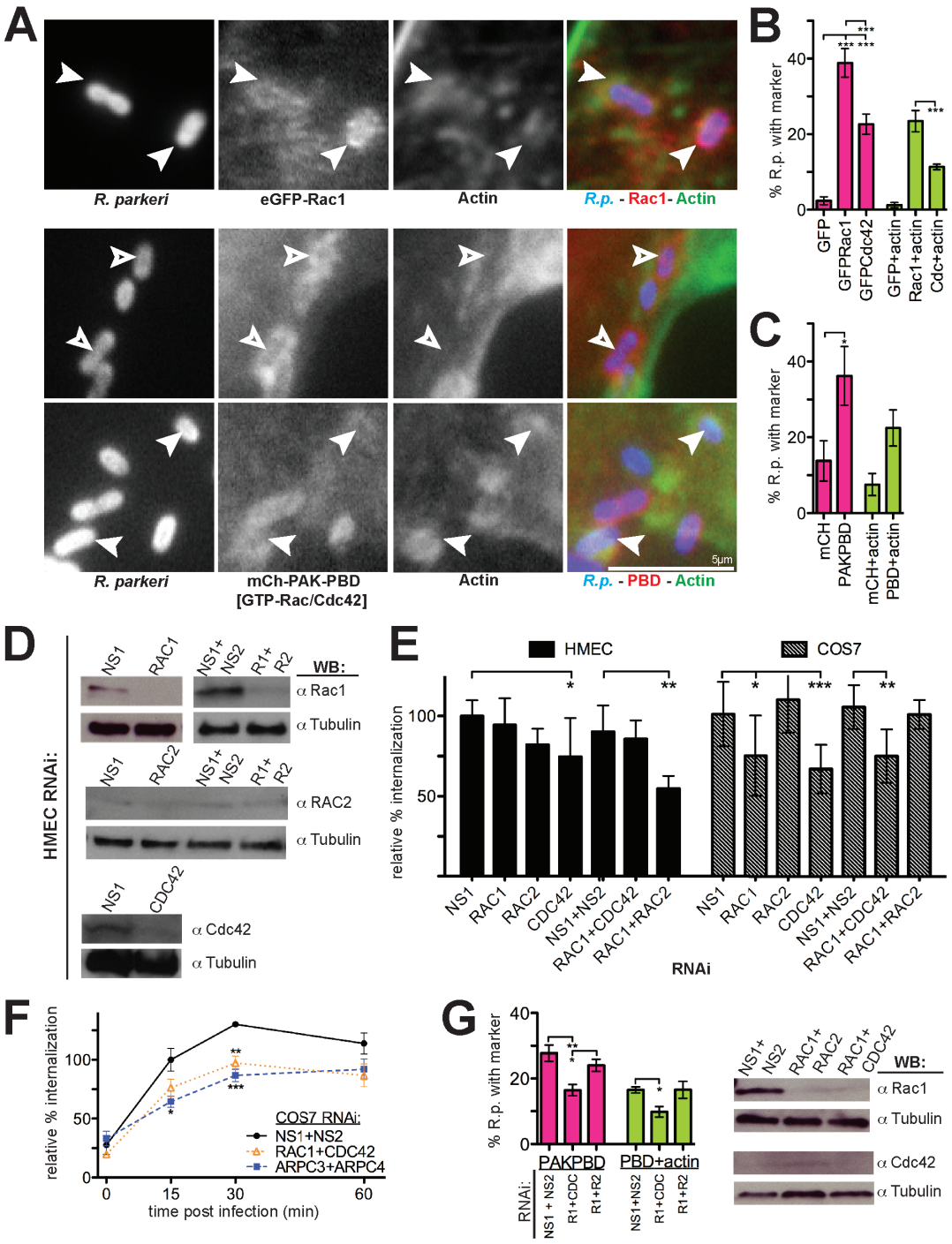

Figure 2.4. Rho-family GTPases are recruited to invading *R. parkeri* in mammalian cells and are important for invasion. (A) *R. parkeri* (left, blue in merge) are surrounded by eGFP-Rac1 or PAK1-PBD-mCherry (middle, red in merge) and actin (right, green in merge) in HMEC-1 cells at 10 min post-infection. Open arrowheads, *Rickettsia* associated with PAK1-PBD alone; filled arrowheads, *Rickettsia* surrounded by actin and eGFP-Rac1 or PAK1-PBD. **(B)** Percentage of *Rickettsia* associated with GFP, eGFP-Rac1, eGFP-Cdc42 and actin 10 min post-infection. Pink bars, mean association with marker; light green bars, mean association with both GFP-

marker and actin. **(C)** Percentage of *Rickettsia* associated with mCherry, PAK1-PBD-mCherry, and actin as in panel (B). **(D)** Western blots of HMEC-1 cell lysates 48 h post-transfection with the indicated siRNAs, corresponding to one experiment represented in (E). COS-7 cell Western blots are shown in Fig S2A. **(E)** Relative percent internalization at 15 min post-infection with *R. parkeri* in either HMEC-1 (solid bars) or COS-7 cells (hashed bars), normalized to nonspecific-RNA treated cells. **(F)** Relative percentage internalization in COS-7 cells from 0-60 min post-infection with *R. parkeri*, normalized to 15 min nonspecific-RNA treated cells. **(G)** Percentage of *Rickettsia* associated with PAK1-PBD-mCherry and actin after cotransfection with indicated siRNAs, as in (C), with corresponding Western blots. Abbreviations: NS1, nonspecific control siRNA 1; NS2, nonspecific control siRNA 2; R1 + R2, Rac1 and Rac2. Error bars, SEM (B-C, F-G) and SD (E). * $p<0.05$, ** $p<0.01$, *** $p<0.001$ versus indicated control by unpaired Student's t-test (E-F) or ANOVA with Bonferroni's post-test (B,C,G). (B-C, F-G) are the mean of two independent experiments performed in duplicate. (E) are the mean of at least three independent experiments performed in duplicate.

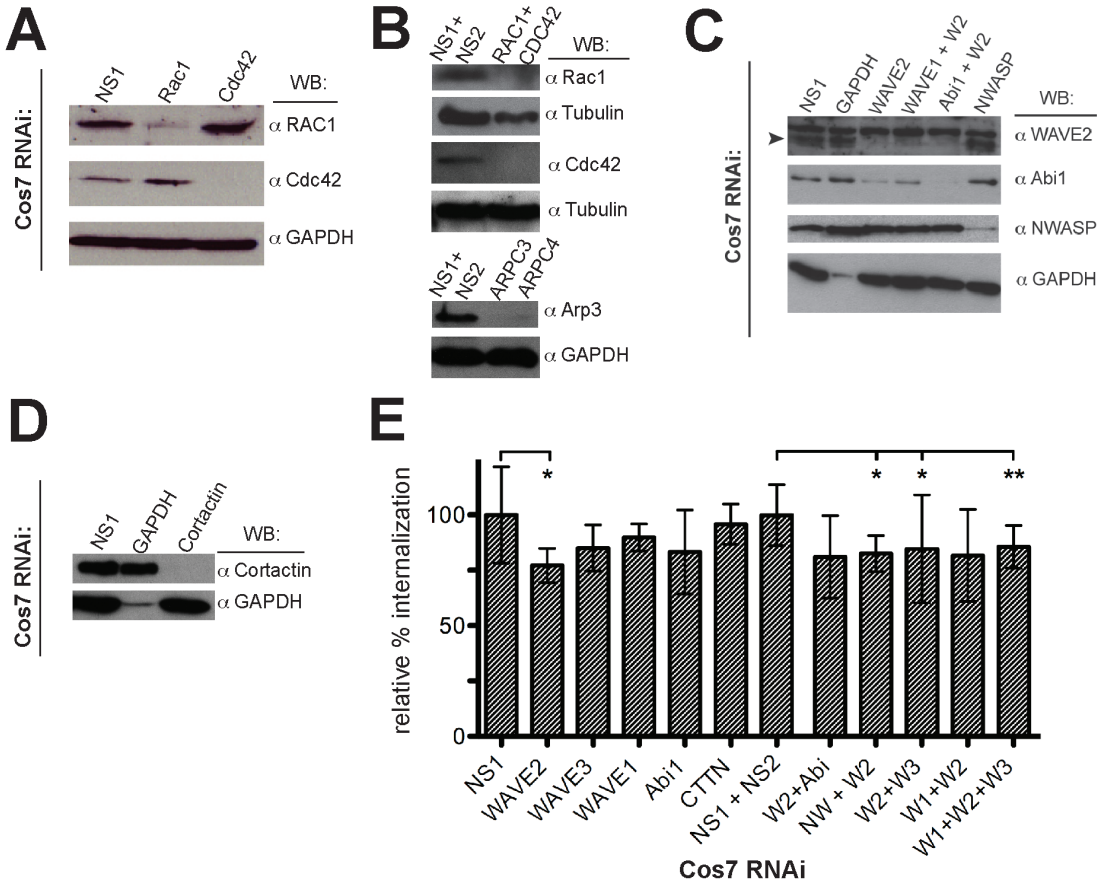

Figure 2.5 –Invasion of COS-7 cells does not require Cortactin or Abi.
(A) Western blots of lysates from cells treated with the indicated siRNAs and collected in parallel during one experiment represented in Figure 3E. **(B)** Western blots of lysates from cells treated with the indicated siRNAs and collected in parallel during one experiment represented in Figure 3F **(C)** Western blots of lysates from cells treated with the indicated siRNAs and collected in parallel during one experiment represented in Figure 4B and in panel (E) of this figure. **(D)** Western blots of lysates from cells treated with the indicated siRNAs and collected in parallel during one experiment represented in panel (E) of this figure. **(E)** Relative percentage internalization at 15 min post infection with *R. parkeri* in COS-7 cells. Data represent the average of at least three independent and were normalized with nonspecific-RNA transfected COS-7 cells set as 100%. Abbreviations: NS1, nonspecific control RNA 1; NS2, nonspecific control RNA 2; W1, W2, W3, WAVE1, WAVE2, WAVE3 respectively; NW, N-WASP; CTTN, Cortactin; *=$p<0.05$, **=$p<0.01$ indicate values significantly different from indicated controls by unpaired t-test.

In HMEC-1 cells, siRNA targeting Cdc42 alone or Rac1 and Rac2 in combination caused a significant decrease in invasion compared to control-siRNA transfected cells (Figure 2.4E). Co-transfection of siRNAs with PAK1-PBD-mCherry revealed that recruitment of PAK1-PBD, and PAK1-PBD together with actin, were significantly reduced ($p<0.05$) after Rac1 and Cdc42 codepletion, to levels similar to mCherry-only controls (Figure 2.4C, 2.4G). In COS-7 cells, knockdown of Rac1, Cdc42, or both GTPases resulted in a significant reduction in invasion (Figure 2.4E) at 15 min, and this decrease persisted through 30-60 min post-infection (Figure 2.4F). The overall requirement for Rac1 and Cdc42 was generally independent of an effect on bacterial binding to cells, as siRNA treatments had little or no effect on binding (Figure 2.6A-B). Thus, Rho-family GTPases play a role during *R. parkeri* invasion of mammalian host cells, while the specific requirements for Rac1 and Cdc42 vary between cell types.

WAVE, but not N-WASP, is the NPF important for optimal **R. parkeri** *invasion of mammalian cells*

Downstream of Rho-family GTPases, *R. parkeri* invasion of *Drosophila* cells required the NPF WAVE and its binding partner Abi, but not the NPF WASP (Figure 2.3D). There are three mammalian isoforms of WAVE, and two isoforms of WASP: WAVE1 and WAVE3 are expressed in brain and hematopoietic cells, whereas WAVE2 is expressed ubiquitously, while WASP is expressed in hematopoietic cells and N-WASP is ubiquitous (Campellone *et al.*, 2010). We first sought to determine which of these NPF proteins were expressed in the mammalian cell lines used for our experiments. Immunoblotting of extracts from various mammalian cell lines revealed that WAVE2, WAVE3 and N-WASP were abundant in HMEC-1 and COS-7 cells whereas WAVE1 and WASP were not expressed at detectable levels (Figure 2.7). Neither immunolocalization of N-WASP and WAVE2, nor expression of GFP or mCherry-fused N-WASP, WAVE2, WHAMM, WASH, and JMY, indicated specific colocalization of NPF proteins with invading *R. parkeri* (data not shown).

To examine the functional importance of NPF proteins during *R. parkeri* invasion, WAVE2, WAVE3, and N-WASP were targeted by RNAi in both HMEC-1 and COS-7 cells and bacterial internalization and binding were measured. Protein depletion was confirmed by immunoblotting (Figure 2.8A, Figure 2.5B). RNAi targeting of WAVEs had little to no effect on bacterial binding, and targeting of N-WASP increased binding in Cos7 cells (Figure 2.6). Silencing of WAVE2 resulted in an approximately 20% decrease of invasion in COS-7 cells, but had no significant effect in HMEC-1 cells. However, in both HMEC-1 and COS-7 cells, silencing WAVE2 in combination with WAVE3 or N-WASP caused a 20-25% decrease of invasion. Knockdown of N-WASP alone had no discernable affect on entry in either cell type (Figure 2.8B). We also treated HMEC-1 cells with wiskostatin, a specific inhibitor of N-WASP (Peterson *et al.*, 2001) and saw no significant change in invasion efficiency or bacterial association (Figure 2.2). Therefore, WAVE2 appears to be consistently important for invasion, and WAVE3 or N-WASP may functionally replace WAVE2 if present, especially in HMEC-1 cells.

To further examine the role of WAVE2 in *R. parkeri* invasion of HMEC-1 cells, we tested whether expression of full-length WAVE2 or truncation derivatives might inhibit the process. HMEC-1 cells were transfected with plasmids expressing either the full-length WAVE2 protein (mChWAVE2), or the N-terminal (mChW2ΔWCA) or C-terminal (mChW2WCA) domains fused to mCherry, and invasion efficiency and binding were quantified in cells visibly

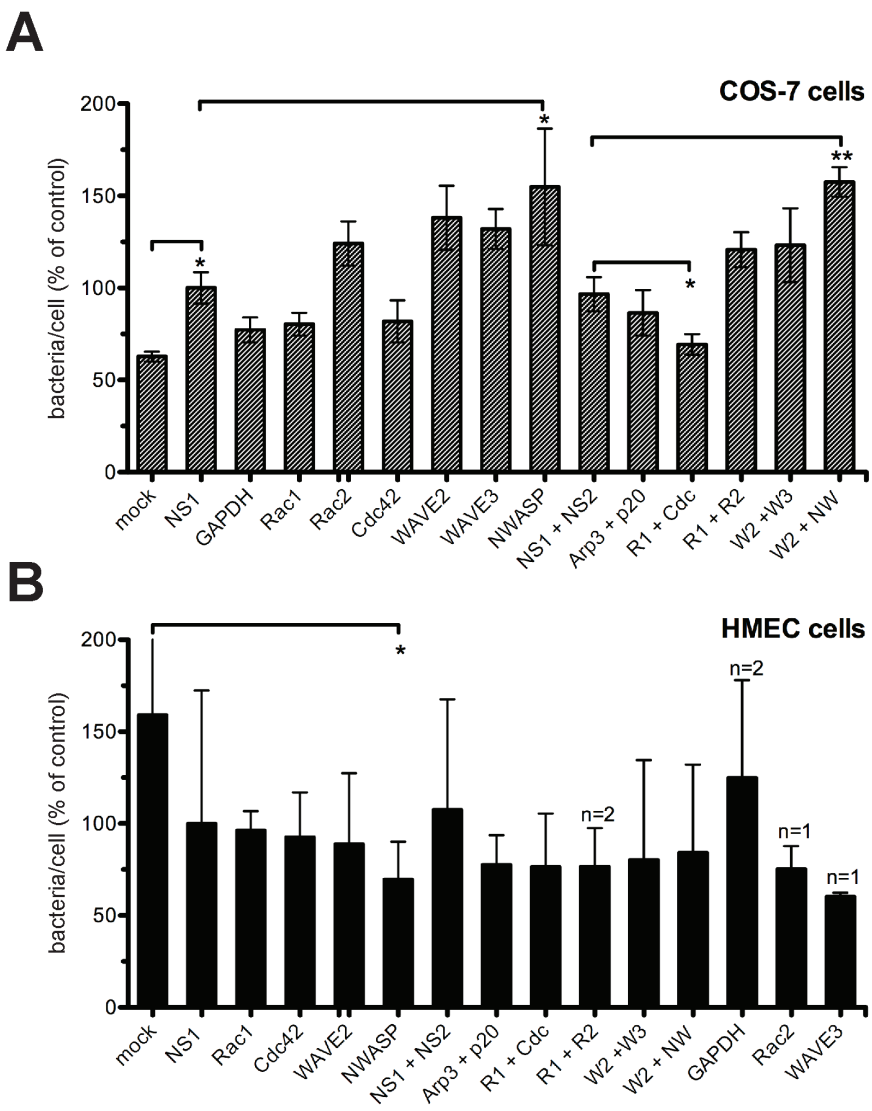

Figure 2.6 – Relative changes in *R. parkeri* adherence to host cells following siRNA treatment. Percentage of bacteria associated with each host cell, relative to NS1 RNAi treatment, in **(A)** COS-7 cells, hashed bars or **(B)** HMEC-1 cells, black bars. Data are the mean of three independent experiments unless otherwise indicated and were normalized with the average of NS1-treated control cells set as 100%. Error bars, SEM, * $p<0.05$, ** $p<0.01$, raw data compared versus indicated control by unpaired t-test.

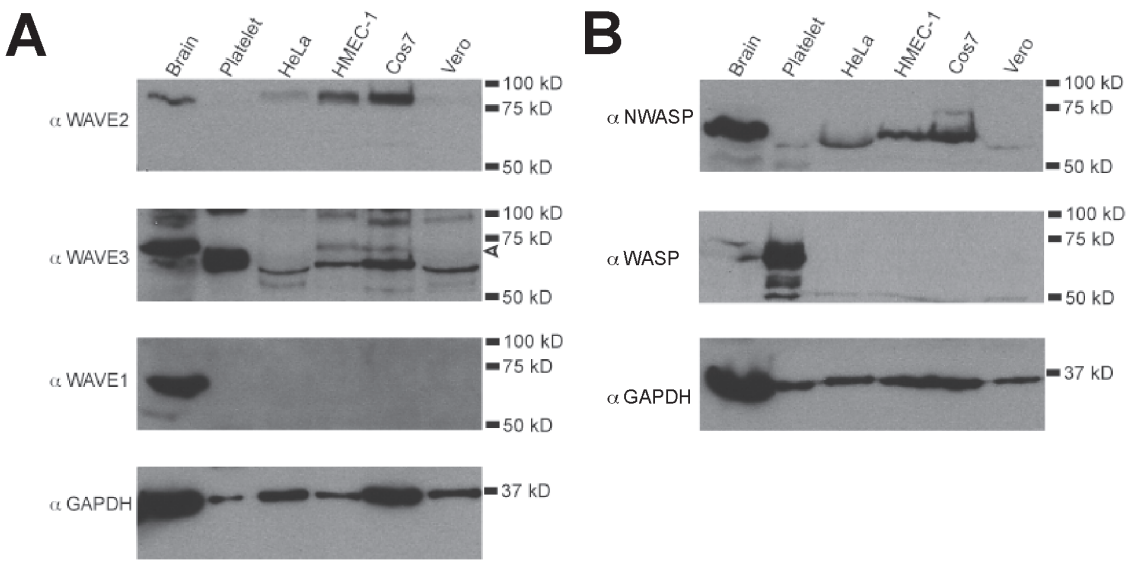

Figure 2.7 - WAVE and WASP family protein expression in various mammalian cell lines. Western blots of cell lysates from pig brain extract, human platelet extract, HeLa, HMEC-1, COS-7, and Vero cells. **(A)** Expression of WAVE1, WAVE2, and WAVE3 in various cell lines. Arrowhead indicates WAVE3-specific band. WAVE1 is expressed only in brain extract. **(B)** Expression of N-WASP and WASP in various cell lines. WASP is expressed only in platelets.

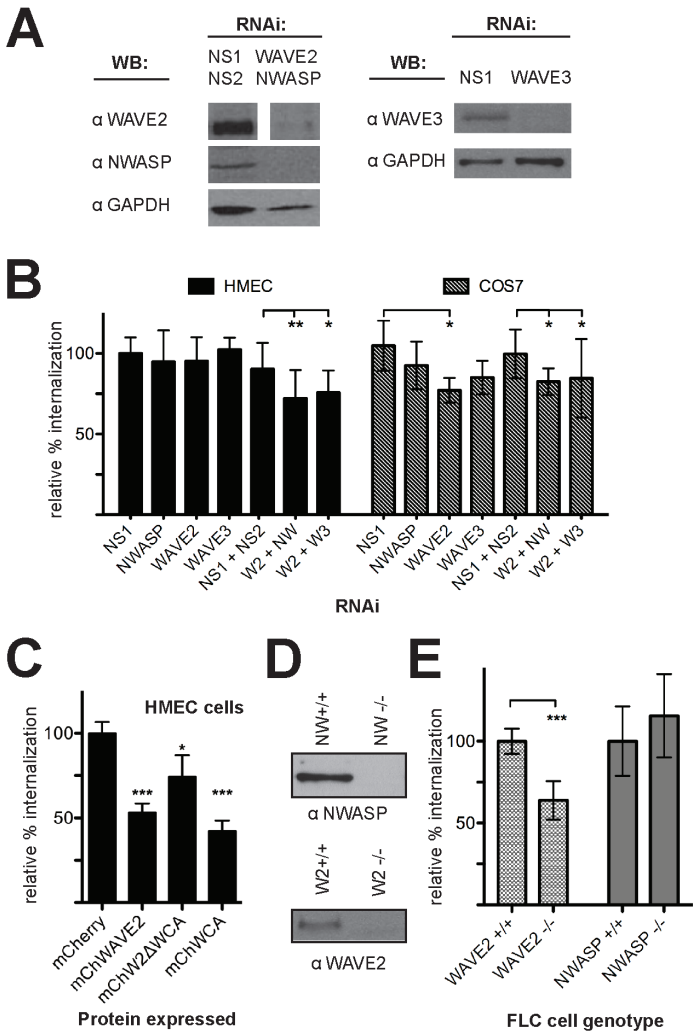

Figure 2.8. Depletion, overexpression or genetic deletion of WAVE2 reduces *R. parkeri* invasion of mammalian cells. (A) Western blots of HMEC-1 cell lysates 48 h post-transfection with the indicated siRNAs, corresponding to one experiment represented in (C). COS-7 Western blots are shown in Figure S2B. **(B)** Relative percent internalization at 15 min post-infection with *R. parkeri* following RNAi of the indicated targets in HMEC-1 (solid bars) or COS-7 cells (hashed bars). **(C)** Relative percent internalization at 15 min post-infection with *R. parkeri* in HMEC-1 cells visibly expressing the indicated proteins. **(D)** Western blots of cell lysates collected from FLC cells showing a lack of expression of N-WASP (top) or WAVE2 (bottom). **(E)** Relative percent internalization at 2 h post-infection with *R. parkeri* in FLC cells with a genetic deletion of WAVE2 or N-WASP. Data represent the mean of at least three independent experiments and were normalized using (B) nonspecific-RNA transfected HMEC-1 cells, (C) mCherry-expressing HMEC-1 cells, or (D) sibling control cells for each deletion line. Abbreviations: NS1, nonspecific control RNA 1; NS2, nonspecific control RNA 2; W2, WAVE2; NW, N-WASP; W3, WAVE3. Error bars indicate SD. * $p<0.05$, ** $p<0.01$, *** $p<0.001$ versus indicated control values by unpaired t-test.

expressing fusion proteins. Expression of either the full-length WAVE2 protein or the C-terminal WCA domain reduced invasion of *R. parkeri* by 50-60% compared with mCherry alone (Figure 2.8C). Interestingly, expression of the WAVE2 N-terminus also reduced invasion by 25% (Figure 2.8C). Binding was not significantly affected by expression of any WAVE derivatives (Figure 2.9A). The dominant negative effect of full-length WAVE2 expression on *Rickettsia* invasion was previously assumed to be due to excess C-terminal WCA domain inhibiting the Arp2/3 complex (Machesky *et al.*, 1998; Magdalena *et al.*, 2003). Our results indicate that inhibition may also involve the N-terminal domain of WAVE binding to and disrupting upstream interacting proteins such as Rac1 (Miki *et al.*, 1998), Abi, or HSPC300 (Shi *et al.*, 2005).

To definitively clarify the roles of WAVE2 or N-WASP during *R. parkeri* invasion of mammalian cells, we measured invasion in mouse embryonic fibroblast-like cell lines (FLC) genetically deficient in each protein. FLC cells deficient for WAVE2 (Yan *et al.*, 2003) or N-WASP (Snapper *et al.*, 2001), along with matched control cells, were infected with *R. parkeri* for 2 h and bacterial internalization and binding were quantified. Absence of NPF expression was confirmed by immunoblotting (Figure 2.8D). WAVE2 knockout cell lines had 40% fewer internalized bacteria than control cells, while there was no significant difference between N-WASP-deleted cell lines and controls (Figure 2.8E). Genetic deletion of WAVE2 or N-WASP did not significantly affect bacterial binding (Figure 2.9B). Therefore, similar to HMEC-1 cells, WAVE2 is important during invasion of murine fibroblasts and N-WASP is dispensable. Overall, these results suggest that N-WASP is not crucial for *R. parkeri* entry, and that WAVE2 is important, with the extent of the requirement depending on the cell type being infected.

The host Arp2/3 complex is recruited by **R. parkeri** *and is required for invasion*

The results of our RNAi screen in S2R+ cells, along with the involvement of Rac1 and the WAVE family proteins in mammalian cells, strongly suggested a role for the Arp2/3 complex during invasion of mammalian cells by *R. parkeri.* Indeed, we observed robust localization of Arp3 protein around *R. parkeri* invading HMEC-1 cells (Figure 2.10A) and COS-7 cells (Figure 2.11) at 5-15 min post-infection. On average, Arp2/3 complex was associated with a higher proportion of invading *Rickettsia* than was actin (Figure 2.10B), suggesting that the Arp2/3 complex is recruited before F-actin is polymerized around entering bacteria.
To investigate the functional importance of the Arp2/3 complex during bacterial invasion, HMEC-1 and COS-7 cells were transfected with two siRNAs targeting the Arp3 and ARPC4 subunits, which were previously shown to deplete the entire complex (Campellone *et al.*, 2008), or with control siRNAs, and silencing was confirmed using immunoblotting (Figure 2.10C, Figure 2.5B). Fifteen min after invasion, an average of 45% fewer intracellular bacteria were observed in Arp3/ARPC4-depleted cells (Figure 2.10D) while bacterial binding was unaffected (Figure 2.6). This invasion defect persisted through 30-60 min post-infection in COS-7 cells (Figure 2.4F). To further confirm the requirement for Arp2/3 complex activity, HMEC-1 or COS-7 cells were treated for 30 min with either a specific chemical inhibitor of the Arp2/3 complex, CK-548 (Nolen *et al.*, 2009), or with DMSO as a control, and were infected with *R. parkeri* in the presence of the inhibitor. Chemical inhibition of the Arp2/3 complex resulted in approximately 55% fewer intracellular bacteria (Figure 2.10D) and decreased bacterial binding (Figure 2.2B).

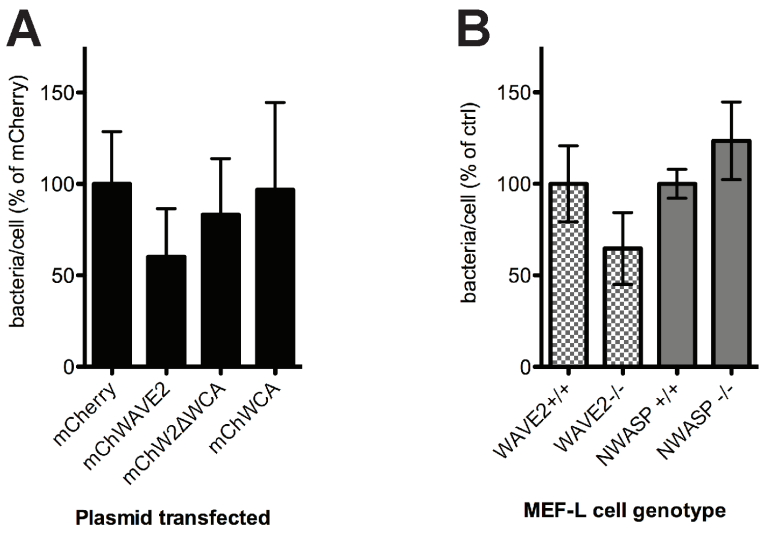

Figure 2.9 – Binding of *R. parkeri* to host cells is not affected by absence or overexpression of WAVE2. (A) Percentage of bacteria associated with each host cell, relative to mCherry control, in HMEC cells transfected with plasmids expressing the indicated proteins. **(B)** Percentage of bacteria associated with each host cell, relative to sibling control cells, in MEF-L cells genetically lacking WAVE2 or NWASP. Data are the mean of three independent experiments and were normalized with the average of control cells set as 100%. Error bars, SEM.

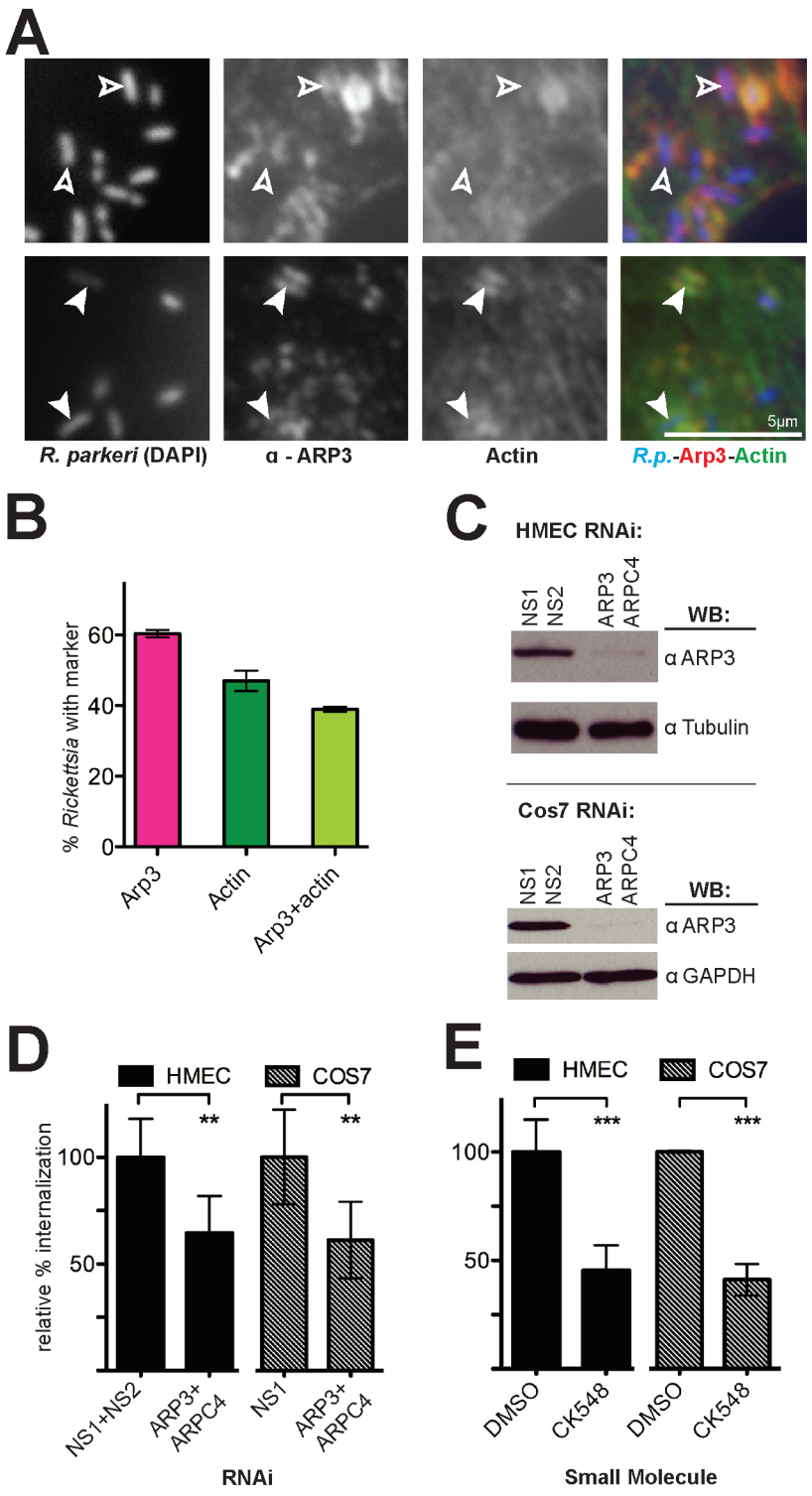

Figure 2.10. The Arp2/3 complex is recruited to invading *R. parkeri* and is required for efficient invasion. **(A)** Bacteria (left, stained with DAPI, blue in merge) are surrounded by Arp3 (middle, anti-Arp3 immunofluorescence, red in merge) and actin (right, anti-RFP immunofluorescence of Lifeact-mCherry, green in merge). Open arrowheads indicate *R. parkeri*

associated with Arp3 protein only, filled arrowheads indicate *R. parkeri* surrounded by both actin and Arp3. **(B)** Percentage of *Rickettsia* associated with Arp3 and actin. Pink, mean association with Arp3; dark green, mean association with actin; light green, subset of cells associated with both Arp3 and actin. For (A-B), HMEC-1 cells were transfected with pLifeact-mCherry for 48 h before infection and fixed 10 min post-infection. **(C)** Western blots of HMEC-1 and COS-7 cell lysates at 48 h post-transfection with the indicated siRNAs, corresponding to one experiment represented in (D). **(D)** Relative percent internalization at 15 min post-infection with *R. parkeri* in either HMEC-1 (solid bars) or COS-7 (hashed bars) cells. **(E)** Relative percent internalization at 15 min post-infection with *R. parkeri* within HMEC-1 or COS-7 cells treated for 30 min prior to infection with either 1% DMSO or 100 μM CK548. (D-E) are the mean of at least three independent experiments and were normalized with nonspecific-RNA transfected cells (D) or DMSO-treated COS-7 cells (E) set as 100%. Abbreviations: NS1, nonspecific control RNA 1; NS2, nonspecific control RNA 2; ** $p<0.01$, *** $p<0.001$, versus indicated control values by unpaired Student's t-test.

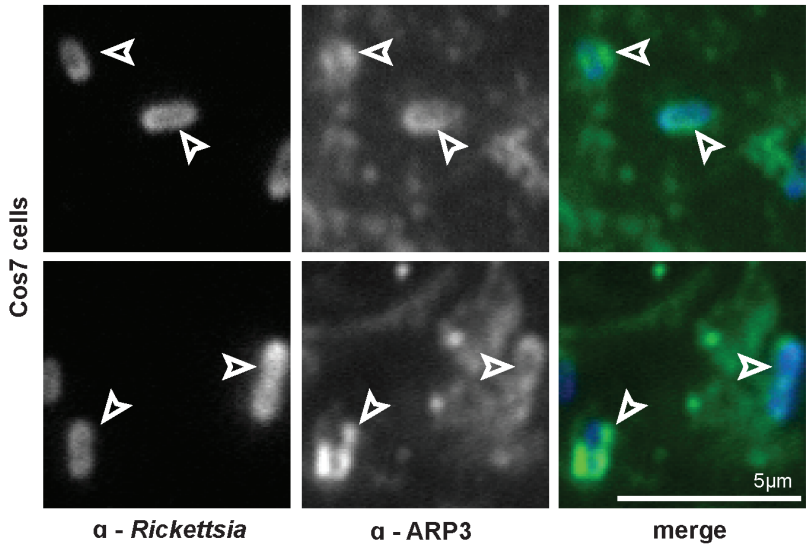

Figure 2.11 – Arp3 is recruited surrounding bacteria invading COS-7 cells.
(A) COS-7 cells infected for 7 min with *R. parkeri*, fixed and stained with anti-*Rickettsia* antibody to visualize bacteria (left, blue in merge), and anti-Arp3 antibody (center, green in merge). Open arrowheads indicate bacteria associated with Arp3 protein.

The inhibition of entry in cells after Arp2/3 complex inactivation or depletion indicates that the complex is a major nucleator of F-actin around entering *Rickettsia* in mammalian cells.

DISCUSSION

As an obligate intracellular pathogen, *Rickettsia parkeri* must invade host cells to survive. Here, we identify core host factors responsible for actin polymerization during invasion of both arthropod and mammalian cells. During invasion, actin is nucleated primarily by the Arp2/3 complex, which is likely activated by a WAVE-dependent and WASP/N-WASP-independent pathway that is in turn controlled by the Rho-family GTPases Rac and Cdc42. Our results reveal differences between actin regulation in arthropod versus mammalian cells due to either different levels of redundancy in the core pathway or to the existence of alternative pathways for polymerizing actin.

We began with an RNAi-based screen in *Drosophila* S2R+ cells that focused on identifying which of ~100 proteins previously shown to be important for actin polymerization, organization and regulation (Rogers *et al.*, 2003) played a role in *R. parkeri* invasion. Our results identified 21 proteins, which include an actin nucleating complex and its regulators, as well as actin organizing and binding proteins likely to contribute to actin network stability (Figure 2.12). A subset of these 21 proteins was also identified in a previous screen for cytoskeletal proteins involved in *Rickettsia* actin tail formation and infection (Serio *et al.*, 2010), indicating that defects in invasion may perturb later steps in the *Rickettsia* life cycle. One question that arises from our work is, what upstream signaling pathways regulate actin cytoskeletal proteins during invasion? Multiple *Rickettsia* outer-membrane autotransporter proteins mediate adherence to host cells and bind to receptors including Ku70 (Chan *et al.*, 2009; Martinez *et al.*, 2005; silencing Ku70 caused a modest but significant defect in invasion of S2R+ cells; Appendix 1). Downstream of receptor engagement, a general inhibitor of tyrosine kinase activity blocks *Rickettsia* invasion of *Drosophila* and mammalian cells (Martinez *et al.*, 2004; this study), but our results did not implicate any individual tyrosine kinases. This suggests that multiple tyrosine kinase signaling pathways converge to activate Rho-family GTPases during *Rickettsia* invasion of host cells.

R. parkeri invasion of both *Drosophila* and mammalian cells was sensitive to depletion of the Rho GTPases Rac or Cdc42, or the combined depletion of both.
Cdc42 was initially thought to activate WASP-dependent filopodia extension while Rac1 and Rac2 activate WAVE-dependent lamellipodia formation (Hall, 1998; Miki *et al.*, 1998), but more recent findings indicate that both GTPases can contribute to lamellipodia formation in *Drosophila* (Rogers *et al.*, 2003) and mammalian cells (Kurokawa *et al.*, 2004). Moreover, Rac1, Rac2 and/or Cdc42 have been previously identified as important for the invasion of S2R+ cells by several pathogens in RNAi screens (Agaisse *et al.*, 2005; Elwell *et al.*, 2008; Serio *et al.*, 2010; Stroschein-Stevenson *et al.*, 2005). Only Cdc42 was previously implicated in a *R. conorii* invasion of Vero cells (Martinez *et al.*, 2004), in a study making use of dominant-negative Rho GTPase mutants.

Because expression of mutant proteins may cause more severe phenotypes than knockdown of the same proteins (Pertz, 2010) and may inhibit GEFs for both GTPases (Ladwein *et al.*, 2008; Pertz, 2010; Rabiet *et al.*, 2002), an RNAi approach provides a clearer picture of specific GTPase requirements for *Rickettsia* invasion. Interestingly, we observed a varying

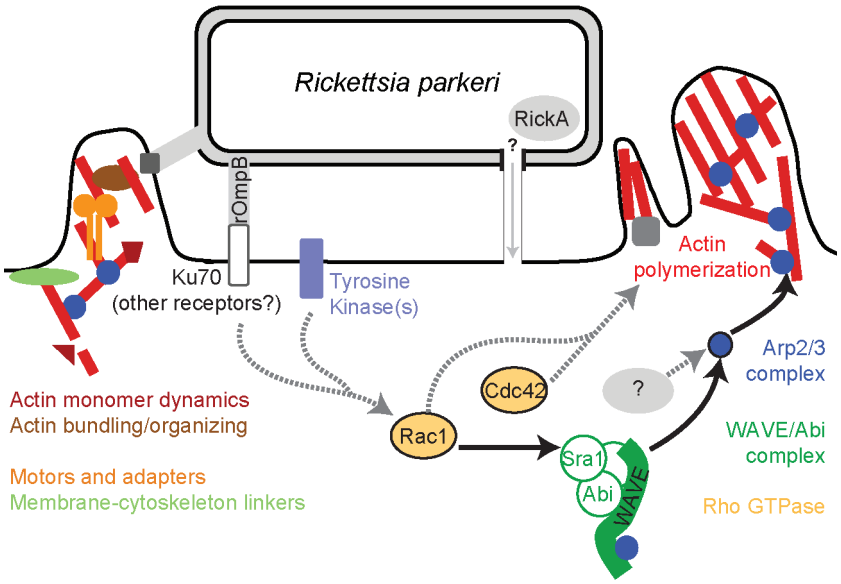

Figure 2.12. Model of host pathways activated during *Rickettsia* invasion. Multiple pathways are likely to be activated during *R. parkeri* invasion of host cells. Solid arrows and colored proteins were identified in this work, while grey proteins and dashed arrows indicate potential pathways suggested from previous work.

phenotype after RNAi targeting Rac1, Rac2 and Cdc42, depending on the cell line. Thus, during *R. parkeri* invasion of host cells, we propose a model where the Rho GTPases cooperatively promote actin polymerization, with Cdc42 and Rac1 playing parallel roles (Figure 2.12). We also observed a strong inhibition of *R. parkeri* invasion after RNAi silencing of WAVE and WAVE-interacting proteins in *Drosophila* S2R+ cells, whereas depletion of WASP had no discernible effect. WAVE and Abi1 were shown to be required for both lamellipodia and filopodia formation and were identified in all previous RNAi-based screens for pathogen invasion in S2R+ cells (Table 2.1), while WASP is important for only *P. aeruginosa* invasion (Pielage *et al.*, 2008) and is not required for the formation of cellular protrusions (Biyasheva *et al.*, 2004; Rogers *et al.*, 2003). We conclude that WAVE is required for actin-dependent cell surface remodeling in S2R+ cells, especially during the invasion of intracellular pathogens including *R. parkeri* (Figure 2.12).

We found that *R. parkeri* invasion of a variety of mammalian cell lines was reduced when WAVE2 was depleted, overexpressed or genetically deleted. On the other hand, our data do not support the previously suggested role for N-WASP (Martinez *et al.*, 2004), nor do they support a role for other host NPFs. Thus, of the many host NPF proteins, only WAVE is important for *R. parkeri* invasion of cell lines from diverse species (Figure 2.12). WAVE2 and WAVE3 have been previously implicated in lamellipodia formation, cell migration, and the invasion of mammalian cells by *Chlamydia* and *Salmonella*, indicating that their function in membrane remodeling and pathogen invasion is conserved (Carabeo *et al.*, 2007; Shi *et al.*, 2005; Yamazaki *et al.*, 2003). Interestingly, the combined depletion of WAVE2 and WAVE3 or WAVE2 and N-WASP caused a more modest decrease in *R. parkeri* invasion in HMEC-1 or COS-7 cells than that observed after WAVE depletion in S2R+ cells, suggesting that other host or bacterial proteins may provide an additional degree of redundancy in mammalian cells.

Downstream of the WAVE complex, our results clearly indicate that depletion, inhibition, or sequestration of the Arp2/3 complex strongly inhibits *R. parkeri* invasion of both *Drosophila* and mammalian cells, implying that upstream pathways that stimulate actin nucleation converge on the Arp2/3 complex. This is consistent with our observation that invasion of S2R+ cells was not significantly affected by RNAi silencing of other actin nucleators. Although a recent report demonstrated that *Salmonella enterica* Typhimurium invades cells via both Arp2/3- and Rho/Myosin II-mediated pathways (Hänisch *et al.*, 2011), and we observed reduced invasion of *Drosophila* cells after Myosin II depletion, treatment of *Drosophila* and mammalian cells with the Myosin II inhibitor blebbistatin had no effect on invasion, suggesting that *R. parkeri* invasion can occur independently of Myosin II. Invasion of S2R+ cells by *L. monocytogenes, Candida albicans, E. coli, C. trachomatis,* and *P. aeruginosa* is also reduced by knockdown of Arp2/3 complex subunits (Agaisse *et al.*, 2005; Elwell *et al.*, 2008; Pielage *et al.*, 2008; Stroschein-Stevenson *et al.*, 2005). Likewise, the Arp2/3 complex is important for invasion of non-phagocytic mammalian cells by *Yersinia pseudotuberculosis*, *L. monocytogenes, S. enterica* Typhimurium and *C. trachomatis* (Alrutz *et al.*, 2001; Carabeo *et al.*, 2007; Hybiske *et al.*, 2007; Sousa *et al.*, 2007; Unsworth *et al.*, 2004). Thus *Rickettsia*, like other pathogens, primarily utilize Arp2/3-dependent actin nucleation during invasion of host cells.

The robust nature of invasion in mammalian cells following knockdown or inhibition of individual Arp2/3 complex activators suggests that Arp2/3 is activated via redundant pathways. Depletion of multiple Rho family GTPases or NPFs also caused a more modest inhibition of invasion compared with depletion or inhibition of the Arp2/3 complex. Thus it is likely that Arp2/3 activation occurs independently of WAVE and Rac1. Another host NPF

protein could activate Arp2/3, although our results do not support this notion. A second possibility is that a bacterial protein directly activates the Arp2/3 complex during invasion. SFG *Rickettsia* possess an Arp2/3 activating protein, RickA (Gouin *et al.*, 2004; Jeng *et al.*, 2004), that is a candidate for promoting actin assembly during invasion (Figure 2.12). However, it remains to be determined whether RickA is secreted into the host cell during this process.

Integrating our data from *Drosophila* and mammalian cells with previously published research suggests a model for the initiation of actin assembly during *Rickettsia* invasion (Figure 2.12). Receptor binding by *Rickettsia* proteins initiates activation of host protein tyrosine kinases, leading to Cdc42 activation and Rac-dependent activation of WAVE, which may act in parallel with other NPFs to activate Arp2/3. Finally, the Arp2/3 complex acts as the major nucleator of actin filaments during *Rickettsia* invasion of host cells. Our work provides a framework for further exploration of the host factors required for invasion of host cells by rickettsiae. It will be interesting to determine whether the molecular pathways identified in *Drosophila* cells are also critical for infection of cells in *Rickettsia* vectors such as ticks and fleas. The robust nature of *Rickettsia* invasion is probably due to a combination of redundant host pathways available for actin polymerization and the action of multiple bacterial proteins on these pathways, a common strategy of intracellular pathogens to ensure efficient uptake by a host cell. Future work will define the relative contribution of bacterial and host proteins to actin assembly during invasion.

MATERIALS AND METHODS

Antibodies

Antibodies were obtained from the following sources (in parentheses): mouse anti-*Dm*-profilin (developed by L. Cooley at Yale School of Medicine, maintained by the Developmental Studies Hybridoma Bank [DSHB] at the University of Iowa); rat anti-*Dm*-Arp3 (L. Cooley; Hudson *et al.*, 2002); guinea pig anti-*Dm*-SCAR (J. Zallen, Sloan-Kettering Institute; Zallen *et al.*, 2002); anti-*Dm*-WASP (G. Borisy, Northwestern University Medical School; Biyasheva *et al.*, 2004), mouse anti-GAPDH (Ambion); mouse anti-tubulin (developed by M. Klymkowsky at the University of Colorado, Boulder, maintained by the DSHB); mouse anti-RFP ab65856 (Abcam); rabbit anti-Arp3 (Welch *et al.*, 1997a); rabbit anti-ARPC2(p34) (Welch *et al.*, 1997b); rabbit anti-WAVE2 (T. Takenawa, University of Tokyo; Yamazaki *et al.*, 2003); goat anti-WAVE1 (sc-10390) and rabbit anti-WAVE2 (sc-33548) (Santa Cruz Biotechnology); rabbit anti-WAVE3 (09-145) (Millipore); guinea pig anti-N-WASP (Duleh *et al.*, 2010); mouse anti-Rac1 (ARC03) and anti-Cdc42 (ACD03) (Cytoskeleton), rabbit anti-Rac2 (sc-96) (Santa Cruz Biotechnology); mouse anti-*Rickettsia* M14-13 and rabbit anti-*Rickettsia* R4668 and I7205 (T. Hackstadt, NIH/NIAID Rocky Mountain Laboratories; Anacker *et al.*, 1987; Policastro *et al.*, 1997); rabbit polyclonal anti-*Listeria* O antibody (BD Biosciences); horseradish peroxidase conjugated anti-mouse, rabbit and guinea pig secondary antibodies for immunoblotting (GE Healthcare); AlexaFluor 488-, 568-, and AMCA-conjugated anti-rabbit and anti-mouse secondary antibodies for immunofluorescence (Invitrogen Molecular Probes). Abbreviation: *Dm, Drosophila melanogaster.*

Plasmids

To generate the plasmid pLifeact-mCherry, the eGFP-encoding region of a Lifeact-GFP expression plasmid derived from pEGFP-N1 (Clontech) (Serio *et al.*, 2010) was removed and replaced with PCR-amplified DNA encoding mCherry, resulting in a plasmid expressing the Lifeact peptide (Riedl *et al.*, 2008) fused to the N-terminus of mCherry. The plasmid pmCherry was constructed similarly by replacing eGFP in the vector pEGFP-C1 (Clontech). For WAVE2 expression plasmids, DNA encoding full-length *Mus musculus* WAVE2 (amino acids M1-D497), the WAVE2 WCA region (amino acids T423-D497), or WAVE2ΔWCA (amino acids M1-L429) were excised from GFP-fusion expression plasmids (K. Campellone, University of California, Berkeley) and cloned into the KpnI and XbaI sites of pmCherry. The eGFP-Rac1 plasmid (Subauste *et al.*, 2000; Addgene plasmid 12980) was a gift from G. Bokoch via addgene.org. The PAK1-PBD-mCherry expression plasmid, with *Homo sapiens* PAK1 amino acids N65-S149 fused to mCherry, was a gift from O. Weiner (University of California, San Francisco). *Rickettsia* insertional mutagenesis plasmid PMW1650 was a gift from D. Wood (University of South Alabama; Liu *et al.*, 2007).

Bacterial strains, growth and purification

Rickettsia parkeri Portsmouth strain was a gift from C. Paddock (Centers for Disease Control and Prevention, Atlanta). *Listeria monocytogenes* strain 10403S was a gift from D. Portnoy (University of California, Berkeley). *E. coli* strain XL-10 Gold was from Stratagene.

GFP-expressing *R. parkeri* clonal strain GFP_{UV}-3 was generated by electroporating *R. parkeri* suspended in 100 µl 250 mM sucrose with 20 µg of plasmid PMW1650 at 2.5 kV, 200 ohms, 25 µF, for 5 ms using a Gene Pulser Xcell (Bio-Rad). Bacteria were immediately suspended in 500 µl Brain Heart Infusion (BHI) media (Difco), and used to infect a 25 cm^2 flask of Vero cells. Cells were grown overnight at 34°C, 5% CO_2 in DMEM with 2% FBS, and after 24 h media was replaced with media containing 200 ng/ml rifampicin (Sigma). After 6 d, plaques were visible in the cell monolayer. The resulting polyclonal stock was collected, amplified and plaque purified to yield a clonal strain. The insertion site of the transposon cassette was determined essentially as described previously (Liu *et al.*, 2007). Briefly, genomic DNA from *R. parkeri* was digested with HindIII, the restriction enzyme was heat-inactivated, and the DNA fragments were self-ligated. *E. coli* were transformed with the resulting plasmids, and selected for resistance to 100 µg/ml rifampicin. The insertion sites were sequenced using primers 5'-CGCCACCTCTGACTTGAGCGTCG and 5'-CCATATGAAAACACTCCAAAAAAC and found to be in a position corresponding to nucleotides 13,843-13,846 of the *R. rickettsii* Sheila Smith strain (Ellison *et al.*, 2008) in the gene encoding hypothetical protein A1G_00085.

For all other procedures, *R. parkeri* was propagated in Vero cells grown at 33°C with 5% CO_2, purified by Renografin density gradient centrifugation as described previously (Hackstadt *et al.*, 1992), and stored at -80º C. For same-day purification of GFP-expressing *R. parkeri*, infected monolayers of Vero cells were scraped from culture flasks, pelleted by centrifugation, resuspended in K-36 buffer (0.05 M KH_2PO_4, 0.05 M K_2HPO_4, 0.1 M KCl, 0.015 M NaCl, pH 7) and dounced to release intracellular *R. parkeri*. Cell suspensions were centrifuged to remove nuclei and cell debris, and aliquots from the supernatant were centrifuged at 16000 *g* for 5 min to pellet *R. parkeri*, then resuspended in the appropriate culture medium and added to cells for infection and visualization. *L. monocytogenes* was grown in liquid Brain Heart Infusion (BHI; Difco) at 37°C without agitation. *E. coli* strain XL-10 Gold was grown in Luria Broth (LB) at 37°C with agitation.

Cell growth and bacterial infection

Drosophila S2R$^+$ cells were a gift from R. Tjian (University of California, Berkeley), and were grown at 28°C in M3 Shields and Sang media (Sigma), supplemented with 0.5 g/L $KHCO_3$, 1 g/L yeast extract (Biotech Sources LLC), 2.5 g/L meat peptone extract (Merck) and 10% FBS (Invitrogen). African green monkey kidney fibroblast cells (COS-7) and epithelial cells (Vero) were from the University of California, Berkeley tissue culture facility, and were grown at 37°C with 5% CO_2 in DMEM (Invitrogen) with 2-10% FBS (JR Scientific). Mouse embryonic fibroblast-like cells with genetic deletions of WAVE2 (Yan *et al.*, 2003) or N-WASP (Snapper *et al.*, 2001) and matched control cells were a gift from S. Snapper (Harvard Medical School). The human microvascular endothelial cell line HMEC-1 (Ades *et al.*, 1992) was obtained via material transfer agreement from the Centers for Disease Control, Biological Products Branch, and was grown at 37°C with 5% CO_2 in MCDB 131 (Invitrogen) with 10% FBS (Hyclone), 2 mM L-Glutamine (Gibco), 10 ng/mL Epidermal Growth Factor (BD Biosciences), and 1 µg/mL Hydrocortisone (Sigma).

To measure invasion, bacterial infections were carried out as follows: cells were seeded onto glass coverslips in 24-well plates 4 d (S2R+ cells) or 24 h (mammalian cells) prior to infection. For most experiments, culture medium was removed and replaced with 0.5 mL ice-cold growth media, and bacteria were added to each well (*R. parkeri* at a final MOI of 1-5 or ~$5x10^5$ pfu/well, *L. monocytogenes* and *E. coli* at an MOI of 5-10). Infected cells were then centrifuged at 200 *g* for 5 min at 4ºC, followed by addition of 0.5 mL of 37ºC media per well. Cells were incubated at 28ºC (S2R+) or 37ºC (HMEC-1, COS-7) for the remainder of infection times. For drug treatments, colocalization and live-cell imaging, infections were carried out in culture medium at 37ºC or 28ºC (S2R+) without replacement and centrifuge steps were at room temperature. Drugs were diluted in culture medium in 1% DMSO for a final concentration of 250 µM genistein (Sigma), 4 µM latrunculin A, 20 µM nocodazole, 100 µM CK-666 (all three from EMD Chemicals), 100 µM CK-548 (CK-0993548, from Cytokinetics), 200 nM wortmannin, 250 nM dasatinib, 500 nM nilotinib (all three from LC Laboratories), 1 µM PP2, 5 µM wiskostatin, and 1µM AAL-993 (all three from Biomol International) and cells were treated with drugs for 30 min prior to infection.

RNA synthesis and RNAi screening

Primers for PCR amplification of target genes from *Drosophila* genomic DNA were derived from those published by Rogers *et al.* (Rogers *et al.*, 2003) or from the *Drosophila* RNAi Screening Center (http://flyrnai.org), and amplification and reverse transcription were performed as described previously (Serio *et al.*, 2010). For RNAi screening, monolayers of S2R+ cells on 12-mm coverslips were treated with dsRNA at a final concentration of 20 µg/ml for 4 d, and then infected with *R. parkeri* for 15 min to allow for invasion, as described above. Cells were fixed and processed for the fluorescence internalization assay, as described below. The number of intracellular and extracellular bacteria was counted in at least 5 fields of view, with >200 bacteria counted on each coverslip. At least three replicates of RNAi and infection were performed for each individual target or control. The percent internalization was calculated and the value for each target was compared pairwise with the untreated control by the Student's t-test using Prism v5.0 (Graphpad Software). For normalized data, the mean of three no-RNA control coverslips for each day's experiment was set as 1.0 and other data was transformed relative to the mean. Differences were considered to be significant if $p \leq 0.01$.

Immunoblotting and immunofluorescence staining

For immunoblotting, cells were lysed in RIPA buffer (50 mM Tris pH 7.6, 150 mM NaCl, 1 mM EDTA, 1% Triton X-100, 0.1% SDS plus 10 mg/ml of aprotinin, leupeptin, pepstatin, and chymostatin, and 1 mM PMSF) or in Laemmli sample buffer. Equal molar amounts of protein were separated by SDS-PAGE and transferred to nitrocellulose. Membranes were blocked with 5% milk in phosphate buffered saline (PBS), probed with primary followed by secondary antibodies, and visualized with ECL detection reagents (GE Healthcare). For detection of Rac1, Rac2 and Cdc42, proteins were separated using 4-20% TGX polyacrylamide gels and blotted to Immun-blot PVDF membranes (both from Bio-Rad). Membranes were dried completely before blocking and probing with primary and secondary antibodies as described above.

For immunofluorescence staining, cells were fixed with 2.5% formaldehyde in PBS at room temperature for 15 min or using –20˚C Cytoskelfix (Cytoskeleton) for 5 min. Antibodies were diluted in PBS with 2% bovine serum albumin (BSA) (anti-Arp3 and anti-RFP, 1:100; anti-*Rickettsia* 14-13, 1:200) and antibody staining steps were carried out at room temperature using standard procedures. For anti-Arp3 staining, coverslips were blocked in PBS + 2% BSA + 2% dry milk for 30 min prior to staining.

For fluorescence internalization assays, coverslips were incubated with primary antibodies against bacteria followed by AMCA or Alexa 488-conjugated secondary antibodies. Cells were permeabilized in PBS with 0.5% Triton X-100 for 5 min, rinsed, and again incubated with primary antibodies against *R. parkeri* or *Listeria* followed by Alexa 568-conjugated secondary antibodies, or *E. coli* were stained using DAPI. To visualize actin, 4 U/µl of Alexa 488 or 568-conjugated phalloidin (Invitrogen) was included with the secondary antibody. Coverslips were mounted with Prolong Gold anti-fade (Invitrogen) and stored at 4°C.

Transfection and RNAi in mammalian cells

For expression of mCherry/GFP-tagged proteins, 50-250 ng of plasmid DNA was transiently transfected into cells using Lipofectamine 2000 (Invitrogen), according to the manufacturer's instructions. For gene silencing, siRNAs (Ambion) were transfected at a final concentration of 50 nM (COS-7 cells) or 20 nM (HMEC-1 cells) using Lipofectamine-RNAi-MAX (Invitrogen), according to the manufacturer's instructions. At 24 h post-transfection, cells were reseeded from 6-well culture plates to 24-well plates containing glass coverslips and parallel 6-well plates for protein lysate collection. At 48 h post-transfection, cells were infected with *R. parkeri* and processed for immunofluorescence microscopy, and uninfected cell lysates were collected for immunoblotting, as described above. For RNA/DNA cotransfections, siRNAs were transfected with RNAiMAX, and siRNA and plasmid DNA were transfected 24h later with Lipofectamine 2000. Cells were reseeded at 48h and infections were carried out at 72h post-transfection. For RNAi-internalization assays, the number of intracellular and extracellular bacteria were counted in at least 5 fields of view, with >200 bacteria counted on each of 2-3 coverslips. An average of ~1000 (301-2562) *Rickettsia* per experiment were scored for protein recruitment in ≥20 cells from 2-3 coverslips.

Imaging

Images were captured using an Olympus IX71 microscope equipped with a 100X (1.35 NA) PlanApo objective lens and a Photometrics CoolSNAP HQ camera. Fixed and live-cell

images were captured in the TIFF 16-bit format using MetaMorph software (Molecular Devices) or Micro-Manager Software (http://www.micro-manager.org). Following image acquisition, Adobe Photoshop was used to convert to 8-bit images, brightness/contrast levels were adjusted, and images were cropped. For *Listeria* and *E. coli* internalization assays, WAVE-fusion internalization assays and colocalization quantitation, images were imported into ImageJ and counted using the Cell Counter plugin (http://rsbweb.nih.gov/ij/plugins/cell-counter.html). For live-cell experiments, cells were plated on glass-bottomed 24-well culture dishes (MatTek) and transfected with Lifeact-mCherry or PAK1-PBD-mCherry plasmids 48 h before infection with freshly prepared GFP-expressing *R. parkeri* at room temperature. Movies were assembled and adjusted using ImageJ and Adobe Photoshop. Deconvolution images were taken using an Applied Precision DeltaVision 4 Spectris microscope with a 100X (1.4 NA) PlanApo objective equipped with a Photometrics CH350 CCD camera. Images were captured using SoftWoRx v3.3.6 software (Applied Precision), deconvolved with Huygens Professional v3.1.0p0 software (Scientific Volume Imaging), and processed using Imaris (Bitplane).

REFERENCES

Ades, E.W., Candal, F.J., Swerlick, R.A., George, V.G., Summers, S., Bosse, D.C. and Lawley, T.J. (1992). HMEC-1: Establishment of an Immortalized Human Microvascular Endothelial Cell Line. *J Investig Dermatol* **99,** 683-690.

Agaisse, H., Burrack, L.S., Philips, J.A., Rubin, E.J., Perrimon, N. and Higgins, D.E. (2005). Genome-wide RNAi screen for host factors required for intracellular bacterial infection. *Science* **309,** 1248-1251.

Alrutz, M.A., Srivastava, A., Wong, K.-W., D'Souza-Schorey, C., Tang, M., Ch'ng, L.-E*., et al.* (2001). Efficient uptake of Yersinia pseudotuberculosis via integrin receptors involves a Rac1-Arp 2/3 pathway that bypasses N-WASP function. *Molecular Microbiology* **42,** 689-703.

Anacker, R.L., Mann, R.E. and Gonzales, C. (1987). Reactivity of monoclonal antibodies to Rickettsia rickettsii with spotted fever and typhus group rickettsiae. *Journal of Clinical Microbiology* **25,** 167-171.

Biyasheva, A., Svitkina, T., Kunda, P., Baum, B. and Borisy, G. (2004). Cascade pathway of filopodia formation downstream of SCAR. *Journal of Cell Science* **117,** 837-848.

Campellone, K.G., Webb, N.J., Znameroski, E.A. and Welch, M.D. (2008). WHAMM Is an Arp2/3 Complex Activator That Binds Microtubules and Functions in ER to Golgi Transport. *Cell* **134,** 148-161.

Campellone, K.G. and Welch, M.D. (2010). A nucleator arms race: cellular control of actin assembly. *Nat Rev Mol Cell Biol* **11,** 237-251.

Carabeo, R.A., Dooley, C.A., Grieshaber, S.S. and Hackstadt, T. (2007). Rac interacts with Abi-1 and WAVE2 to promote an Arp2/3-dependent actin recruitment during chlamydial invasion. *Cellular Microbiology* **9,** 2278-2288.

Cardwell, M.M. and Martinez, J.J. (2009). The Sca2 Autotransporter Protein from *Rickettsia conorii* Is Sufficient To Mediate Adherence to and Invasion of Cultured Mammalian Cells. *Infection and Immunity* **77,** 5272-5280.

Chan, Y.G.Y., Cardwell, M.M., Hermanas, T.M., Uchiyama, T. and Martinez, J.J. (2009). Rickettsial outer-membrane protein B (rOmpB) mediates bacterial invasion through Ku70 in an actin, c-Cbl, clathrin and caveolin 2-dependent manner. *Cellular Microbiology* **11,** 629-644.

Chenette, E.J., Mitin, N.Y. and Der, C.J. (2006). Multiple Sequence Elements Facilitate Chp Rho GTPase Subcellular Location, Membrane Association, and Transforming Activity. *Mol. Biol. Cell* **17,** 3108-3121.

Cossart, P. and Sansonetti, P.J. (2004). Bacterial Invasion: The Paradigms of Enteroinvasive Pathogens. *Science* **304,** 242-248.

Duleh, S.N. and Welch, M.D. (2010). WASH and the Arp2/3 complex regulate endosome shape and trafficking. *Cytoskeleton* **67,** 193-206.

Ellison, D.W., Clark, T.R., Sturdevant, D.E., Virtaneva, K., Porcella, S.F. and Hackstadt, T. (2008). Genomic Comparison of Virulent Rickettsia rickettsii Sheila Smith and Avirulent *Rickettsia rickettsii* Iowa. *Infect. Immun.* **76,** 542-550.

Elwell, C.A., Ceesay, A., Kim, J.H., Kalman, D. and Engel, J.N. (2008). RNA Interference Screen Identifies Abl Kinase and PDGFR Signaling in *Chlamydia trachomatis* Entry. *PLoS Pathogens* **4,** e1000021.

Gillespie, J.J., Ammerman, N.C., Dreher-Lesnick, S.M., Rahman, M.S., Worley, M.J., Setubal, J.C.*, et al.* (2009). An Anomalous Type IV Secretion System in *Rickettsia* Is Evolutionarily Conserved. *PLoS ONE* **4,** e4833.

Gouin, E., Egile, C., Dehoux, P., Villiers, V., Adams, J., Gertler, F.*, et al.* (2004). The RickA protein of Rickettsia conorii activates the Arp2/3 complex. *Nature* **427,** 457-461.

Greiffenberg, L., Goebel, W., Kim, K.S., Weiglein, I., Bubert, A., Engelbrecht, F.*, et al.* (1998). Interaction of Listeria monocytogenes with Human Brain Microvascular Endothelial Cells: InlB-Dependent Invasion, Long-Term Intracellular Growth, and Spread from Macrophages to Endothelial Cells. *Infect. Immun.* **66,** 5260-5267.

Hackstadt, T., Messer, R., Cieplak, W. and Peacock, M.G. (1992). Evidence for proteolytic cleavage of the 120-kilodalton outer membrane protein of rickettsiae: identification of an avirulent mutant deficient in processing. *Infect. Immun.* **60,** 159-165.

Hall, A. (1998). Rho GTPases and the Actin Cytoskeleton. *Science* **279,** 509-514.

Hänisch, J., Kölm, R., Wozniczka, M., Bumann, D., Rottner, K. and Stradal, T.E.B. (2011). Activation of a RhoA/Myosin II-Dependent but Arp2/3 Complex-Independent Pathway Facilitates *Salmonella* Invasion. *Cell Host & Microbe* **9,** 273-285.

Hudson, A.M. and Cooley, L. (2002). A subset of dynamic actin rearrangements in *Drosophila* requires the Arp2/3 complex. *J Cell Biol* **156,** 677-687.

Hybiske, K. and Stephens, R.S. (2007). Mechanisms of *Chlamydia trachomatis* Entry into Nonphagocytic Cells. *Infection and Immunity* **75,** 3925-3934.

Jeng, R.L., Goley, E.D., D'Alessio, J.A., Chaga, O.Y., Svitkina, T.M., Borisy, G.G.*, et al.* (2004). A Rickettsia WASP-like protein activates the Arp2/3 complex and mediates actin-based motility. *Cell Microbiol* **6,** 761-769.

Kurokawa, K., Itoh, R.E., Yoshizaki, H., Nakamura, Y.O.T. and Matsuda, M. (2004). Coactivation of Rac1 and Cdc42 at Lamellipodia and Membrane Ruffles Induced by Epidermal Growth Factor. *Molecular Biology of the Cell* **15,** 1003-1010.

Ladwein, M. and Rottner, K. (2008). On the Rho'd: The regulation of membrane protrusions by Rho-GTPases. *FEBS Letters* **582,** 2066-2074.

Li, H. and Walker, D.H. (1998). rOmpA is a critical protein for the adhesion of Rickettsia rickettsii to host cells. *Microbial Pathogenesis* **24,** 289-298.

Liu, Z.-M., Tucker, A.M., Driskell, L.O. and Wood, D.O. (2007). mariner-Based Transposon Mutagenesis of Rickettsia prowazekii. *Appl. Environ. Microbiol.* **73,** 6644-6649.

Machesky, L.M. and Insall, R.H. (1998). Scar1 and the related Wiskott-Aldrich syndrome protein, WASP, regulate the actin cytoskeleton through the Arp2/3 complex. *Current Biology* **8,** 1347-1356.

Magdalena, J., Millard, T.H., Etienne-Manneville, S., Launay, S., Warwick, H.K. and Machesky, L.M. (2003). Involvement of the Arp2/3 Complex and Scar2 in Golgi Polarity in Scratch Wound Models. *Mol. Biol. Cell* **14,** 670-684.

Martinez, J.J. and Cossart, P. (2004). Early signaling events involved in the entry of Rickettsia conorii into mammalian cells. *J Cell Sci* **117,** 5097-5106.

Martinez, J.J., Seveau, S., Veiga, E., Matsuyama, S. and Cossart, P. (2005). Ku70, a component of DNA-dependent protein kinase, is a mammalian receptor for Rickettsia conorii. *Cell* **123,** 1013-1023.

Miki, H., Suetsugu, S. and Takenawa, T. (1998). WAVE, a novel WASP-family protein involved in actin reorganization induced by Rac. *Embo J* **17,** 6932-6941.

Nolen, B.J., Tomasevic, N., Russell, A., Pierce, D.W., Jia, Z., McCormick, C.D.*, et al.* (2009). Characterization of two classes of small molecule inhibitors of Arp2/3 complex. *Nature* **460,** 1031-1034.

Paddock, C., Sumner, J., Comer, J., Zaki, S., Goldsmith, C., Goddard, J.*, et al.* (2004). Rickettsia parkeri: A Newly Recognized Cause of Spotted Fever Rickettsiosis in the United States. *Clinical Infectious Diseases* **38,** 805-811.

Paddock, C.D., Finley, R.W., Wright, C.S., Robinson, H.N., Schrodt, B.J., Lane, C.C.*, et al.* (2008). Rickettsia parkeri Rickettsiosis and Its Clinical Distinction from Rocky Mountain Spotted Fever. *Clinical Infectious Diseases* **47,** 1188-1196.

Pertz, O. (2010). Spatio-temporal Rho GTPase signaling - where are we now? *Journal of Cell Science* **123,** 1841-1850.

Peterson, J.R., Lokey, R.S., Mitchison, T.J. and Kirschner, M.W. (2001). A chemical inhibitor of N-WASP reveals a new mechanism for targeting protein interactions. *Proceedings of the National Academy of Sciences of the United States of America* **98,** 10624-10629.

Pielage, J.F., Powell, K.R., Kalman, D. and Engel, J.N. (2008). RNAi Screen Reveals an Abl Kinase-Dependent Host Cell Pathway Involved in *Pseudomonas aeruginosa* Internalization. *PLoS Pathog* **4,** e1000031.

Policastro, P.F., Munderloh, U.G., Fischer, E.R. and Hackstadt, T. (1997). Rickettsia rickettsii growth and temperature-inducible protein expression in embryonic tick cell lines. *J Med Microbiol* **46,** 839-845.

Rabiet, M.-J., Tardif, M., Braun, L. and Boulay, F. (2002). Inhibitory effects of a dominant-interfering form of the Rho-GTPase Cdc42 in the chemoattractant-elicited signaling pathways leading to NADPH oxidase activation in differentiated HL-60 cells. *Blood* **100,** 1835-1844.

Ralph, D., Pretzman, C., Daugherty, N. and Poetter, K. (1990). Genetic Relationships among the Members of the Family Rickettsiaceae As Shown by DNA Restriction Fragment Polymorphism Analysis. *Annals of the New York Academy of Sciences* **590,** 541-552.

Riedl, J., Crevenna, A.H., Kessenbrock, K., Yu, J.H., Neukirchen, D., Bista, M.*, et al.* (2008). Lifeact: a versatile marker to visualize F-actin. *Nat Meth* **5,** 605-607.

Riley, S.P., Goh, K.C., Hermanas, T.M., Cardwell, M.M., Chan, Y.G.Y. and Martinez, J.J. (2010). The Rickettsia conorii Autotransporter Protein Sca1 Promotes Adherence to Nonphagocytic Mammalian Cells. *Infection and Immunity* **78,** 1895-1904.

Rogers, S.L., Wiedemann, U., Stuurman, N. and Vale, R.D. (2003). Molecular requirements for actin-based lamella formation in *Drosophila* S2 cells. *J Cell Biol* **162,** 1079-1088.

Serio, A.W., Jeng, R.L., Haglund, C.M., Reed, S.C. and Welch, M.D. (2010). Defining a Core Set of Actin Cytoskeletal Proteins Critical for Actin-Based Motility of *Rickettsia*. *Cell Host & Microbe* **7,** 388-398.

Shi, J., Scita, G. and Casanova, J.E. (2005). WAVE2 Signaling Mediates Invasion of Polarized Epithelial Cells by Salmonella Typhimurium. *J. Biol. Chem.* **280,** 29849-29855.

Snapper, S.B., Takeshima, F., Anton, I., Liu, C.H., Thomas, S.M., Nguyen, D.*, et al.* (2001). N-WASP deficiency reveals distinct pathways for cell surface projections and microbial actin-based motility. *Nat Cell Biol* **3,** 897-904.

Sousa, S., Cabanes, D., Bougneres, L., Lecuit, M., Sansonetti, P., Tran-Van-Nhieu, G. and Cossart, P. (2007). Src, cortactin and Arp2/3 complex are required for E-cadherin-mediated internalization of *Listeria* into cells. *Cellular Microbiology* **9,** 2629-2643.

Srinivasan, S., Wang, F., Glavas, S., Ott, A., Hofmann, F., Aktories, K.*, et al.* (2003). Rac and Cdc42 play distinct roles in regulating PI(3,4,5)P3 and polarity during neutrophil chemotaxis. *The Journal of Cell Biology* **160,** 375-385.

Stroschein-Stevenson, S.L., Foley, E., O'Farrell, P.H. and Johnson, A.D. (2005). Identification of Drosophila Gene Products Required for Phagocytosis of *Candida albicans*. *PLoS Biol* **4,** e4.

Subauste, M.C., Von Herrath, M., Benard, V., Chamberlain, C.E., Chuang, T.-H., Chu, K.*, et al.* (2000). Rho Family Proteins Modulate Rapid Apoptosis Induced by Cytotoxic T Lymphocytes and Fas. *Journal of Biological Chemistry* **275,** 9725-9733.

Teysseire, N., Boudier, J.A. and Raoult, D. (1995). Rickettsia conorii entry into Vero cells. *Infect Immun* **63,** 366-374.

Uchiyama, T., Kawano, H. and Kusuhara, Y. (2006). The major outer membrane protein rOmpB of spotted fever group rickettsiae functions in the rickettsial adherence to and invasion of Vero cells. *Microbes and Infection* **8,** 801-809.

Unsworth, K.E., Way, M., McNiven, M., Machesky, L. and Holden, D.W. (2004). Analysis of the mechanisms of Salmonella-induced actin assembly during invasion of host cells and intracellular replication. *Cellular Microbiology* **6,** 1041-1055.

Walker, D.H. and Ismail, N. (2008). Emerging and re-emerging rickettsioses: endothelial cell infection and early disease events. *Nat Rev Microbiol* **6,** 375-386.

Walker, T.S. (1984). Rickettsial interactions with human endothelial cells in vitro: adherence and entry. *Infect. Immun.* **44,** 205-210.

Walker, T.S. and Winkler, H.H. (1978). Penetration of Cultured Mouse Fibroblasts (L Cells) by Rickettsia prowazeki. *Infect. Immun.* **22,** 200-208.

Welch, M.D., DePace, A.H., Verma, S., Iwamatsu, A. and Mitchison, T.J. (1997a). The human Arp2/3 complex is composed of evolutionarily conserved subunits and is localized to cellular regions of dynamic actin filament assembly. *J Cell Biol* **138,** 375-384.

Welch, M.D., Iwamatsu, A. and Mitchison, T.J. (1997b). Actin polymerization is induced by Arp2/3 protein complex at the surface of Listeria monocytogenes. *Nature* **385,** 265-269.

Yamazaki, D., Suetsugu, S., Miki, H., Kataoka, Y., Nishikawa, S.-I., Fujiwara, T.*, et al.* (2003). WAVE2 is required for directed cell migration and cardiovascular development. *Nature* **424,** 452-456.

Yan, C., Martinez-Quiles, N., Eden, S., Shibata, T., Takeshima, F., Shinkura, R.*, et al.* (2003). WAVE2 deficiency reveals distinct roles in embryogenesis and Rac-mediated actin-based motility. *Embo J* **22,** 3602-3612.

Zallen, J.A., Cohen, Y., Hudson, A.M., Cooley, L., Wieschaus, E. and Schejter, E.D. (2002). SCAR is a primary regulator of Arp2/3-dependent morphological events in *Drosophila*. *J Cell Biol* **156,** 689-701.

CHAPTER THREE

RickA and Sca2 independently activate temporally and mechanistically distinct phases of Rickettsia *actin-based motility.*

INTRODUCTION

Actin-based motility is a strategy used by many intracellular pathogens to move within the host cell cytosol and into adjacent cells (Haglund *et al.*, 2011). In addition to mediating cell-to-cell spread, emerging evidence suggests that actin-based motility can allow pathogens such as *Listeria monocytogenes* and *Shigella flexneri* to evade septin and ubiquitin recruitment and subsequent targeting by host autophagy pathways, including innate immune sensing of intracellular bacteria (Mostowy *et al.*, 2012). *Rickettsia* species are Gram-negative, obligate intracellular pathogens that undergo actin-based motility. They polymerize characteristic long actin tails composed of helical bundles of linear, unbranched filaments (Gouin *et al.*, 1999; Heinzen *et al.*, 1993; Serio *et al.*, 2010), in contrast to actin tails formed by *Listeria* and *Shigella*, which consist of branched filament networks nucleated by the host Arp2/3 complex (Haglund *et al.*, 2011). *Rickettsia* actin-based motility also requires profilin and fimbrin (T-plastin), which are dispensable for *Listeria* motility, while capping protein and ADF/cofilin are essential for proper actin tail morphology and motility in both species (Serio *et al.*, 2010).

Recently, the differences in actin structure between *Listeria* and *Rickettsia* were explained by the discovery and characterization of the *Rickettsia* Sca2 protein. In both *R. parkeri* and *R. rickettsii*, the Sca2 autotransporter protein acts as a mimic of host formin-family actin nucleators. Sca2 is localized to the bacterial outer membrane, often at the actin-tail associated pole (Haglund *et al.*, 2010) Biochemically, Sca2 directly nucleates linear actin filaments and enables filament elongation in a profilin-dependent manner (Haglund *et al.*, 2010). A critical role for Sca2 during *Rickettsia* motility is bolstered by two observations: first, profilin depletion causes aberrant motility in both insect and mammalian cells (Serio *et al.*, 2010), and second, a mutation in the *sca2* gene eliminates long actin tail formation and causes a defect in cell-cell spread and virulence (Kleba *et al.*, 2010). Sca2 also mediates adherence to and invasion of host cells by *R. conorii*, in a function that is separable from its actin nucleation activity (Cardwell *et al.*, 2009; Cardwell *et al.*, 2012).

Interestingly, another *Rickettsia* protein, RickA, was initially proposed to mediate actin-based motility. RickA is an Arp2/3 complex nucleation-promoting factor (NPF) that is sufficient to activate nucleation of branched actin filament networks by Arp2/3 *in vitro* (Jeng *et al.*, 2004). Biochemically, RickA functions similarly to the *Listeria* surface protein ActA, and to host NPFs such as N-WASP, which is recruited to the *Shigella* surface (Haglund *et al.*, 2011). However, the role of RickA in actin-based motility remained unclear. For example, there were conflicting reports as to whether the Arp2/3 complex was localized to *Rickettsia* actin tails and functionally important for motility (Gouin *et al.*, 2004) or was absent from actin tails (Gouin *et al.*, 1999; Serio *et al.*, 2010; Van Kirk *et al.*, 2000) and dispensable for motility (Balraj *et al.*, 2008; Harlander *et al.*, 2003; Heinzen, 2003; Serio *et al.*, 2010). RickA might function cooperatively with Sca2 under certain circumstances, or mediate the initial association of actin with *Rickettsia* or the initiation of actin-based motility. Alternatively, RickA might function in another step of the bacterial life cycle, such as Arp2/3 complex-dependent invasion of host cells (Chapter 2; Reed *et al.*, 2012), a process that occurs within the initial 5-30 min of infection (Figure 2.1; Martinez *et al.*, 2004; Reed *et al.*, 2012; Teysseire *et al.*, 1995).

Actin-based motility of *R. rickettsii, R. conorii,* and *R. parkeri* has been reported to occur primarily after 24 h of infection (Gouin *et al.*, 1999; Heinzen *et al.*, 1993; Serio *et al.*, 2010), with a single report of rare actin tail formation at 30 min post-infection (Heinzen *et al.*, 1993). While investigating actin association immediately following invasion, we observed distinctive

short, curved actin tails formed by *R. parkeri* during the first hour of host cell infection. Here, we report that these early actin tails are temporally restricted to early infection, and that early motility has distinct parameters when compared to previously characterized, Sca2-dependant late actin-based motility. In addition, we find that early actin-based motility of *R. parkeri* requires both the host Arp2/3 complex and the bacterial NPF RickA. This is the first example of a bacterium using two distinct, temporally regulated mechanisms of actin-based motility. This work raises important questions about the evolution of actin-based motility in the genus *Rickettsia*, and the function of motility at different times during the bacterial life cycle and for purposes other than cell-to-cell spread.

RESULTS

Rickettsia parkeri *actin-based motility is distinct during early infection*

In a previous report, we investigated the host cytoskeletal proteins required for *R. parkeri* invasion of various tissue culture cell lines (Chapter 2; Reed *et al.*, 2012). While studying invasion, we observed distinctive shorter, curved actin tails associated with *R. parkeri* 15-30 min after infection of host cells including HMEC-1, COS7, and *Drosophila* S2R+ cells (Figure 3.1A and data not shown). *R. parkeri* is rarely associated with actin from 1 h -12 h post-infection, while distinctive longer, helical actin tails become common 24 h – 48 h post-infection (Figure 3.1B-D and data not shown). Quantification of actin tails associated with *R. parkeri* at various times after synchronous infection of HMEC-1 cells indicated that curved actin tails were exclusively associated with early infection, while longer actin tails (>2 bacterial body lengths) did not appear with any frequency until 24-48 h post-infection (Figure 3.1D). Live-cell confocal microscopy of HMEC-1 cells transfected with lifeact-GFP and infected with *R. parkeri* expressing codon-optimized mCherry (Welch *et al.*, 2012a) revealed that early actin-based motility was irregular (Figure 3.1E) compared to the directionally-persistent motility at 24-48 h post-infection (Serio *et al.*, 2010). Thus, the appearance and frequency of *R. parkeri* actin tails varies during the infectious cycle in a temporally regulated manner.

Because the parameters of movement appeared distinct, we used confocal spinning-disc microscopy to image multiple cells either transfected with a lifeact-GFP actin marker and infected with mCherry-expressing *R. parkeri* or stably expressing lifeact-mCherry and infected with GFP-expressing *L. monocytogenes* (Shen *et al.*, 2005). It was immediately apparent that *R. parkeri* moved in more curved paths through the host cytosol during early infection (Figure 3.2A, upper panel) than during late infection (Figure 3.2A, lower panel). Bacterial movement was tracked for multiple cells infected for either 15-60 min or 48 h with *R. parkeri* or for 9-11 h with *Listeria*. Maximum intensity projections of all tracks in representative cells infected with *R. parkeri* for 24 min (blue box) and 48 h (red box) are shown in Figure 3.2B.

We compared the speed of *R. parkeri* early and late actin-based motility in HMEC-1 cells (Figure 3.2C) and found that early motility (25 ± 8 μm/min) was significantly slower both than late motility (24 ± 7 μm/min) and Listeria motility (22 ± 10 μm/min). While previous reports have indicated that *Rickettsia* movement is slower than that of *Listeria* (Goldberg, 2001), we found that in HMEC-1 cells, as in COS7 cells (Serio *et al*., 2010), the rate of *R. parkeri* late motility is not significantly different than that of *Listeria*. As we observed microscopically (Figure 3.1A, E; Figure 3.2A), the length of actin tails produced by *R. parkeri* during early

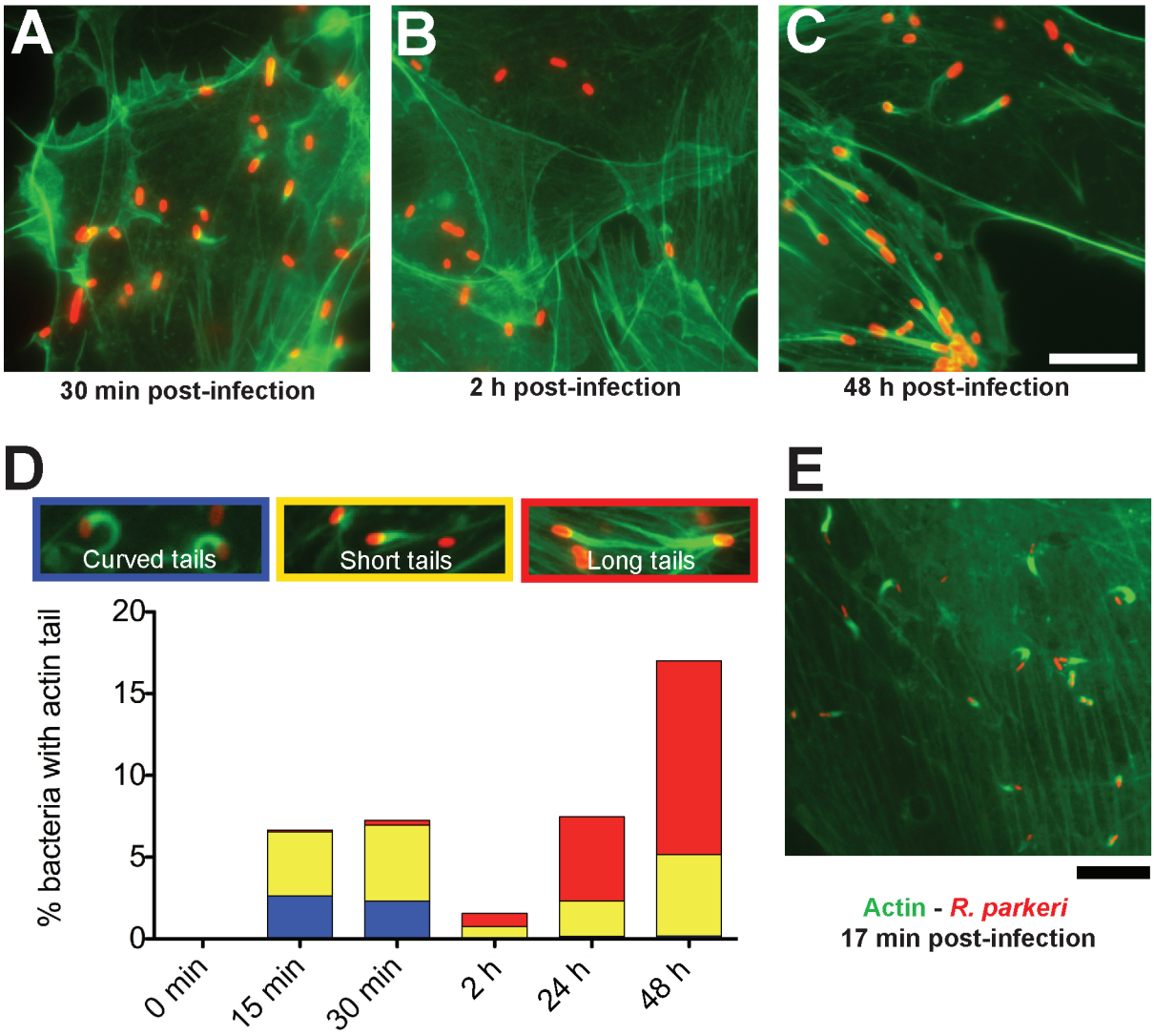

Figure 3.1 – *Rickettsia parkeri* forms short, curved actin tails during early infection. (A-C) HMEC-1 cells fixed 30 min (A), 2 h (B), or 48 h (C) after a synchronized infection. (D) HMEC-1 cells were infected with *R. parkeri* for the indicated times, fixed, and the percent of bacteria associated with each type of actin structure was counted: blue, curved actin tails; yellow, actin tails <2 bacteria lengths; red, actin tails >2 bacteria lengths. Results are the average from three independent experiments performed in duplicate. (A-D) Red, anti-*Rickettsia* antibody; green, actin stained with Alexa 488-phalloidin. (E) Still confocal image of a live cell, showing mCherry-expressing *R. parkeri* (red) actively moving at 17 min after infection of HMEC-1 cells transfected with LifeAct-GFP (green). Scale bars, 10μm.

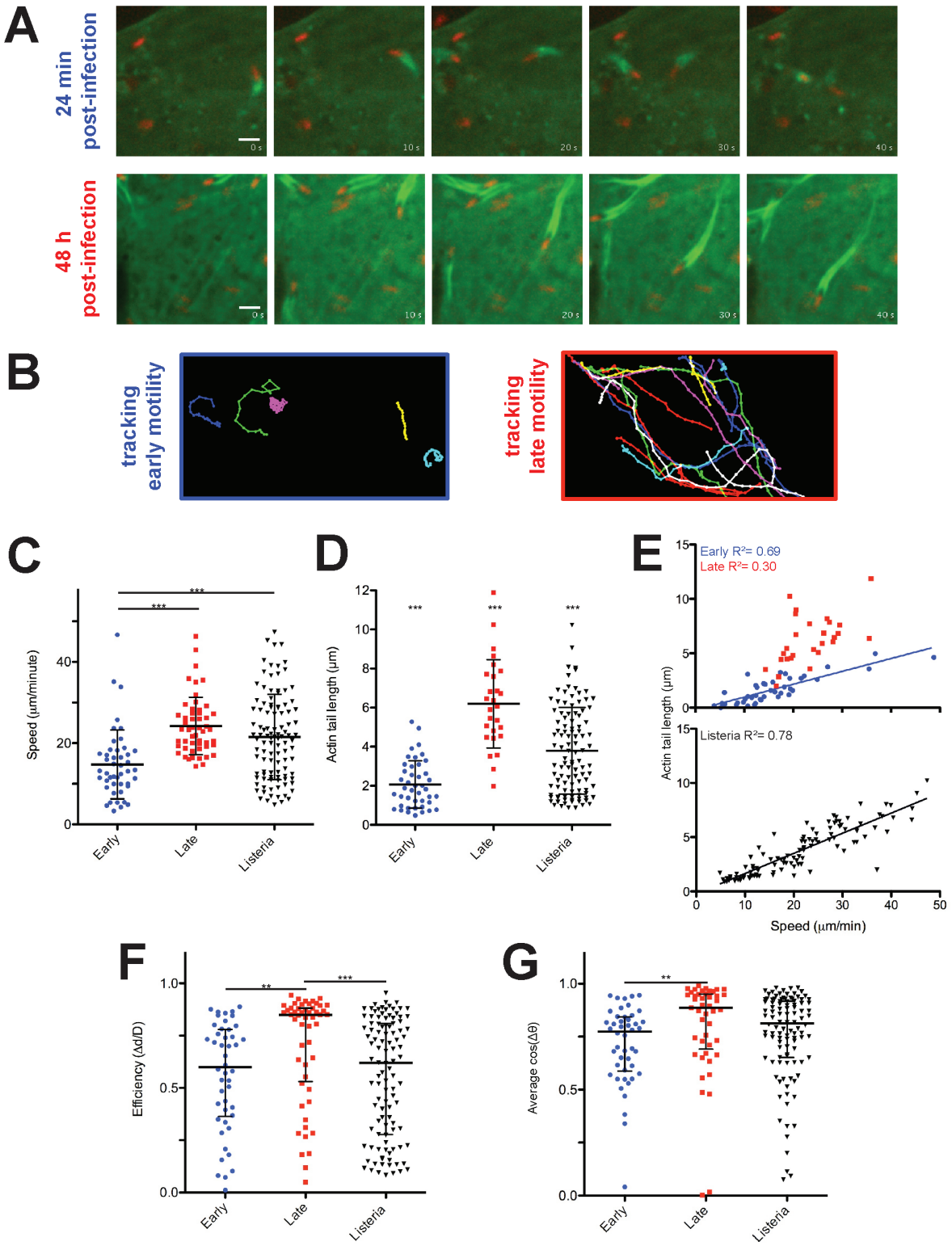

Figure 3.2 – Parameters of early and late *Rickettsia* actin-based motility (A) Still images of bacterial movement at 24 min (upper panels) and 48 h (lower panels) post-infection, taken at10 s intervals from Movie 3.2 (upper panels) and Movie 3.3 (lower panels), in HMEC-1 cells

transfected with lifeact-GFP (green) and infected with mCherry-expressing *R. parkeri*. Scale bars, 2 μm. (B) Maximum intensity projections of all movement tracks from *R. parkeri* in cells infected for 24 min (left, Movie 3.2) or 48 h (right, Movie 3.3). (C-G) parameters of movement for *R. parkeri* early motility (blue circles), *R. parkeri* late motility (red squares), and *L. monocytogenes* actin-based motility (black triangles). Multiple cells imaged on at least three separate occasions, with tracking and speed data trimmed to single 60 s intervals for each bacterium. (C) Average speed of each bacterium over 60 s. (D) Average actin tail length per bacterium over same interval as in (C). (E) Relationship between average speed and actin tail length for each bacterium, with best-fit linear regression. (F) Average efficiency of movement, calculated by dividing the net x-y displacement by the total path distance over 60 s for each individual bacterium. (G) Path straightness for each bacterium, calculated by averaging cosines of the change in tangent angle between adjacent track segments ($\Delta\theta$) over 60 s of movement. Statistical representations: (C-D); mean ± SD, *** $p<0.001$ by ANOVA with Bonferroni's multiple comparison; (D) all means are significantly different from one another. (F-G); median ± interquartile range, *** $p<0.001$, ** $p<0.01$ by Kruskal-Wallis test with Dunn's multiple comparison.

movement (mean 2 ± 1 μm, range, 0.5-5 μm) are significantly shorter than during late movement (mean 6 ± 2 μm, range, 2-12 μm; Figure 3.2D). In addition, *Rickettsia* actin tails are significantly shorter (for early) or longer (for late) than Listeria tails (mean 4 ± 2 μm, range, 1-10 μm) produced under similar conditions (Figure 3.2D).

To further examine the quantitative differences between early and late actin-based motility, we explored the relationship between speed and actin tail length. Previous reports have shown that a linear correlation ($R^2 > 0.96$) exists between speed and actin tail length for individual *Listeria* (Theriot *et al.*, 1992), but not for *R. parkeri* motility at 24-48 h post-infection ($R^2 = 0.02$) (Serio *et al.*, 2010). We found a similar, weak correlation between tail length and speed during *R. parkeri* late motility ($R^2 = 0.30$, Figure 3.2E, red squares). However, there was a much stronger linear correlation ($R^2 = 0.69$) between tail length and speed for early motility (Figure 3.2E, blue circles). Interestingly, the correlation was similar to that observed for *Listeria* motility under these conditions ($R^2 = 0.78$, figure 3.2E, lower panel).

Finally, we quantified the observed differences in path curvature during early and late *Rickettsia* motility and compared them to *Listeria* motility using two mathematical parameters. First, we calculated the persistence and efficiency of movement by dividing the x-y displacement for each track by the total distance moved by each bacterium over 60 s (Figure 3.2F). We found that the movements of both *R. parkeri* at 15-60 min post-infection, as well as of *Listeria*, were significantly less efficient than *R. parkeri* late actin-based movements (medians: early = 0.60, late = 0.85, Listeria = 0.62, $p < 0.05$ by Kruskal-Wallis test with Dunn's multiple comparison). As a geometric measure of path curvature, we also calculated the cosine of the change in tangent angle between adjacent path segments ($\cos[\Delta\theta]$) averaged over 60 s for each bacterium (Figure 3.2G). We found that movement paths during early motility were significantly more curved than during late motility (medians: early = 0.77, late = 0.89, $p < 0.05$ by Kruskal-Wallis test with Dunn's multiple comparison). However, *Listeria* motility showed a broad curvature range and was not significantly different than either type of *Rickettsia* motility by this measurement (median = 0.81). Thus, early actin-based movement of *R. parkeri* is slow and associated with distinct actin tails, with geometric parameters of movement more similar to *Listeria* motility than to *R. parkeri* late actin-based motility.

Early actin-based motility is Arp2/3-dependent and is associated with RickA

We hypothesized that the differences in temporal regulation and quality of movement during early and late actin-based motility results from the action of different bacterial or host actin nucleators. Late motility has been shown to depend on the *Rickettsia* protein Sca2, which is localized to the actin-tail associated pole (Haglund *et al.*, 2010; Kleba *et al.*, 2010). In *Shigella* and *Listeria*, mediators of actin-based motility (IcsA and ActA, respectively) are also localized to the bacterial pole (Goldberg, 2001). Previously, RickA has been reported to localize throughout the bacterial outer membrane without a polar concentration (Gouin *et al.*, 2004). When we visualized RickA localization in HMEC-1 cells fixed 30 min post-infection with *R. parkeri*, we found that bacteria with early actin tails did have polar concentrations of RickA protein (Figure 3.3A). In contrast, when HMEC-1 cells were imaged after 48 h of infection, RickA was present mostly in the bacterial cytoplasm, while Sca2 was localized to the actin-associated pole (Figure 3.3B and data not shown).

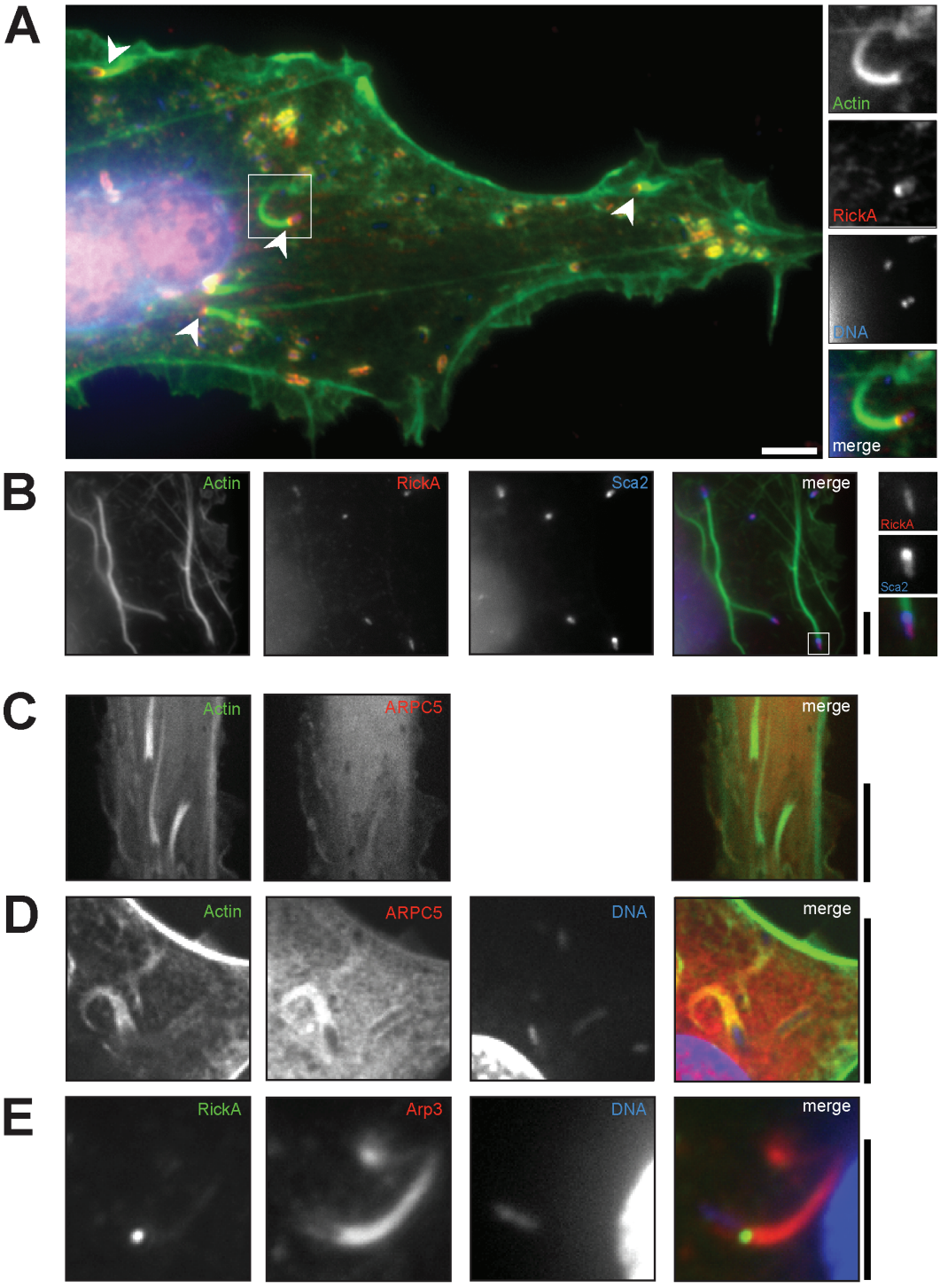

Figure 3.3 – RickA and the Arp2/3 complex localize to early, but not to late, *Rickettsia* actin tails. (A) HMEC-1 cells infected with *R. parkeri* for 30 min. Actin stained with 488-phalloidin (green), RickA with anti-RickA antibody (red), and bacterial/host DNA stained with DAPI (blue). Arrows indicate bacteria with early actin tails and polar RickA staining. Box, bacterium magnified on right. (B) HMEC-1 cells infected with FLAG-RickA expressing *R. parkeri* for 48 h. Actin stained with 488-phalloidin (green), RickA with anti-FLAG M2 antibody (red), and

Sca2 with anti-Sca2 antibody (blue). (C) HMEC-1 cell transfected with Lifeact-mCherry (green) and eGFP-ARPC5 (red) and infected with *R. parkeri* for 48 h, confocal micrograph of a live cell. (D) HMEC-1 cell infected with *R. parkeri* for 30 min and fixed. Cells transfected with GFP-ARPC5 (red) actin stained with 568-phalloidin (green), and DNA stained with DAPI (blue). (E) HMEC-1 cell infected with FLAG-RickA expressing *R. parkeri* for 30 min and fixed with Cytoskelfix. RickA visualized with anti-FLAG M2 antibody (green), Arp3 with anti-Arp3C antibody (red), and DNA with DAPI (blue). Scale bars, 5μm for all panels.

Should RickA activate the Arp2/3 complex during early motility, Arp3 and other complex proteins should localize throughout the actin tail as they do in *Listeria* (Welch *et al.*, 1997b) and *Shigella* (Gouin *et al.*, 1999) actin tails. In contrast, while Arp3 has been reported at the *R. conorii* bacterial surface during actin-based motility (Gouin *et al.*, 2004), complex members do not localize to late *Rickettsia* actin tails (Gouin *et al.*, 1999; Heinzen, 2003; Serio *et al.*, 2010). In HMEC-1 cells infected with *R. parkeri* for 30 min, GFP-ARPC5 strongly co-localized with early actin tails (Figure 3.3D). In addition, we observed both polar RickA (visualized with anti-FLAG antibody) and strong Arp3 staining consistent with early tails in HMEC-1 cells infected with FLAG-RickA *R. parkeri* for 30 min (Figure 3.3D). In agreement with previous reports, we found that neither Arp3 nor GFP-ARPC5 (p16), a member of the Arp2/3 complex, localize to late *R. parkeri* actin tails (Figure 3.3C and data not shown). Therefore, unlike late *Rickettsia* tails, early actin tails are associated with Arp2/3 complex-rich actin networks and polar RickA protein.

The differential localization of RickA and Arp2/3 during early actin-based motility, along with the similarities between early and *Listeria* movement, led us to hypothesize that early actin tails were nucleated by the Arp2/3 complex rather than by *Rickettsia* Sca2. Late actin-based motility of *R. parkeri* has previously shown to be unaffected or modestly inhibited by depletion of Arp2/3 complex subunits (Serio *et al*., 2010). Depletion of Arp2/3 complex using RNA interference inhibits and delays invasion (Figure 2.4, 2.10; Reed *et al*., 2012), which would confound analysis of actin tails occurring at 30 min post-infection. We utilized fast acting chemical inhibitors of the Arp2/3 complex (Nolen *et al.*, 2009) to interfere with Arp2/3 function during early and late *R. parkeri* motility. These inhibitors block Arp2/3-dependent *Listeria* motility (Nolen *et al*., 2009), but would not be expected to influence Sca2-mediated nucleation of late actin tails.

We infected HMEC-1 and COS7 cells for 15 min to allow most invasion to occur (Figure 2.1; Reed *et al*., 2012), then added media containing inactive control (CK312) or Arp2/3 inhibitor (CK869) at a final concentration of 100 μM, and fixed after 30 total min of infection. *R. parkeri* early actin tails were reduced by 88% (HMEC-1) or 73% (COS-7) relative to DMSO-treated controls after treatment with CK869 (Figure 3.4A-B). The difference between control and treated cells was more dramatic inHMEC-1 cells, since *R. parkeri* form 2-3 fold more early tails in this cell type (Figure 3.4A). Therefore, formation of early actin tails requires Arp2/3 complex activity.

We also investigated whether late actin tail polymerization or formation required Arp2/3 complex activity. We utilized COS7 cells to examine late *Rickettsia* tail formation, as they remained adherent during long-term treatment with the Arp2/3 inhibitor. We infected COS7 cells for 48 h with *R. parkeri*, exchanging culture media at 24, 32, 40, and 48 h post-infection with medium containing 100 μM inactive control (CK312) or Arp2/3 inhibitor (CK869) in 1% DMSO. Cells were fixed 30 min after the final treatment. When actin tail formation was quantified, we found that there was no change in the average percent of bacteria associated with actin tails after 24 h of Arp2/3 inhibition (Figure 3.4C). We also treated COS7 cells infected for 48 h for only 30 min before fixation. For this treatment, we found modest decrease in actin tail formation after both CK312 and CK869 treatment compared to the DMSO-treated control (Figure 3.4D, DMSO mean 13.65 ± 3.44% with tails). Nevertheless, there was no difference between treatment with the inactive control (CK312, mean 9 ± 1.4%) or the Arp2/3 inhibitor (CK869, mean 9 ± 2.4%), indicating that the effect was nonspecific.

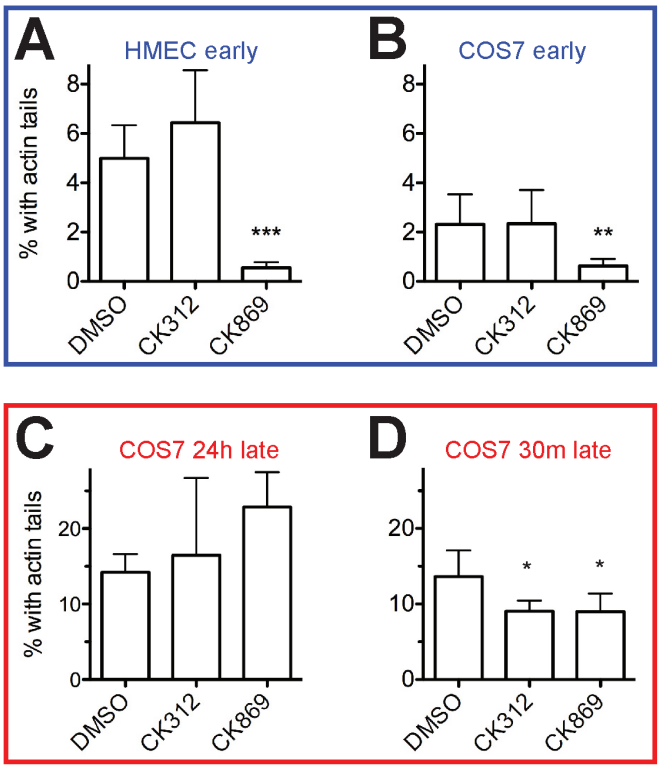

Figure 3.4 – Arp2/3 complex activity is required for early, but not late, *Rickettsia* actin-based motility. (A) HMEC-1 cells or (B) COS7 cells infected with *R. parkeri* for 15 min to allow invasion, then treated with 1% DMSO or 100 μM inactive control (CK312) or Arp2/3 inhibitor (CK869) for 15 min, then fixed. (C) COS7 cells infected with *R. parkeri* for 24 h, then treated with 1% DMSO or 100μM CK312 or CK869, with fresh media exchanged (including inhibitors) at 32 h, 40 h, and 48 h. Cells were fixed 30 min after final treatment. (D) COS7 cells infected with *R. parkeri* for 48 h, then treated with 1% DMSO or 100μM CK312 or CK869 for 30 min before fixation. (A-D) All cells were stained with 488-phalloidin and anti-*Rickettsia* antibody, 5 random fields of view were imaged, and percent of bacteria associated with any actin tail were counted. Results represent the mean ± SD of three independent experiments performed in duplicate, * $p<0.05$, ** $p<0.01$, *** $p<0.001$ mean varies significantly from DMSO control by student's t-test.

In conclusion, we have found that unlike late *Rickettsia* actin-based motility, early *R. parkeri* motility depends on actin tails nucleated by the host Arp2/3 complex and associated with polar localization of the Arp2/3 activator, RickA.

RickA is required for early actin tail formation.

To conclusively demonstrate that RickA and Sca2 act independently during the two phases of *Rickettsia* actin-based motility, we needed to generate strains of *R. parkeri* lacking each protein. Unfortunately, the obligate intracellular nature of *Rickettsia* has hampered development of robust genetic tools for these bacteria. Our attempts at using homologous recombination (Driskell *et al.*, 2009) to delete the *rickA* and *sca2* genes have thus far been unsuccessful. However, a *mariner*-based *Himar1* transposition system has been used successfully for limited transposon mutagenesis and for expression of fluorescent proteins in *R. parkeri* (Liu *et al.*, 2007; Welch *et al.*, 2012a). Recently, a strain of *R. rickettsii* with a transposon insertion in the *sca2* gene was isolated, and this strain is unable to form actin tails at 48 h post-infection, and forms small plaques in tissue culture cells, indicating a defect in cell-to-cell spread (Kleba *et al.*, 2010). In addition, multiple experiments using the same *mariner* transposon (plasmid PMW1650) resulted in semi-random transposition events, at a rate of approximately 1.1×10^{-7}, throughout the *R. rickettsii* and *R. prowazekii* genomes (Clark *et al.*, 2011).

We utilized methods similar to Clark and colleagues to isolate strains with insertions in the *rickA* and *sca2* genes using PMW1650, a transposon cassette encoding both rifampicin-resistance and GFP_{UV}. We electroporated *R. parkeri* with PMW1650, immediately plaque purifying to select for resistant clonal populations, followed by semi-random PCR to determine insertion sites of the transposon in each clone. After identification of insertion sites, strains were expanded, plaque purified again to ensure clonality, resequenced, and assayed for GFP, RickA and Sca2 protein expression.

We isolated *R. parkeri* strains with insertions in both *sca2* (strain Sp2, *sca2::himar1*, insertion at bp 112315) and *rickA* (strain Sp34, *rickA::himar1*, insertion at bp 888003) (Figure 3.5A). Given the monocistronic nature of the *sca2* and *rickA* genetic loci, these insertions are unlikely to have polar effects (Figure 3.5A). Both strains Sp2 and Sp34, as well as a previously generated control strain (GFP3) with an insertion in an unrelated protein (Reed *et al.*, 2012), express the GFP_{UV} protein to similar levels (Figure 3.5B, lower panel of blot). Strain Sp34 lacked any detectable RickA expression by either Western blot or immuno-fluorescence microscopy (Figure 3.5B and data not shown). Strain Sp2 expressed a 50 kD polypeptide, consistent with a predicted 480 amino acid Sca2 passenger domain fragment translated before the insertion site (Figure 3.5A, 3.5B). This fragment lacks the predicted proline-rich and WH2 (actin-binding) domains, as well as the autotransporter domain responsible for delivering Sca2 to the bacterial outer membrane (Haglund *et al.*, 2010; Kleba *et al.*, 2010). This 50 kD polypeptide reacted with a Sca2-specific antibody by Western blot (Figure 3.5B, asterisk) and appeared periplasmic by immunofluorescence microscopy (data not shown).

Based on our previous results, we hypothesized that *R. parkeri* strains lacking functional Sca2 and RickA proteins would have defects in late and early actin-based motility, respectively. The *sca2::himar1* strain formed plaques in cultured Vero cells which were significantly smaller (area, 0.60 ± 0.36 μm^2) than those formed by wild-type (0.95 ± 0.63 μm^2), control rifampicin-

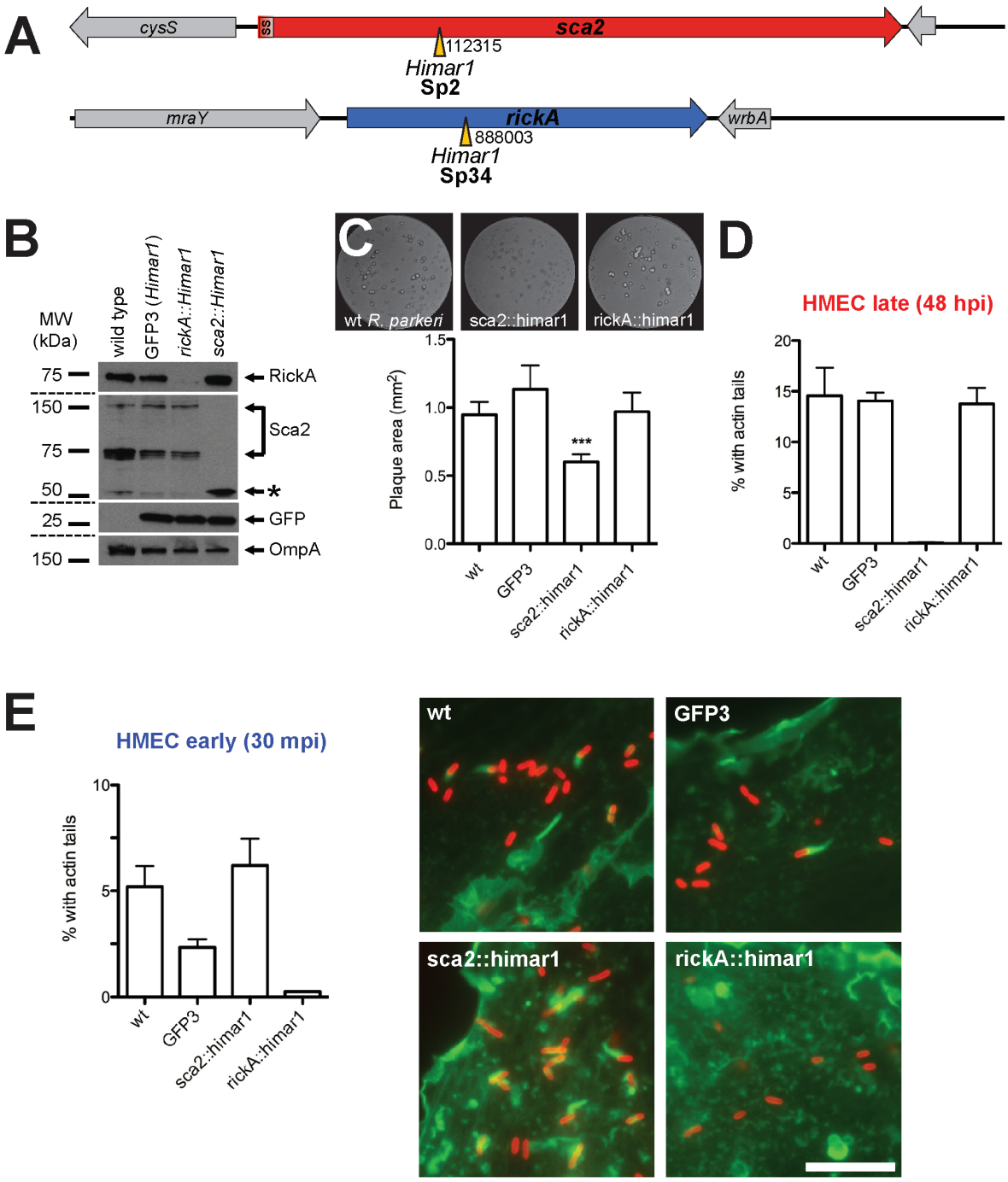

Figure 3.5 – RickA is required for early actin tail formation, but dispensable for late tail formation and cell-cell spread. (A) Schematic of *sca2* and *rickA* genes in the *R. parkeri* genome. Locations of *himar1*[GFP_{UV}-Rif^R] transposon insertions in strains Sp2 and Sp34 are indicated with yellow arrowheads along with genomic position. (B) Western Blot showing RickA, Sca2, and GFP expression in wild-type *R. parkeri*, an unrelated *Himar1* insertion line (GFP3), Sp34 (*rickA::himar1*), and Sp2 (*sca2::himar1*) strains. OmpA *Rickettsia* outer-membrane protein is used as a loading control. Note the truncated Sca2 fragment (asterisk) expressed in *sca2::himar1* strain. (C) Plaque assay stained 5 d post-infection with neutral red (upper panels) and quantification of plaque area (lower panel) for each strain. Results represent

mean ± SEM of two independent experiments. *** $p<0.001$, mean varies significantly from wt *R. parkeri* by student's t-test. (D-E) HMEC-1 cells were infected with various strains for 48 h (D) or 30 min (E), fixed and stained with 488-phalloidin and anti-*Rickettsia* antibody. 5 random fields of view were imaged for each duplicate coverslip, and percent of bacteria associated with any actin tail were counted. (E), right panel: representative images from samples infected for 30 min.

resistant (GFP3, 1.13 ± 0.77 μm^2) and the *rickA::himar1* strain (0.97 ±0.84 μm^2, Figure 3.5C). These data indicate that Sca2 is required for efficient cell-to-cell spread, and agree with the small-plaque phenotype previously observed for a *sca2::himar1* strain of *R. rickettsii* (Kleba *et al.*, 2010).

If RickA and Sca2 acted independently to mediate each phase of motility, we would expect strain Sp34 to have few early actin tails, while strain Sp2 would lack late actin tails. Indeed, when we infected HMEC-1 cells with each strain of *R. parkeri* and fixed cells 30 min post-infection, we found that wild-type and *sca2::himar1* strains formed similar numbers of actin tails, while the *rickA::himar1* strain formed almost no actin tails (0.25% with tails, Figure 3.5E). The GFP3 strain had a modest reduction in actin tail formation, possibly due to viability of the stock used for this experiment. When we infected HMEC-1 cells with each of the four strains for 48 h, we observed a dramatic lack of actin tail association in the *sca2::himar1* strain (0.07% with actin tails), while there was no difference in actin tail formation between wild-type, GFP3, and *rickA::himar1* strains (Figure 3.5D).

Taken together, these results indicate that RickA is required only for early actin-based motility, while Sca2 is required for late actin-based motility leading to cell-cell spread of *R. parkeri*. The lack of a defect in late actin tail formation by the *rickA::himar1* mutant strain, combined with our results after long-term inhibition of the Arp2/3 complex, indicate that RickA is dispensable for late actin-based motility of *R. parkeri*. Similarly, the absence of a defect in early actin tail formation by the *sca2::himar1* mutant indicates that Sca2 is dispensable for this process. Thus, the two phases of *Rickettsia* motility occur by mechanistically independent pathways.

DISCUSSION

Actin-based motility is a feature that has evolved independently in multiple intracellular parasites, including spotted-fever group *Rickettsia* species. Understanding how pathogens such as *Rickettsia* polymerize and organize actin to enable motility will enhance our understanding of bacterial pathogenesis as well as the complex regulation of actin function in the host cell (Haglund *et al.*, 2011). Here we report is the first observation of two entirely distinct mechanisms of actin-based motility by the same pathogen, and raise new questions about the regulation and function of actin-based motility for *R. parkeri* as well as for other pathogens.

We found that the parameters of movement vary for the same bacterium, depending on the type of actin network being produced. While previous reports found that *Rickettsia* move more slowly in Vero cells than do *Listeria* and *Shigella* (Goldberg, 2001), we observe *R. parkeri* and *Listeria* moving at similar speeds in both COS7 (Serio *et al.*, 2010) and HMEC-1 cell lines. Our measurements of *Rickettsia* late motility and of *Listeria* motility are faster than some previously reported speeds (Goldberg, 2001; Lacayo *et al.*, 2004), which may be related to cell type-specific factors, or imaging at ~37°C rather than ~25°C (Serio *et al.*, 2010). Variations in *Listeria* and *Rickettsia* motility have been reported to occur between cell types, because of interference from mitochondria or other cellular structures, or because of changes in the availability of profilin and other proteins important for motility (Goldberg, 2001; Lacayo *et al.*, 2004; Serio *et al.*, 2010). We conclude that HMEC-1 cells are more amenable to both *Rickettsia* and *Listeria* motility than other cell types, due to either a lack of interference from microtubules and mitochondria, an increased availability of actin and related proteins, or both.

Previously, RickA and Sca2 were proposed to act cooperatively to nucleate *Rickettsia* actin tails (Haglund *et al.*, 2010; Kleba *et al.*, 2010). In this work, we report multiple lines of evidence indicating that each protein acts independently to nucleate actin at different times in infection. First, there is a clear temporal separation between early and late motility (Figure 3.1). In addition, the insensitivity of Sca2-nucleated late motility to extended Arp2/3 inhibition (Figure 3.4) and the complete separability of *rickA* and *sca2* mutant phenotypes (Figure 3.5) indicate that each type of motility is independent. Therefore, we conclude that early tails are nucleated by the combined action of RickA and Arp2/3 complex, while late tails are nucleated only by Sca2.

Interestingly, we found that early *R. parkeri* motility, nucleated by RickA, was significantly slower than late motility, nucleated by Sca2. This result was somewhat unexpected, given that RickA and Arp2/3 are more efficient nucleators of actin filaments *in vitro* than is Sca2 (Haglund *et al.*, 2010; Jeng *et al.*, 2004). The difference in speed is probably not due to a defect in Arp2/3-mediated nucleation in HMEC-1 cells, since *Listeria* motility is not significantly slower than *R. parkeri* Sca2-dependent motility. Rather, we propose that this difference may be due to an intrinsic difference in the nucleation or elongation of actin filaments in early actin tails.

Sca2 is an outer-membrane autotransporter, like *Shigella* IcsA, and is predicted to be stably tethered to the outer surface of the bacterium (Goldberg *et al.*, 1995). On the other hand, while RickA has been reported to localize to the bacterial surface (Gouin *et al.*, 2004), it is not predicted to be secreted by the Sec, Tat, or autotransporter pathways. Nevertheless, the protein must be secreted into the host cytosol in order to potentiate motility. Indeed, *Rickettsia* genomes, including that of *R. parkeri*, encode an *rvh* type IV secretion system (T4SS), and the C-terminus of RickA indicates that it may be secreted through this pathway (Gillespie *et al.*, 2009; Vellaiswamy *et al.*, 2011; our unpublished observations). One intriguing hypothesis for the reduced motility rate of *R. parkeri* during early movement is that secretion of an Arp2/3 activating protein is less efficient at mediating actin nucleation/elongation or at generating force at the surface of the bacterium. Further studies of *rickA* and *sca2* mutant strains of *Rickettsia* may illuminate the differences in force generation and network stability between linear and branched networks moving the same particle.

The expression, localization, or activity of RickA and Sca2 proteins must be tightly regulated by *R. parkeri* to maintain the separation of actin tail phenotypes. If RickA is secreted, regulation of the T4SS could determine its ability to nucleate short actin tails. Likewise, regulation of Sca2 autotransporter activity, incorporation into the outer membrane, or unipolar localization could regulate its activity as has been observed for IcsA and ActA (Gouin *et al.*, 2005; Robbins *et al.*, 2001). Finally, regulated proteolysis of both proteins could serve to tightly regulate their expression. We are beginning careful analyses of gene transcription, protein abundance, and subcellular localization of each protein to address this question.

The primary function of actin-based motility is proposed to be the promotion of spread between host cells while avoiding the extracellular milieu and recognition by complement and phagocytes. However, growing evidence indicates that actin-based motility may potentiate evasion of cellular autophagy pathways by enabling escape from damaged phagolysosomes, evading ubiquitination and outrunning septin "caging" (Mostowy *et al.*, 2012). Intriguingly, *Rickettsia* do not recruit septin cages late in infection, while early colocalization with septins has not been examined (Mostowy *et al.*, 2010). One possibility is that RickA-driven motility evolved to evade autophagy, while Sca2-driven motility functions in cell-cell spread (Figure 3.5; Kleba *et*

al., 2010). *Rickettsia* would be the first pathogens to have evolved separable forms of motility to carry out both functions during the infectious cycle.

An alternate possibility is that RickA-driven motility functions in cell-cell spread, but in a manner more similar to virus actin-based movement. Both vaccinia virus (through 'surfing') and Baculovirus (through Arp2/3 mediated motility) have been reported to use actin-based motility to move from cell to cell before replication, thus increasing the chances of a successful infection (Doceul *et al.*, 2010; Ohkawa *et al.*, 2010). Because SFG *Rickettsia* do not divide until 10 h after infection, any spread resulting from early motility would have to be pre-replicative (Wisseman *et al.*, 1976). On the other hand, Sca2-mediated motility does not occur with any frequency until after 1-3 cycles of replication have occurred. This change from pre-replicative, RickA-driven motility to actively dividing, Sca2-driven motility suggests that *Rickettsia* may undergo previously unappreciated phenotypic switching, as do *Chlamydia* and *Legionella*, between infectious and replicative forms.

Overall, we have described the evolution of a heretofore unknown, bimodal separation of actin-based motility in an intracellular pathogen. The separability of each type of motility in *R. parkeri* will allow us to address important questions about the different functions of actin based motility during intracellular infection. In addition, the generation of two types of actin networks by the same pathogen will allow a comparison of the biophysical properties of Arp2/3- and formin-nucleated actin networks and their roles in intracellular motility. Further exploration of each type of motility in other species of *Rickettsia* will illuminate the evolutionary function of actin-based motility in both pathogenic and avirulent organisms.

MATERIALS AND METHODS

Antibodies

Antibodies were obtained from the following sources: mouse anti-FLAG M2 monoclonal antibody (Sigma-Aldrich); rabbit anti-Arp3 (Welch *et al.*, 1997a); rabbit anti-GFP (Firat-Karalar *et al.*, 2011); rabbit anti-RickA (Jeng *et al.*, 2004); rabbit anti-Sca2 (Haglund *et al.*, 2010); mouse anti-*Rickettsia* OmpA M13-3, and mouse anti-*Rickettsia* M14-13 (Anacker *et al.*, 1987) (T. Hackstadt, NIH/NIAID Rocky Mountain Laboratories; rabbit polyclonal anti-*Listeria* O antibody (BD Biosciences); horseradish peroxidase conjugated anti-mouse and rabbit secondary antibodies for immunoblotting (GE Healthcare); AlexaFluor 488-, and 568-conjugated anti-rabbit and anti-mouse secondary antibodies for immunofluorescence (Invitrogen Molecular Probes).

Plasmids

To generate the plasmid pGFP-ARPC5, the *Homo sapiens* ARPC5 (p16) cDNA was PCR-amplified with HindIII and XbaI restriction sites and ligated into a modified pEGFP-C1 vector (Clontech), resulting in a plasmid expressing eGFP fused to the N-terminus of ARPC5. The Lifeact (Riedl *et al.*, 2008) expression plasmids were pLifeact-GFP (Serio *et al.*, 2010) and pLifeact-mCherry (Reed *et al.*, 2012). *Rickettsia* insertional mutagenesis plasmid PMW1650 was a gift from D. Wood (University of South Alabama; (Liu *et al.*, 2007). To generate the plasmid pCLIP2B-Lifeact-mCherry, the Lifeact-mCherry ORF was PCR-amplified with XhoI and Pac1 restriction sites and ligated into plasmid pCLIP2B, a murine moloney leukemia virus that is derived from pCLIP3 (Lamason *et al.*, 2010) with expression driven by a CMV-derived Chicken

β-actin promoter. pCLIP2B and the packaging vectors pCMV-VSVg and pCL-SIN-Ampho were gifts from J. Pomerantz (Johns Hopkins University).

Bacterial strains, growth and purification

R. parkeri Portsmouth strain was a gift from C. Paddock (Centers for Disease Control and Prevention). GFP-expressing *R. parkeri* clonal strain GFP_{UV}-3 (Reed *et al.*, 2012) and codon-optimized mCherry-expressing *R. parkeri* clonal strains mCherry-1 and 3XmCherry-2 (Welch *et al.*, 2012a) were previously described. *Listeria monocytogenes* strain 10403S and GFP-expressing *L. monocytogenes* (Shen *et al.*, 2005) were a gift from D. Portnoy (University of California, Berkeley).

R. parkeri strains were propagated in Vero cells grown at 33°C with 5% CO_2, and purified by density gradient centrifugation as described previously (Hackstadt *et al.*, 1992), with the exception that MD-76R (Merry X-Ray) was substituted for Renografin, and stored at -80º C. For 30 min infections with GFP- or mCherry-expressing *R. parkeri*, infected monolayers of Vero cells were scraped from culture flasks, pelleted by centrifugation, resuspended in K-36 buffer (0.05 M KH_2PO_4, 0.05 M K_2HPO_4, 0.1 M KCl, 0.015 M NaCl, pH 7) and lysed using a dounce or syringe to release intracellular *R. parkeri*. Cell suspensions were centrifuged to remove nuclei and cell debris, and aliquots from the supernatant were centrifuged at 16000 *g* for 5 min to pellet *R. parkeri*, then resuspended in the appropriate culture medium and added to cells for infection and visualization. Alternately, supernatant from heavily infected Vero cells was used to directly infect HMEC-1 cells. *L. monocytogenes* was grown in liquid Brain Heart Infusion (BHI; Difco) at 37°C without agitation.

Isolation and characterization of* R. parkeri *with transposon insertions

Strains Sp2 (*sca2::himar1*) and Sp34 (*rickA::himar1*) were generated in separate experiments by harvesting a 75 cm^2 flask of Vero cells infected with *R. parkeri*, purifying through a syringe, washing in 250 mM sucrose, and electroporating with 1 µg of plasmid PMW1650 at 2.5 kV, 200 ohms, 25 µF, for 5 ms using a Gene Pulser Xcell (Bio-Rad). Bacteria were immediately suspended in 1.4-2.4 µl Brain Heart Infusion (BHI) media (Difco), and used to infect a 6-well plates of confluent Vero cells with an overlay of DMEM with 2% FBS and 0.5% agarose. Cells were grown overnight at 34°C, 5% CO_2, and after 20 h an additional overlay containing 500 ng/ml rifampicin was added for a final concentration of 200 ng/ml rifampicin (Sigma). Selection with 200 ng/ml rifampicin was continued for all subsequent growth. After 6-8 d, plaques were visible in the cell monolayer. Plaques were isolated and expanded in individual wells of Vero cells growing in 6-well plates. Once cells were heavily infected, each well was collected, *R. parkeri* isolated via syringe lysis and stored in 100 µl BHI at -80C. For sequencing of insertion sites, 1-2 µl of each strain was boiled and used in semi-random nested PCR.
Reaction #1 used primers:
Ex Tn1 5'-CACCAATTGCTAAATTAGCTTTAGTTCC-3' or
ExTn2 5'-GTGAGCTATGAGAAAGCGCCACGC-3' with
Univ1 5'-GCTAGCGGCCGCACTAGTCGANNNNNNNNNNCTTCT-3'
and reaction #2 used primers:
InTn1 5'-GCTAGCGGCCGCGGTCCTTGTACTTGTTTATAATTATCATGAG-3' or InTn2 5'-GCTAGCGGCCGCCCTGGTATCTTTATAGTCCTGTCGG-3' with

Univ2 5'-GCTAGCGGCCGCACTAGTCGA-3'. The PCR products were cleaned using column purification or ExoSAP-IT (Affymetrix), and insertion sites were sequenced using primers SR095 5'-CGCCACCTCTGACTTGAGCGTCG-3' and SR096 5'-CCATATGAAAACACTCCAAAAAAC-3'. Following sequencing, strains were expanded and re-plaque purified as in (Clark *et al.*, 2011) and re-sequenced. Genomic locations were determined using BLAST to search for the sequence adjacent to the transposon insertion in the *R. parkeri* strain Portsmouth genome (GenBank/NCBI accession NC_017044.1).

Cell growth and transfections

African green monkey kidney fibroblast cells (COS-7) and epithelial cells (Vero) were from the University of California, Berkeley, tissue culture facility, and were grown at 37°C with 5% CO_2 in DMEM (Invitrogen) with 2-10% FBS (JR Scientific, Gibco). The human microvascular endothelial cell line HMEC-1 (Ades *et al.*, 1992) was obtained via material transfer agreement from the Centers for Disease Control, Biological Products Branch, and was grown at 37°C with 5% CO_2 in MCDB 131 (Invitrogen) with 10% FBS (Hyclone), 2 mM L-Glutamine (Gibco), 10 ng/mL Epidermal Growth Factor (BD Biosciences), and 1 μg/mL Hydrocortisone (Sigma).

For expression of mCherry/GFP-tagged proteins, 250-500 ng of plasmid DNA was transiently transfected into HMEC-1 cells using Lipofectamine 2000 (Invitrogen), according to the manufacturer's instructions. 24 h later, cells were infected *with R. parkeri* mCherry-1 or 3XmCherry-2. Imaging or fixation was at 48-72 h post-transfection. A polyclonal HMEC-1 cell line stably expressing mCherry-Lifeact was generated by retroviral transduction using pCLIP2B-mCherry Lifeact, pCMV-VSVg, and pCL-SIN-Ampho to package virus in HEK293T cells, essentially as described in (Lamason *et al.*, 2010), selected using 2.5 μg/ml Puromycin (EMD Millipore), and sorted for strong expression using Cytopeia INFLUX Sorter (UC Berkeley Flow Cytometry Facility).

Bacterial infections

Plaque assays were performed as described in (Cory *et al.*, 1974). For plaque size measurements, wells were overlaid 5 d after infection with PBS + 0.5% agarose + 2% Neutral Red (Sigma) for a final concentration of 1% Neutral Red, incubated overnight and imaged using an AlphaInnotech AlphaImager EP (ProteinSimple). Plaque area was manually measured using ImageJ.

Rickettsia infections were carried out as follows: HMEC-1 cells were seeded either onto glass coverslips in 24-well plates, or to 24-well, 6-well, or 3 cm^2 glass-bottom dishes (MatTek) at about 50% cell density. Cells were infected with ~$1.5x10^5$ pfu/well for 48 h, ~$3x10^5$ pfu/well for 24 h or with ~$6x10^5$ pfu/well *R. parkeri* for less than 24 h. For infection times from 0 min – 2 h, *R. parkeri* were added directly to culture medium, plates were centrifuged at 200 *g* for 5 min at 22-25ºC and incubated at 37ºC for the remainder of infection times. *L. monocytogenes* infections of HMEC-1 cells were conducted at an MOI of about 100 as follows: overnight *Listeria*-GFP cultures were diluted 1:40 in HMEC-1 growth medium and incubated at 37ºC for 15 min, then added to culture dishes and incubated for 1 h at 37°C with 5% CO_2, after which extracellular *Listeria* were rinsed off with PBS, and cells were maintained in HMEC growth medium containing 10 μg/ml gentamicin for the remainder of infections.

For drug treatments, CK-312 or CK-869 (EMD Chemicals) were diluted in culture medium in 1% DMSO for a final concentration of 100 μM, warmed to 37°C and used to replace

medium at the indicated times post-infection; for 30 min inhibition, drugs were prepared at 2X concentration and added directly to infected cells. After infections were complete, cells were imaged using live-cell microscopy or fixed and processed for immunofluorescence as described below.

Immunoblotting and immunofluorescence staining

For immunoblotting, bacteria purified by density gradient centrifugation or syringe lysis were diluted in Laemmli lysis/sample buffer and boiled at 95˚C for 10 min. Equal molar amounts of protein were separated by SDS-PAGE and transferred to nitrocellulose. Membranes were blocked with 5% milk in phosphate buffered saline (PBS), probed with primary followed by secondary antibodies, and visualized with ECL detection reagents (GE Healthcare).

For immunofluorescence staining, cells were fixed with 2.5% formaldehyde in PBS at room temperature for 15 min or using –20˚C Cytoskelfix (Cytoskeleton) for 5 min. Cells were permeabilized in PBS with 0.5% Triton X-100 and 1 mg/ml lysozyme (Sigma-Aldrich) for 5 min. Antibodies were diluted in PBS with 2% bovine serum albumin (BSA) and antibody staining steps were carried out at room temperature using standard procedures. For anti-Arp3 staining, coverslips were blocked in PBS + 2% BSA + 2% dry milk for 30 min prior to staining. To visualize actin, 4 U/µl of Alexa 488 or 568-conjugated phalloidin (Invitrogen) was included with the secondary antibody. DNA was stained with DAPI (Invitrogen) included with secondary antibody. Coverslips were mounted with Prolong Gold anti-fade (Invitrogen), sealed, and stored at 4°C.

Imaging and analysis

Confocal images of live and fixed cells were captured using a Nikon Ti Eclipse (Melville, NY) equipped with a Yokogawa CSU-XI spinning confocal disc (Tokyo, Japan), a 100X (1.4 NA) Plan Apo objective and a Clara Interline CCD camera (Andor, Belfast, Northern Ireland). Wide-field images were captured using an Olympus IX71 microscope equipped with a 100X (1.35 NA) PlanApo objective lens and a Photometrics CoolSNAP HQ camera (Figures 3.2 B,E), or a Nikon Ti Eclipse equipped with a 100X or 60X (1.49 NA) TIRF objective and an Andor Clara Interline CCD camera (Figures 3.1A-C, 3.3A, 3.5E).

Fixed and live-cell images were captured in the TIFF 16-bit format using MetaMorph software (Molecular Devices) or Micro-Manager Software (http://www.micro-manager.org) and then processed to 8 bit files, cropped and adjusted for brightness/contrast using ImageJ and Adobe Photoshop. Movies were assembled and adjusted using ImageJ, bacterial motility was tracked using the Manual Tracking plugin (http://rsbweb.nih.gov/ij/plugins/track/track.html), and actin tails were measured using the Segmented Line function for each of 12 frames (60 s) per bacterium. Only tracks where a bacterium moved in the plane of focus for at least 60 s were kept, and for all analyses each track was cropped to 60 s. 50-100 bacteria were tracked and measured from cells infected on at least three separate occasions.

For quantification of actin tails, five semi-random fields of view were chosen for each of two coverslips using only bacterial staining for focus/centering, images were imported into ImageJ, bacteria were counted using the Threshold function, and the Cell Counter plugin (http://rsbweb.nih.gov/ij/plugins/cell-counter.html) was used to correct manual counting of bacteria and quantify actin tail association. For actin tail quantification, an average of 300-500 bacteria and 20-30 host cells were counted per experimental sample (range: 76-2140 bacteria).

Images of mutant *R. parkeri* strains were collected, processed and analyzed by a blinded observer.

Average cosines of the change in tangent angle between adjacent track segments ($\Delta\theta$) were calculated using Matlab (Mathworks) to analyze the x-y coordinates of each track, code available on request. Average efficiency of movement was calculated by dividing the net x-y displacement by the total path distance over 60 s for each individual bacterium. All data were analyzed using Prism v5.0 (Graphpad Software) and groups were either compared pairwise by Student's t-test, using a one-way ANOVA with Bonferroni's multiple comparison or by Kruskal-Wallis test with Dunn's multiple comparison. Differences with p-values < 0.05 were designated statistically significant.

REFERENCES

Ades, E.W., Candal, F.J., Swerlick, R.A., George, V.G., Summers, S., Bosse, D.C. and Lawley, T.J. (1992). HMEC-1: Establishment of an Immortalized Human Microvascular Endothelial Cell Line. *J Investig Dermatol* **99,** 683-690.

Anacker, R.L., Mann, R.E. and Gonzales, C. (1987). Reactivity of monoclonal antibodies to Rickettsia rickettsii with spotted fever and typhus group rickettsiae. *Journal of Clinical Microbiology* **25,** 167-171.

Balraj, P., El Karkouri, K., Vestris, G., Espinosa, L., Raoult, D. and Renesto, P. (2008). RickA expression is not sufficient to promote actin-based motility of Rickettsia raoultii. *PLoS ONE* **3,** e2582.

Cardwell, M.M. and Martinez, J.J. (2009). The Sca2 Autotransporter Protein from Rickettsia conorii Is Sufficient To Mediate Adherence to and Invasion of Cultured Mammalian Cells. *Infection and Immunity* **77,** 5272-5280.

Cardwell, M.M. and Martinez, J.J. (2012). Identification and characterization of the mammalian association and actin-nucleating domains in the Rickettsia conorii autotransporter protein, Sca2. *Cellular Microbiology***,** n/a-n/a.

Clark, T.R., Lackey, A.M., Kleba, B., Driskell, L.O., Lutter, E.I., Martens, C*., et al.* (2011). Transformation Frequency of a mariner-Based Transposon in Rickettsia rickettsii. *Journal of Bacteriology* **193,** 4993-4995.

Cory, J., Yunker, C.E., Ormsbee, R.A., Peacock, M., Meibos, H. and Tallent, G. (1974). Plaque assay of rickettsiae in a mammalian cell line. *Appl Microbiol* **27,** 1157-1161.

Doceul, V., Hollinshead, M., van der Linden, L. and Smith, G.L. (2010). Repulsion of Superinfecting Virions: A Mechanism for Rapid Virus Spread. *Science* **327,** 873-876.

Driskell, L.O., Yu, X., Zhang, L., Liu, Y., Popov, V.L., Walker, D.H*., et al.* (2009). Directed Mutagenesis of the Rickettsia prowazekii pld Gene Encoding Phospholipase D. *Infect. Immun.***,** IAI.00395-00309.

Firat-Karalar, E.N., Hsiue, P.P. and Welch, M.D. (2011). The actin nucleation factor JMY is a negative regulator of neuritogenesis. *Molecular Biology of the Cell* **22,** 4563-4574.

Gillespie, J.J., Ammerman, N.C., Dreher-Lesnick, S.M., Rahman, M.S., Worley, M.J., Setubal, J.C*., et al.* (2009). An Anomalous Type IV Secretion System in Rickettsia Is Evolutionarily Conserved. *PLoS ONE* **4,** e4833.

Goldberg, M.B. (2001). Actin-based motility of intracellular microbial pathogens. *Microbiol Mol Biol Rev* **65,** 595-626, table of contents.

Goldberg, M.B. and Theriot, J.A. (1995). Shigella flexneri surface protein IcsA is sufficient to direct actin-based motility. *Proc Natl Acad Sci U S A* **92,** 6572-6576.

Gouin, E., Egile, C., Dehoux, P., Villiers, V., Adams, J., Gertler, F*., et al.* (2004). The RickA protein of Rickettsia conorii activates the Arp2/3 complex. *Nature* **427,** 457-461.

Gouin, E., Gantelet, H., Egile, C., Lasa, I., Ohayon, H., Villiers, V*., et al.* (1999). A comparative study of the actin-based motilities of the pathogenic bacteria Listeria monocytogenes, Shigella flexneri and Rickettsia conorii. *J Cell Sci* **112 (Pt 11),** 1697-1708.

Gouin, E., Welch, M.D. and Cossart, P. (2005). Actin-based motility of intracellular pathogens. *Curr Opin Microbiol* **8,** 35-45.

Hackstadt, T., Messer, R., Cieplak, W. and Peacock, M.G. (1992). Evidence for proteolytic cleavage of the 120-kilodalton outer membrane protein of rickettsiae: identification of an avirulent mutant deficient in processing. *Infect. Immun.* **60,** 159-165.

Haglund, C.M., Choe, J.E., Skau, C.T., Kovar, D.R. and Welch, M.D. (2010). Rickettsia Sca2 is a bacterial formin-like mediator of actin-based motility. *Nat Cell Biol* **12,** 1057-1063.

Haglund, C.M. and Welch, M.D. (2011). Pathogens and polymers: Microbe-host interactions illuminate the cytoskeleton. *The Journal of Cell Biology* **195,** 7-17.

Harlander, R.S., Way, M., Ren, Q., Howe, D., Grieshaber, S.S. and Heinzen, R.A. (2003). Effects of ectopically expressed neuronal Wiskott-Aldrich syndrome protein domains on Rickettsia rickettsii actin-based motility. *Infect Immun* **71,** 1551-1556.

Heinzen, R.A. (2003). Rickettsial actin-based motility: behavior and involvement of cytoskeletal regulators. *Ann N Y Acad Sci* **990,** 535-547.

Heinzen, R.A., Hayes, S.F., Peacock, M.G. and Hackstadt, T. (1993). Directional actin polymerization associated with spotted fever group Rickettsia infection of Vero cells. *Infect Immun* **61,** 1926-1935.

Jeng, R.L., Goley, E.D., D'Alessio, J.A., Chaga, O.Y., Svitkina, T.M., Borisy, G.G.*, et al.* (2004). A Rickettsia WASP-like protein activates the Arp2/3 complex and mediates actin-based motility. *Cell Microbiol* **6,** 761-769.

Kleba, B., Clark, T.R., Lutter, E.I., Ellison, D.W. and Hackstadt, T. (2010). Disruption of the Rickettsia rickettsii Sca2 Autotransporter Inhibits Actin-Based Motility. *Infection and Immunity* **78,** 2240-2247.

Lacayo, C.I. and Theriot, J.A. (2004). Listeria monocytogenes actin-based motility varies depending on subcellular location: a kinematic probe for cytoarchitecture. *Mol Biol Cell* **15,** 2164-2175.

Lamason, R.L., Kupfer, A. and Pomerantz, J.L. (2010). The Dynamic Distribution of CARD11 at the Immunological Synapse Is Regulated by the Inhibitory Kinesin GAKIN. *Molecular Cell* **40,** 798-809.

Liu, Z.-M., Tucker, A.M., Driskell, L.O. and Wood, D.O. (2007). mariner-Based Transposon Mutagenesis of Rickettsia prowazekii. *Appl. Environ. Microbiol.* **73,** 6644-6649.

Martinez, J.J. and Cossart, P. (2004). Early signaling events involved in the entry of Rickettsia conorii into mammalian cells. *J Cell Sci* **117,** 5097-5106.

Mostowy, S., Bonazzi, M., Hamon, M.l.A., Tham, T.N., Mallet, A., Lelek, M.l.*, et al.* (2010). Entrapment of Intracytosolic Bacteria by Septin Cage-like Structures. *Cell Host & Microbe* **8,** 433-444.

Mostowy, S. and Cossart, P. (2012). Bacterial autophagy: restriction or promotion of bacterial replication? *Trends in Cell Biology* **22,** 283-291.

Nolen, B.J., Tomasevic, N., Russell, A., Pierce, D.W., Jia, Z., McCormick, C.D.*, et al.* (2009). Characterization of two classes of small molecule inhibitors of Arp2/3 complex. *Nature* **460,** 1031-1034.

Ohkawa, T., Volkman, L.E. and Welch, M.D. (2010). Actin-based motility drives baculovirus transit to the nucleus and cell surface. *The Journal of Cell Biology* **190,** 187-195.

Reed, S.C.O., Serio, A.W. and Welch, M.D. (2012). Rickettsia parkeri invasion of diverse host cells involves an Arp2/3 complex, WAVE complex and Rho-family GTPase-dependent pathway. *Cellular Microbiology* **14,** 529-545.

Riedl, J., Crevenna, A.H., Kessenbrock, K., Yu, J.H., Neukirchen, D., Bista, M.*, et al.* (2008). Lifeact: a versatile marker to visualize F-actin. *Nat Meth* **5,** 605-607.

Robbins, J.R., Monack, D., McCallum, S.J., Vegas, A., Pham, E., Goldberg, M.B. and Theriot, J.A. (2001). The making of a gradient: IcsA (VirG) polarity in Shigella flexneri. *Molecular Microbiology* **41,** 861-872.

Serio, A.W., Jeng, R.L., Haglund, C.M., Reed, S.C. and Welch, M.D. (2010). Defining a Core Set of Actin Cytoskeletal Proteins Critical for Actin-Based Motility of Rickettsia. *Cell Host & Microbe* **7,** 388-398.

Shen, A. and Higgins, D.E. (2005). The 5′ untranslated region-mediated enhancement of intracellular listeriolysin O production is required for Listeria monocytogenes pathogenicity. *Molecular Microbiology* **57,** 1460-1473.

Teysseire, N., Boudier, J.A. and Raoult, D. (1995). Rickettsia conorii entry into Vero cells. *Infect Immun* **63,** 366-374.

Theriot, J.A., Mitchison, T.J., Tilney, L.G. and Portnoy, D.A. (1992). The rate of actin-based motility of intracellular Listeria monocytogenes equals the rate of actin polymerization. *Nature* **357,** 257-260.

Van Kirk, L.S., Hayes, S.F. and Heinzen, R.A. (2000). Ultrastructure of Rickettsia rickettsii actin tails and localization of cytoskeletal proteins. *Infect Immun* **68,** 4706-4713.

Vellaiswamy, M., Campagna, B. and Raoult, D. (2011). Transmission electron microscopy as a tool for exploring bacterial proteins: model of RickA in Rickettsia conorii. *New Microbiol* **34,** 209-218.

Welch, M.D., DePace, A.H., Verma, S., Iwamatsu, A. and Mitchison, T.J. (1997a). The human Arp2/3 complex is composed of evolutionarily conserved subunits and is localized to cellular regions of dynamic actin filament assembly. *J Cell Biol* **138,** 375-384.

Welch, M.D., Iwamatsu, A. and Mitchison, T.J. (1997b). Actin polymerization is induced by Arp2/3 protein complex at the surface of Listeria monocytogenes. *Nature* **385,** 265-269.

Welch, M.D., Reed, S.C.O., Lamason, R.L. and Serio, A.W. (2012a). Expression of an Epitope-Tagged Virulence Protein in Rickettsia parkeri Using Transposon Insertion. *PLoS ONE* **7,** e37310.

Wisseman, C.L., Edlinger, E.A., Waddell, A.D. and Jones, M.R. (1976). Infection cycle of Rickettsia rickettsii in chicken embryo and L-929 cells in culture. *Infection and Immunity* **14,** 1052-1064.

CHAPTER FOUR

Future Directions

The research described in this thesis, including the elucidation of a major *R. parkeri* invasion pathway, as well as the discovery of bimodal *Rickettsia* actin-based motility mechanisms, raises a number of important questions worthy of future research. Our enhanced understanding of *Rickettsia* invasion opens the door to examining other cellular receptors and bacterial factors that could activate host pathways during this process. In addition, intriguing preliminary results suggest that RickA may potentiate host cell invasion as well as early actin tail formation. A role for RickA during early motility, and possibly invasion, brings this protein back to the forefront of *Rickettsia* pathogenesis. The clear separation between early and late modes of movement raises important questions about the regulation of *Rickettsia* gene expression throughout the intracellular life cycle and the function of each type of motility. Finally, an examination of the cellular requirements and biophysical properties of two distinct actin networks may shed light on the function of actin in the host cell and the evolution of actin-based motility in the *Rickettsiae*.

Does RickA contribute to* Rickettsia *invasion?

Although *R. parkeri* invasion occurs through a Rac1, WAVE, and Arp2/3 dependant pathway, as described in Chapter 2, the requirement for Arp2/3 complex is much more stringent than the requirement for host NPFs that activate the complex. We hypothesize that RickA might enhance invasion by activating the Arp2/3 complex (Figure 2.10). Preliminary evidence suggests that RickA may be secreted into the host cell during invasion to target the Arp2/3 complex. For example, wide-field microscopy reveals that bacteria associated with actin 'clouds' during invasion (at 15-30 min post-infection) also have a 'halo' of punctate RickA staining (Figure 4.1A). RickA also co-localizes with Arp3 around these bacteria (Figure 4.1B). In contrast, bacteria without actin association have RickA concentrated in the their cytosol (Figure 4.1A). When deconvolution microscopy is used to resolve RickA localization, the protein appears in puncta surrounding the bacterium, clearly in a distinct compartment from GFP in the bacterial cytosol (Figure 4.1C).

These data suggest that RickA might be secreted into the host cell, probably through the *Rickettsia* Type IV Secretion System (T4SS). Two lines of evidence suggest that RickA may be a T4SS effector protein. First, the C-terminus of T4SS substrates has a characteristic pattern of positively charged amino acid residues with a hydrophobic residue at position -3/4 (Burstein *et al.*, 2009). Indeed, the RickA C-terminal 20 amino acids match this pattern well (Figure 4.2A). Second, we have constructed a *R. parkeri* secretion reporter strain stably expressing a TEM1-RickA (β-lactamase) fusion protein, which successfully cleaves the lactam-containing substrate CCF4-AM only 30 min post-infection (Figure 4.2B). Work is underway to construct alternate reporter strains using a GSK-phosphorylation tag as well as control strains for both TEM1 and GSK assays, including RickA fusion proteins lacking the C-terminal signal, which would likely be defective in secretion (Torruellas Garcia *et al.*, 2006). If RickA were secreted, it would be the first example of a *Rickettsia* T4SS substrate, as well as the first example of an Arp2/3 NPF secreted to potentiate invasion. If RickA acts during invasion, we would expect the *rickA::himar1* mutant strain to show reduced and delayed invasion of HMEC-1 cells, as observed upon Arp2/3 complex depletion in COS7 and HMEC-1 cells (Figure 2.4, 2.10).

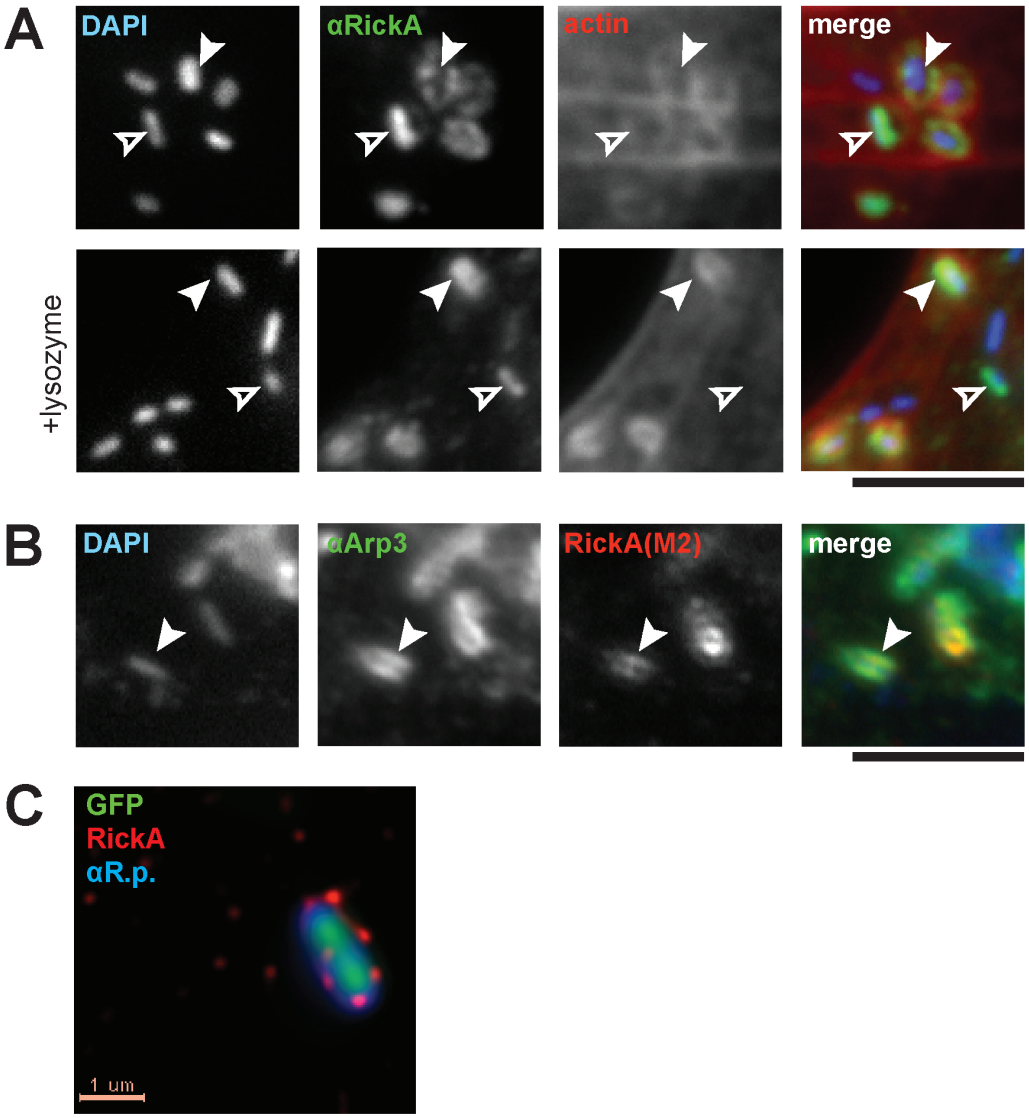

Figure 4.1 – RickA localization during invasion of host cells.
(A) HMEC-1 cells infected with *R. parkeri* for 30 min and fixed with Cytoskelfix. Bacteria stained with DAPI (blue), anti-RickA antibody (green) and anti-RFP antibody to visualize the Lifeact-mCherry marker (red). Closed arrowheads, bacteria with punctate/extracellular RickA; open arrowhead, bacterium with cytoplasmic RickA. (B) HMEC-1 cell infected with FLAG-RickA *R. parkeri* for 30 min and fixed with Cytoskelfix. Staining with anti-FLAG M2 antibody (RickA, green), anti-Arp3C antibody (red), DAPI (blue). (C) HMEC-1 cells infected with GFP3-*R. parkeri* for 30 min, fixed with formaldehyde, and stained with anti-RickA antibody (red) and anti-*Rickettsia* antibody (blue). Scale bars, 5 μm for (A-B), 1 μm for (C). (A-B) Sample preparation, antibodies, and widefield microscopy methods as described in Chapter 3. (C) Deconvolution image captured with an Applied Precision DeltaVision 4 Spectris microscope with a 100X objective, deconvolved with Huygens Professional (Scientific Volume Imaging), and processed using Imaris (Bitplane).

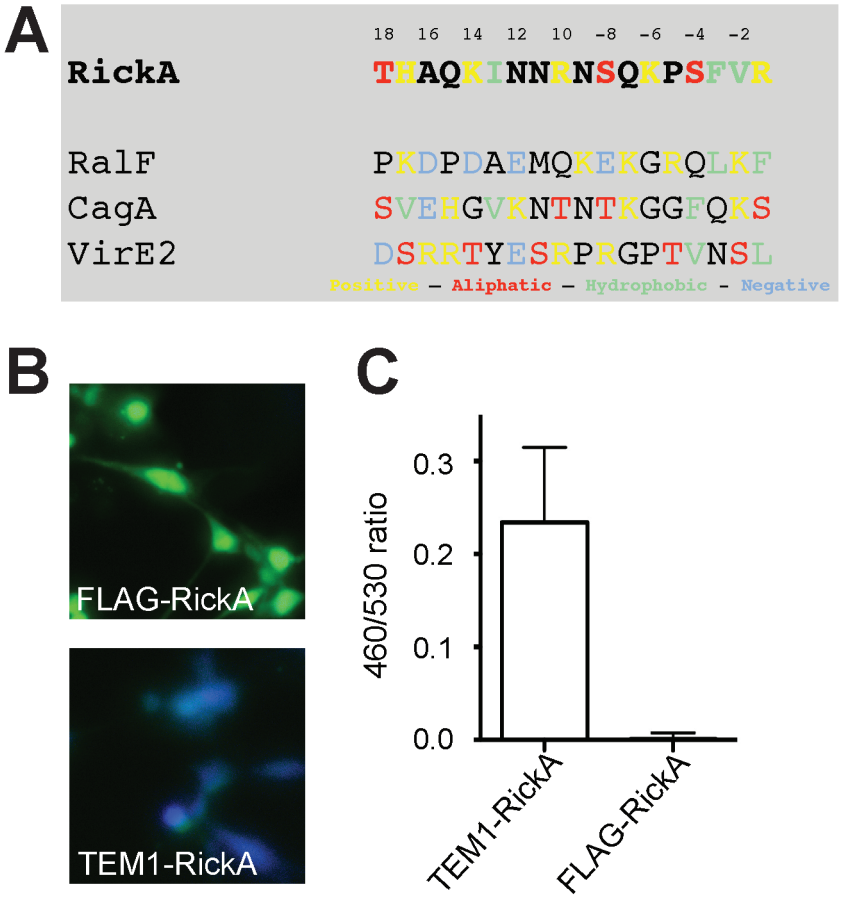

Figure 4.2 – RickA is secreted into host cells during invasion and early motility.
(A) C-terminal 20 amino acids of putative T4SS substrate RickA (*R. parkeri*) aligned with C-terminal sequences from *bona fide* T4SS substrates RalF (*Legionella pneumophila*), CagA (*Helicobacter pylori*), and VirE2 (*Agrobacterium tumefaciens*). Selected amino acid characteristics noted by yellow (positively charged), red (aliphatic), green (hydrophobic), and blue (negatively charged) colors. Position from C-terminus of protein indicated above alignment. (B) Widefield microscopy of HMEC-1 cells infected with TEM1-RickA or FLAG-RickA *R. parkeri* for 24 h, and loaded with CCF4-AM substrate using LIVEBLAzer-FRET B/G loading kit (Invitrogen) according to manufacturer's instructions. Blue cells contain cleaved CCF4-AM substrate while green cells contain uncleaved substrate. (C) HMEC-1 cells plated into 96-well black, clear-bottom tissue culture plates, loaded with CCF4-AM for 90 min, infected with *R. parkeri* and incubated at 34˚C for 30 min before reading light emission at 460 nm (blue) and 530 nm (green) using an Infinite F200 Pro plate reader (Tecan).

Regardless of the role of RickA, *R. parkeri* invasion is not fully understood. Despite the fact that the outer membrane autotransporter proteins rOmpA, Sca1, rOmpB, and Sca2 have been implicated during attachment and invasion, only one host receptor, Ku70, has been identified (Cardwell *et al.*, 2009; Chan *et al.*, 2009; Li *et al.*, 1998; Martinez *et al.*, 2005; Riley *et al.*, 2010). One explanation for the high level of redundancy observed during *R. parkeri* invasion is that multiple host pathways could be activated (Chapter 2). Future discoveries of host receptors or molecules that associate with invasion/adhesion factors other than rOmpB might illuminate the nature of these pathways. Interestingly, RNAi experiments in *Drosophila* S2R+ cells identified one such pathway. Depletion of RhoA, *Drosophila* Rho Kinase, and Myosin II caused a modest decrease in *R. parkeri* invasion (Table 2.1, Appendix 1 and data not shown). An identical pathway was recently shown to potentiate stress fiber contractility, acting in parallel to Arp2/3-mediated actin nucleation, during *Salmonella enterica* Typhimurium invasion of epithelial cells (Hänisch *et al.*, 2011). Residual *R. parkeri* invasion after Arp2/3 complex inhibition (Figure 2.10) suggests that this or other secondary pathways may contribute to actin nucleation during invasion. The complexity of bacterial invasion makes this a fertile area for future research.

How are RickA and Sca2 regulated?

In order to potentiate temporally and mechanistically distinct forms of actin-based motility, RickA and Sca2 activity must be tightly regulated by *R. parkeri*. Knowledge of the regulation of each protein is critical to understanding the biology of *Rickettsia* actin-based motility. Interestingly, we have noted that the ability of *R. parkeri* to efficiently invade host cells and produce early actin tails depends on the time when bacteria are collected for infections. Preparations of frozen or fresh *R. parkeri* are generally collected from Vero cells at 5-7 d post-infection, when cells are heavily infected and pulling away from the substrate, and free *Rickettsia* are abundant in the culture medium (see Materials and Methods for Chapter 2 and Chapter 3). When experiments were attempted using *R. parkeri* collected at 3-4 d post-infection, even from heavily infected cells, invasion and early actin tail formation appeared to be inhibited (data not shown). These data are intriguing, because they suggest that *Rickettsia* may be either infectious (and competent for invasion) or replicative (and competent for cell-cell spread) at different stages of the life cycle. *Chlamydia*, also an intracellular pathogen, transitions from an infectious, electron-dense Elementary Body (EB) form to a replicative, electron-lucent Reticulate Body (RB), then back to the EB form in response to nutrient and ATP depletion (Wyrick, 2010). As mentioned in Chapter 1, host cells infected with SFG *Rickettsia* show signs of ATP depletion and nutrient stress 4-7 d after infection.

As a first step to understanding their regulation, transcriptional analysis of *rickA* and *sca2* gene expression over a timecourse of infection (5 min to 48 or 72 h post-infection) using quantitative reverse-transcription and PCR will illuminate whether each gene is expressed during early or late actin-based motility. Transcriptional studies could easily be adapted to examine other putative effectors, or components of the T4SS, which might be co-regulated with RickA. In addition, RickA and Sca2-specific antibodies (Figure 3.5B) allow bulk protein abundance to be determined over the course of infection. As an alternate approach to population-level analyses, a recently developed *Rickettsia* plasmid (pRAM; Burkhardt *et al.*, 2011) would allow construction of reporter strains with the *rickA* or *sca2* promoter regions upstream of a GFP variant with a short half-life (Longo *et al.*, 2006). These single-cell reporter strains could allow assessment of

the transcriptional state of individual bacteria before and during actin-based motility and invasion. Importantly, a previous study of *R. rickettsii* transcription under various conditions found almost no transcriptional variation (Ellison *et al.*, 2009), and *Rickettsia* genomes encode only two sigma factors (σ^{70} and σ^{34}) and a handful of two-component systems, and no predicted transcriptional repressors (McLeod *et al.*, 2004). Therefore, regulation of *rickA* and *sca2* may not occur at the level of transcription initiation, confounding transcriptional analyses.

Protein activity and localization may represent an alternate strategy for regulation, and indeed, preliminary experiments indicate that the localization of RickA and Sca2 varies during the *Rickettsia* life cycle. Specifically, Sca2 localization is often unipolar during late motility but bipolar during invasion and early motility. RickA localization is variable, with cytoplasmic, periplasmic/outer membrane, punctate extracellular, and polar localizations all present to different degrees during infection (Figure 3.3, Figure 4.1, Figure 4.3, data not shown). A careful single-cell analysis of bacterial association with actin, along with Sca2 and RickA localization patterns, may reveal that localization is as important as transcript or protein abundance in controlling actin-based motility. In *Chlamydiae*, the Type III Secretion System and invasion-associated early effector proteins are transcribed late during infection, during the RB-to-EB transition, to ensure that bacteria are competent to invade as soon as they encounter a host cell (AbdelRahman *et al.*, 2005). If RickA were regulated in a similar fashion, we would expect to see greater protein abundance before and during invasion and early motility, consistent with a strong cytosolic 'payload' of RickA observed in some bacteria (Figure 4.1, open arrowhead). Transcription of *rickA* might occur at later stages (72 h or more) of infection. Alternately, regulated proteolysis or functional inhibition of RickA and Sca2 could modulate their abundance and activity throughout the life cycle. We plan to first undertake transcriptional and single-cell localization experiments to illuminate the general regulation of RickA and Sca2 activity, informing future experiments in this vein.

Functions of RickA-mediated actin-based motility

The generation of *R. parkeri* strains lacking functional RickA and Sca2 proteins (Figure 3.5) expands our ability to examine the function of each protein, as well as of each type of actin-based motility, in infection. However, the expression of a Sca2 fragment (Figure 3.5B) confounds some analyses. An essential next step is to generate clean deletions of each gene using homologous recombination (Driskell *et al.*, 2009). In addition, both our existing *rickA* and *sca2* insertional mutants, as well as any deletion strains, must be complemented with a functional copy of the deleted gene to conclusively demonstrate that a lack of early or late actin tail formation derives from a lack of RickA or Sca2. These experiments will be accomplished by using recently developed *Rickettsia* pRAM plasmids (Burkhardt *et al.*, 2011) modified to express a second selectable marker (Spectinomycin resistance) as well as the *rickA* or *sca2* loci, and used to transform RickA/Sca2 deletion strains.

An important question is whether RickA and Sca2 are virulence factors in the context of a mammalian or tick infection by *R. parkeri*. We are beginning a collaboration to use a recently developed C3H/HeJ mice mouse model of *R. parkeri* eschar-associated rickettsiosis (Grasperge *et al.*, 2012) to test for a virulence phenotype in each strain. When used to infect guinea pigs, the *R. rickettsii sca2::himar1* insertion mutant does not cause fever but induces a robust immune response (Kleba *et al.*, 2010). We expect that the *sca2::himar1* strain of *R. parkeri* will have a similar phenotype in mice, causing an inflammatory leukogram but likely with reduced vasculitis

and edema when compared to wild-type *R. parkeri* (Grasperge *et al.*, 2012). The infectious phenotype of a *rickA* mutant in mice will allow us to generate new hypotheses about the function of RickA-mediated invasion and early actin tail formation during the *Rickettsia* life cycle.

In order to understand the function of early actin-based motility, we require a more complete picture of the cytoskeletal structures that are produced during this process. While a dependence on Arp2/3 complex and RickA suggests that actin filaments form a branched network in early tails, conclusive demonstration of network structure requires transmission electron microscopy and/or myosin S1 decoration (Gouin *et al.*, 1999). At this time, preliminary data from super resolution microscopy has revealed a more diffuse actin network in early *R. parkeri* tails along with the expected linear, bundled actin network in late *R. parkeri* tails (Figure 4.3A,B). We will also examine the localization of cytoskeletal regulators such as cofilin, fascin, fimbrin, moesin, and profilin, which are differentially recruited or required between *Listeria* motility and *Rickettsia* late motility (Gouin *et al.*, 1999; Serio *et al.*, 2010). We expect that *R. parkeri* early motility will share many features with *Listeria* ActA-mediated motility, and that cellular factors may contribute to the slower movement and shorter tail lengths of *R. parkeri* early motility.

One possibility, raised in Chapter 3, is that both early and late *Rickettsia* actin-based motility could contribute to cell-to-cell spread. Pre-replication spread could assist *Rickettsia* in establishing a stable infection, as proposed for viruses such as vaccinia and baculovirus (Doceul *et al.*, 2010; Ohkawa *et al.*, 2010). Plaque assays suggest that Sca2 is the major contributor to cell-cell spread in a monolayer (Figure 3.5), but our preliminary data indicates that *R. parkeri* lacking RickA may form smaller infectious foci after only 24-48 h (data not shown). In addition, we have observed cellular protrusions forming after only 30 min of infection (Figure 4.3C), suggesting that some cell-cell spread may take place during early motility. We will continue to actively investigate early cell-cell spread associated with RickA-mediated motility.

Recent evidence points to another intriguing hypothesis regarding early *Rickettsia* actin-based motility. As mentioned in Chapter 3, actin-based motility appears to help bacteria outrun or interfere with host ubiquitin, septin, and autophagosome (e.g. LC3) recruitment aimed at containing cytosolic pathogens (Mostowy *et al.*, 2012). While *Shigella* appear to constitutively recruit septins, requiring motility to escape septin 'caging', *Listeria* recruit septins less robustly, and *Mycobacterium marinum* only recruits autophagy markers at the onset of motility (Mostowy *et al.*, 2010; Mostowy *et al.*, 2012). *Rickettsia* have not been observed to recruit septins or any autophagy markers, such as Atg5 or LC3, to the actin tail (Mostowy *et al.*, 2010). Interestingly, a *Listeria ΔactA* mutant is ubiquitylated and recruits autophagosomes, suggesting that ActA protects against autophagy (Campoy *et al.*, 2009). On the other hand, *Shigella* IcsA binds to Atg5 to recruit LC3 and other autophagy markers, while IcsB prevents this recruitment (Ogawa *et al.*, 2005). Therefore, proteins that activate actin-based motility (e.g. ActA, IcsA) may either enhance or inhibit autophagic recognition.

R. parkeri might use early, RickA-mediated actin-based motility to evade autophagic recognition, or might switch to Sca2-mediated motility to avoid recognition of RickA. It seems more likely that early motility could help *Rickettsia* species evade autophagy, because damaged phagocytic membranes would be proximal to the bacterium during invasion and vacuole escape, immediately before actin-based motility begins. A careful analysis of the *rickA* and *sca2* mutant strains of *R. parkeri* in a variety of cell types should reveal whether and when *Rickettsia* are evading cytosolic recognition pathways via actin-based motility. We speculate that *rickA* mutant

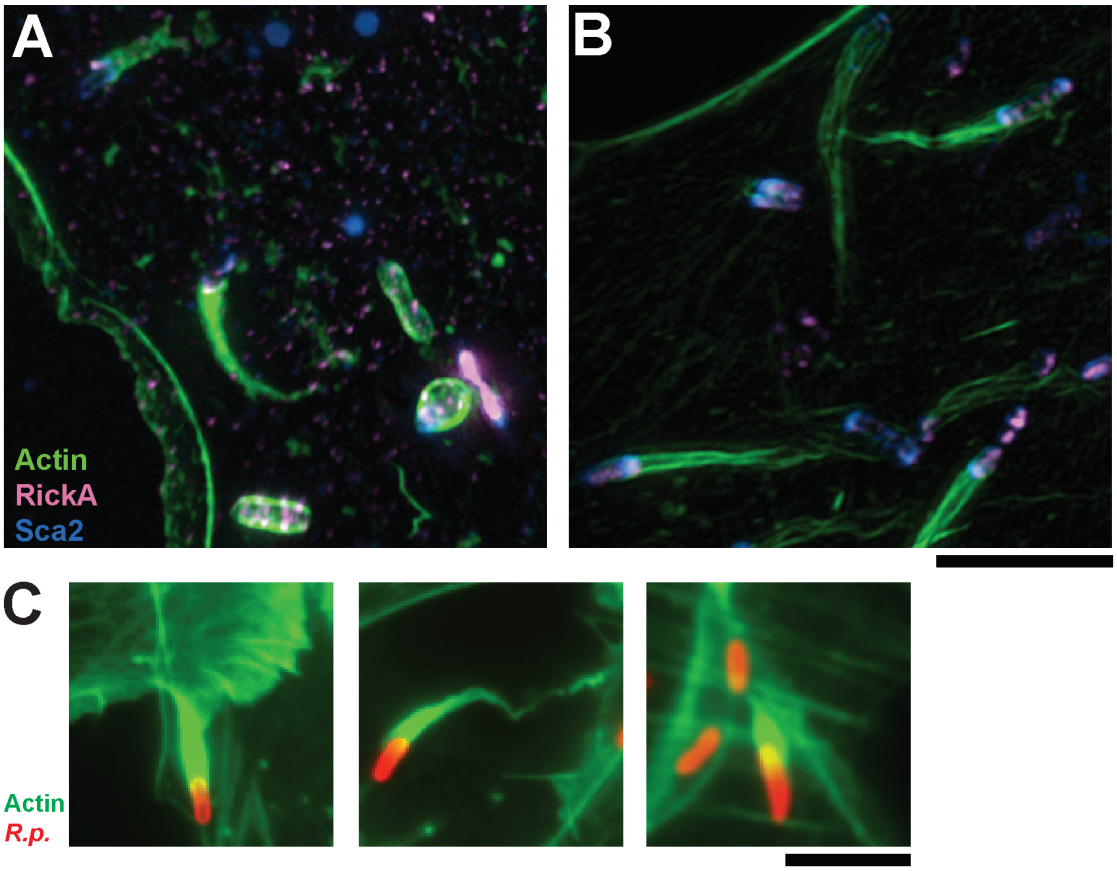

Figure 4.3. Actin network structure and protrusion formation during early motility
(A) Structured illumination microscopy of HMEC-1 cells infected with *R. parkeri* for 30 min (A) or 48 h (B), and stained with phalloidin (actin, green), anti-RickA (pink), and anti-Sca2 (blue) antibodies. Images collected using 100X objective on an ELYRA S.1 superresolution microscope (Carl Zeiss) at the UC Berkeley Biological Imaging Facility and processed using Imaris. (C) Widefield microscopy of protrusions formed by *R. parkeri* in HMEC cells infected for 30 min and treated with DMSO, images from experiments represented in Figure 3.4A. Red, anti-*Rickettsia* antibody, Green, phalloidin staining of actin. (A-C) Scale bars, 5 µm.

strains may have reduced survival in some cell types, such as macrophages, where autophagic pathways are basally induced.

The work presented in this thesis will bolster future investigations of other *Rickettsia* species, especially those with divergent *rickA* and *sca2* genes (Table 1.1). In addition, our improved understanding of *Rickettsia* actin-based motility, along with a comparison of early and late motility to the movement of other pathogens, will continue to shed light on actin nucleation and regulation – a critical process for all eukaryotic cells. Continued investigation of *R. parkeri* interaction with the host cell actin cytoskeleton will illuminate not only our understanding of *Rickettsia* biology, but also the general principles of microbial pathogenesis and cell biology.

REFERENCES

AbdelRahman, Y.M. and Belland, R.J. (2005). The chlamydial developmental cycle. *FEMS Microbiology Reviews* **29,** 949-959.

Burkhardt, N.Y., Baldridge, G.D., Williamson, P.C., Billingsley, P.M., Heu, C.C., Felsheim, R.F.*, et al.* (2011). Development of Shuttle Vectors for Transformation of Diverse Rickettsia Species. *PLoS ONE* **6,** e29511.

Burstein, D., Zusman, T., Degtyar, E., Viner, R., Segal, G. and Pupko, T. (2009). Genome-Scale Identification of Legionella pneumophila Effectors Using a Machine Learning Approach. *PLoS Pathog* **5,** e1000508.

Campoy, E. and Colombo, M.a.I. (2009). Autophagy in intracellular bacterial infection. *Biochimica et Biophysica Acta (BBA) - Molecular Cell Research* **1793,** 1465-1477.

Cardwell, M.M. and Martinez, J.J. (2009). The Sca2 Autotransporter Protein from Rickettsia conorii Is Sufficient To Mediate Adherence to and Invasion of Cultured Mammalian Cells. *Infection and Immunity* **77,** 5272-5280.

Chan, Y.G.Y., Cardwell, M.M., Hermanas, T.M., Uchiyama, T. and Martinez, J.J. (2009). Rickettsial outer-membrane protein B (rOmpB) mediates bacterial invasion through Ku70 in an actin, c-Cbl, clathrin and caveolin 2-dependent manner. *Cellular Microbiology* **11,** 629-644.

Doceul, V., Hollinshead, M., van der Linden, L. and Smith, G.L. (2010). Repulsion of Superinfecting Virions: A Mechanism for Rapid Virus Spread. *Science* **327,** 873-876.

Driskell, L.O., Yu, X., Zhang, L., Liu, Y., Popov, V.L., Walker, D.H.*, et al.* (2009). Directed Mutagenesis of the Rickettsia prowazekii pld Gene Encoding Phospholipase D. *Infect. Immun.***,** IAI.00395-00309.

Ellison, D.W., Clark, T.R., Sturdevant, D.E., Virtaneva, K. and Hackstadt, T. (2009). Limited Transcriptional Responses of Rickettsia rickettsii Exposed to Environmental Stimuli. *PLoS ONE* **4,** e5612.

Gouin, E., Gantelet, H., Egile, C., Lasa, I., Ohayon, H., Villiers, V.*, et al.* (1999). A comparative study of the actin-based motilities of the pathogenic bacteria Listeria monocytogenes, Shigella flexneri and Rickettsia conorii. *J Cell Sci* **112 (Pt 11),** 1697-1708.

Grasperge, B.J., Reif, K.E., Morgan, T.D., Sunyakumthorn, P., Bynog, J., Paddock, C.D. and Macaluso, K.R. (2012). Susceptibility of Inbred Mice to Rickettsia parkeri. *Infection and Immunity* **80,** 1846-1852.

Hänisch, J., Kölm, R., Wozniczka, M., Bumann, D., Rottner, K. and Stradal, T.E.B. (2011). Activation of a RhoA/Myosin II-Dependent but Arp2/3 Complex-Independent Pathway Facilitates Salmonella Invasion. *Cell Host & Microbe* **9,** 273-285.

Kleba, B., Clark, T.R., Lutter, E.I., Ellison, D.W. and Hackstadt, T. (2010). Disruption of the Rickettsia rickettsii Sca2 Autotransporter Inhibits Actin-Based Motility. *Infection and Immunity* **78,** 2240-2247.

Li, H. and Walker, D.H. (1998). rOmpA is a critical protein for the adhesion of Rickettsia rickettsiito host cells. *Microbial Pathogenesis* **24,** 289-298.

Longo, D. and Hasty, J. (2006). Dynamics of single-cell gene expression. *Mol Syst Biol* **2**.

Martinez, J.J., Seveau, S., Veiga, E., Matsuyama, S. and Cossart, P. (2005). Ku70, a component of DNA-dependent protein kinase, is a mammalian receptor for Rickettsia conorii. *Cell* **123,** 1013-1023.

McLeod, M.P., Qin, X., Karpathy, S.E., Gioia, J., Highlander, S.K., Fox, G.E., *et al.* (2004). Complete Genome Sequence of Rickettsia typhi and Comparison with Sequences of Other Rickettsiae. *J. Bacteriol.* **186,** 5842-5855.

Mostowy, S., Bonazzi, M., Hamon, M.l.A., Tham, T.N., Mallet, A., Lelek, M.l., *et al.* (2010). Entrapment of Intracytosolic Bacteria by Septin Cage-like Structures. *Cell Host & Microbe* **8,** 433-444.

Mostowy, S. and Cossart, P. (2012). Bacterial autophagy: restriction or promotion of bacterial replication? *Trends in Cell Biology* **22,** 283-291.

Ogawa, M., Yoshimori, T., Suzuki, T., Sagara, H., Mizushima, N. and Sasakawa, C. (2005). Escape of Intracellular Shigella from Autophagy. *Science* **307,** 727-731.

Ohkawa, T., Volkman, L.E. and Welch, M.D. (2010). Actin-based motility drives baculovirus transit to the nucleus and cell surface. *The Journal of Cell Biology* **190,** 187-195.

Riley, S.P., Goh, K.C., Hermanas, T.M., Cardwell, M.M., Chan, Y.G.Y. and Martinez, J.J. (2010). The Rickettsia conorii Autotransporter Protein Sca1 Promotes Adherence to Nonphagocytic Mammalian Cells. *Infection and Immunity* **78,** 1895-1904.

Serio, A.W., Jeng, R.L., Haglund, C.M., Reed, S.C. and Welch, M.D. (2010). Defining a Core Set of Actin Cytoskeletal Proteins Critical for Actin-Based Motility of Rickettsia. *Cell Host & Microbe* **7,** 388-398.

Torruellas Garcia, J., Ferracci, F., Jackson, M.W., Joseph, S.S., Pattis, I., Plano, L.R.W., *et al.* (2006). Measurement of Effector Protein Injection by Type III and Type IV Secretion Systems by Using a 13-Residue Phosphorylatable Glycogen Synthase Kinase Tag. *Infect. Immun.* **74,** 5645-5657.

Wyrick, P.B. (2010). Chlamydia trachomatis Persistence In Vitro: An Overview. *Journal of Infectious Diseases* **201,** S88-S95.

APPENDIX 1

Supplementary Dataset for Chapter 2
Full results of S2R+ cell RNAi screening

Appendix 1. RNAi screen results for Chapter 2						
Gene / control	**CG number**	**Functional Group**	**% internalized bacteria**	**p-value**	**normalized % internalization**	**p-value normalized**
Untreated cells (no RNAi) + *R. parkeri*	-------	-------	54 ± 10	-------	1 ± 0.09	-------
Untreated cells + *Rp*, fixed at time=0	-------	*negative control*	19 ± 9	<0.0001	0.36 ± 0.18	<0.0001
Untreated cells + I, 4mM latrunculin A	-------	*negative control*	15 ± 5	<0.0001	0.33 ± 0.13	<0.0001
Untreated cells + 56C Heat-killed R. parkeri	-------	*negative control*	23 ± 8	<0.0001	0.48 ± 0.1	<0.0001
Untreated cells + *Listeria monocytogenes*	-------	*negative control*	24 ± 5	<0.0001	0.41 ± 0.05	<0.0001
Untreated cells + *E. coli* XL-10	-------	*negative control*	5 ± 6	<0.0001	0.09 ± 0.09	<0.0001
Abi	CG9749	WAVE complex subunit	17 ± 10	<0.0001	0.34 ± 0.18	<0.0001
Abl	CG4032	Kinase	42 ± 10	0.0431	0.86 ± 0.06	0.0068
ADF/cofilin	CG6873	Actin monomer dynamics	51 ± 13	0.5961	0.99 ± 0.16	0.7844
Aip1	CG10724	Actin monomer dynamics	47 ± 9	0.2366	1.06 ± 0.09	0.2799
α-actinin	CG4376	Actin filament bundling/organizing	34 ± 14	0.0004	0.71 ± 0.19	<0.0001
α-actinin 3	CG8953	Actin filament bundling/organizing	51 ± 7	0.5532	0.85 ± 0.12	0.0056
Anillin	CG2092	Actin filament binding / cytokinesis	57 ± 4	0.6946	0.98 ± 0.06	0.6766
Arp2/3 complex ARP3	CG7558	Actin filament nucleator	34 ± 9	0.0002	0.67 ± 0.07	<0.0001
Arp2/3 complex ARP2	CG9901	Actin filament nucleator	29 ± 9	<0.0001	0.59 ± 0.15	<0.0001
Arp2/3 complex ARPC1	CG8978	Actin filament nucleator	33 ± 16	0.0013	0.66 ± 0.25	<0.0001
Arp2/3 complex ARPC2	CG10954	Actin filament nucleator	30 ± 9	<0.0001	0.63 ± 0.21	<0.0001
Arp2/3 complex ARPC3	CG4560	Actin filament nucleator	51 ± 8	0.5061	1.05 ± 0.19	0.3124
Arp2/3 complex ARPC4	CG5972	Actin filament nucleator	36 ± 12	0.001	0.61 ± 0.22	<0.0001

Arp2/3 complex ARPC5	CG9881	Actin filament nucleator	25 ± 6	<0.0001	0.5 ± 0.04	<0.0001
Band 4.1 FERM-like	CG34347	Membrane-cytoskeleton linker	42 ± 9	0.019	0.95 ± 0.14	0.2692
Basket (c-Jun N-terminal kinase)	CG5680	Kinase	56 ± 7	0.7782	0.97 ± 0.17	0.6022
By blistery tensin	CG9379	Membrane-cytoskeleton linker / focal adhesions	49 ± 14	0.397	0.97 ± 0.15	0.5125
CAP1	CG5061	Actin monomer dynamics / filament binding	40 ± 4	0.0211	1.02 ± 0.3	0.708
Capping protein_(beta)	CG17158	Actin monomer dynamics / filament binding	41 ± 12	0.0142	0.87 ± 0.18	0.0088
Cappucino	CG3399	Actin filament nucleator	51 ± 22	0.6488	0.93 ± 0.33	0.2241
Cdc42	CG12530	Rho family GTPases	48 ± 8	0.2047	1.02 ± 0.05	0.7433
Citron kinase	CG10522	Kinase	39 ± 12	0.0156	0.8 ± 0.11	0.0003
Cofilin (twinstar)	CG4254	Actin monomer dynamics	40 ± 12	0.0088	0.8 ± 0.09	<0.0001
Coracle	CG11949	Membrane-cytoskeleton linker	62 ± 5	0.2264	0.94 ± 0.06	0.2558
Coronin	CG9446	Arp2/3 complex regulator	53 ± 15	0.7956	1.03 ± 0.2	0.6399
Cortactin	CG3637	Arp2/3 complex regulator	43 ± 15	0.0669	0.87 ± 0.18	0.0144
Cyclin-dep kinase 5	CG8203	Kinase	59 ± 2	0.4054	1.05 ± 0.09	0.3399
Dab (disabled)	CG9695	Adapter / WASP regulator	66 ± 5	0.0506	1.09 ± 0.13	0.1033
Dah	CG6157	Membrane-cytoskeleton linker / cortical furrow	55 ± 12	0.858	1.17 ± 0.08	0.0003
Dcarmil	CG1399	Arp2/3 complex regulator	52 ± 17	0.7566	0.89 ± 0.12	0.0301
Diaphanous	CG1768	Actin filament nucleator	54 ± 14	0.9939	0.93 ± 0.06	0.1633
DLAR	CG10443	Tyrosine phosphatase	59 ± 9	0.4422	1.05 ± 0.29	0.3746
Drebrin-like	CG10083	Actin filament binding / endocytosis	62 ± 17	0.2443	1.05 ± 0.08	0.3076
Drk	CG6033	Adapter/ WAVE complex subunit	44 ± 9	0.0863	0.96 ± 0.04	0.4541
DROK	CG9774	Kinase	39 ± 3	0.0138	0.88 ± 0.14	0.0272
E-cadherin (shotgun)	CG3722	Membrane-cytoskeleton linker / cell-cell junctions	59 ± 9	0.4101	0.96 ± 0.11	0.3906
Enabled (Ena)	CG15112	Actin monomer dynamics / filament binding	57 ± 13	0.7007	0.98 ± 0.17	0.6929

Fascin	CG1536	Actin filament bundling/organizing	56 ± 16	0.7845	0.98 ± 0.24	0.7512
Filamin	CG3937	Actin filament bundling/organizing	57 ± 4	0.6544	0.93 ± 0.11	0.1922
Fimbrin	CG8649	Actin filament bundling/organizing	38 ± 6	0.0078	0.86 ± 0.05	0.0055
Forked	CG5424	Actin filament bundling/organizing	49 ± 7	0.3574	0.8 ± 0.12	0.0002
Formin/DIA-like	CG14622	Actin filament nucleator	59 ± 8	0.4736	0.95 ± 0.07	0.3161
Form 3	CG33556	Actin filament nucleator	45 ± 12	0.1229	0.92 ± 0.11	0.1347
Formin FRL group	CG32138	Actin filament nucleator	44 ± 21	0.1143	0.87 ± 0.31	0.037
Formin FHOD3 group	CG32030	Actin filament nucleator	46 ± 8	0.1612	0.96 ± 0.08	0.3847
Gelsolin	CG1106	Actin monomer dynamics	55 ± 9	0.8639	0.91 ± 0.15	0.0758
Genghis Kahn	CG4012	Cdc42 effector	54 ± 8	0.9626	0.94 ± 0.06	0.2302
Hemipterous	CG4353	Map kinase kinase	65 ± 10	0.0848	0.99 ± 0.13	0.8308
Hip1R	CG10971	endocytic / phagocytic adapter protein	35 ± 7	0.0005	0.74 ± 0.17	<0.0001
HSPC300	CG30173	WAVE complex subunit	58 ± 6	0.5415	1.01 ± 0.07	0.8098
Kelch	CG7210	Actin filament binding / ring canals	52 ± 11	0.7108	0.85 ± 0.14	0.006
Kette HEM-protein	CG5837	WAVE complex subunit	31 ± 9	<0.0001	0.57 ± 0.24	<0.0001
Ku70	CG5247	Mammalian receptor for *R. conorii* entry	42 ± 16	0.0263	0.83 ± 0.16	0.0005
Lethal (2) giant larvae	CG2671	Membrane-cytoskeleton linker	56 ± 2	0.7352	1.01 ± 0.08	0.9133
Lim kinase	CG1848	Actin binding kinase	61 ± 12	0.3031	0.99 ± 0.15	0.882
Merlin	CG14228	Membrane-cytoskeleton linker	48 ± 15	0.2916	0.81 ± 0.11	0.0005
MIM homolog	CG33558	Membrane-cytoskeleton linker	33 ± 8	0.0001	0.69 ± 0.21	<0.0001
Moesin	CG10701	Membrane-cytoskeleton linker	40 ± 4	0.0183	0.83 ± 0.16	0.0015
ML (rac-like)	CG5588	Rho family GTPases	48 ± 4	0.3279	1.1 ± 0.15	0.0725
Mushroom bodies tiny	CG18582	Kinase	62 ± 8	0.1905	1.01 ± 0.05	0.8091
Myoblast city	CG10379	Membrane-cytoskeleton linker / focal adhesions	38 ± 4	0.0089	0.87 ± 0.11	0.011
Myosin IA	CG7438	Myosin / phagocytosis	28 ± 12	<0.0001	0.62 ± 0.37	<0.0001

Myosin IB	CG9155	Myosin	48 ± 9	0.306	0.85 ± 0.06	0.0032
Myosin II (zipper)	CG15792	Myosin / phagocytosis	33 ± 6	0.0002	0.72 ± 0.27	<0.0001
Myosin V	CG2146	Myosin	47 ± 9	0.216	1.01 ± 0.09	0.9136
Myosin VI	CG5695	Myosin	54 ± 16	0.9636	1.19 ± 0.18	0.0006
Myosin VII	CG7595	Myosin	51 ± 11	0.5934	0.82 ± 0.09	0.0006
Myosin VII (28B)	CG6976	Myosin	67 ± 3	0.0342	1.09 ± 0.12	0.0901
Myosin XV	CG2174	Myosin	66 ± 4	0.0567	1.08 ± 0.14	0.1529
Myosin XVIII (PDZ-myosin)	CG10218	Myosin	47 ± 10	0.2597	1.06 ± 0.17	0.2461
Myosin 29D XX	CG10595	Myosin	67 ± 10	0.0471	1.11 ± 0.09	0.0312
Nck	CG3727	Adapter/ WAVE complex subunit	54 ± 12	0.8843	0.89 ± 0.13	0.0178
Nullo	CG14426	Membrane-cytoskeleton linker / basal junctions	57 ± 5	0.64	0.93 ± 0.09	0.1032
Ovarian tumor	CG12743	Actin filament bundling/organizing	55 ± 10	0.8567	0.93 ± 0.16	0.12
Pak1 kinase	CG10295	Kinase	55 ± 8	0.8561	0.96 ± 0.19	0.4252
PKN	CG2049	Rho, Rac1 kinase	61 ± 8	0.2083	1.02 ± 0.17	0.6535
POD-1/coronin	CG4532	Arp2/3 complex regulator	46 ± 15	0.1467	0.88 ± 0.09	0.0083
Pp2A	CG17291	Phosphatase	52 ± 8	0.6327	0.87 ± 0.13	0.0055
Profilin	CG9553	Actin monomer dynamics	45 ± 5	0.0668	0.87 ± 0.1	0.0055
Pten	CG5671	Membrane-cytoskeleton linker / ring canals	52 ± 14	0.713	0.87 ± 0.18	0.0148
Quail	CG6433	Actin monomer dynamics	60 ± 7	0.2158	1.03 ± 0.06	0.4976
Rab5	CG3664	Rab family GTPase	53 ± 14	0.7785	0.91 ± 0.22	0.0734
Rac1	CG2248	Rho family GTPases	37 ± 17	0.0021	0.84 ± 0.5	0.0237
Rac2	CG8556	Rho family GTPases	37 ± 8	0.002	0.77 ± 0.09	<0.0001
RacGAP50C	CG13345	GAP for Rac GTPase	65 ± 14	0.0532	1.12 ± 0.06	0.0116
Rho1	CG8416	Rho family GTPases	43 ± 4	0.0277	0.89 ± 0.11	0.0142
RhoBTB	CG5701	Rho family GTPases	60 ± 2	0.2575	1.01 ± 0.02	0.8836

RhoL	CG9366	Rho family GTPases	44 ± 7	0.0612	0.76 ± 0.12	<0.0001
Rhophilin	CG8497	Rho GTPase effector	56 ± 6	0.7812	0.93 ± 0.12	0.1205
Slingshot	CG6238	Phosphatase of cofilin	44 ± 15	0.1039	0.96 ± 0.18	0.4078
Spire	CG10076	Actin filament nucleator	50 ± 9	0.4491	0.91 ± 0.13	0.0394
Sra-1	CG4931	WAVE complex subunit	35 ± 6	0.0027	0.55 ± 0.07	<0.0001
Taf110	CG5444	DNA binding, cytokinesis	39 ± 7	0.0124	0.81 ± 0.09	0.0005
Talin	CG6831	Membrane-cytoskeleton linker / cell-cell junctions	48 ± 15	0.2377	0.95 ± 0.17	0.2818
Trio (GEF)	CG18214	GEF for Rho GTPases	48 ± 9	0.2236	0.91 ± 0.17	0.0593
Tropomodulin	CG1539	Actin monomer dynamics / filament binding	57 ± 12	0.5516	0.98 ± 0.09	0.5323
Tropomyosin1	CG4898	Actin monomer dynamics	52 ± 9	0.6681	0.86 ± 0.09	0.0028
Tropomyosin2	CG4843	Actin monomer dynamics	43 ± 13	0.0451	0.72 ± 0.19	<0.0001
Twinfillin	CG3172	Actin monomer dynamics	53 ± 8	0.8331	0.89 ± 0.15	0.0325
Vav	CG7893	GEF for Rac1 GTPase	41 ± 6	0.0319	0.69 ± 0.16	<0.0001
Villin-like	CG33232	Actin monomer dynamics	60 ± 6	0.3213	1.01 ± 0.04	0.8604
Vinculin	CG3299	Membrane-cytoskeleton linker / focal adhesions	41 ± 17	0.0379	0.76 ± 0.17	<0.0001
WASP	CG1520	Arp2/3 Nucleation Promoting Factor	49 ± 16	0.3635	0.99 ± 0.16	0.8127
WAVE (SCAR)	CG4636	Arp2/3 Nucleation Promoting Factor	18 ± 6	<0.0001	0.38 ± 0.08	<0.0001
WIP verprolin	CG13503	WASP binding, regulation	38 ± 16	0.005	0.78 ± 0.34	0.0003
Rac1 + Cdc42	CG2248 + CG12530	Rho family GTPases	34 ± 5	0.0003	0.68 ± 0.11	<0.0001
Rac1 + Rac2	CG2248 + CG8556	Rho family GTPases	39 ± 18	0.0031	0.84 ± 0.46	0.0162

Column A, common gene name. Column B, FlyBase gene annotation symbol. Column C, type of control or protein function. Column D, raw percentage of internalized *R. parkeri* expressed as mean ± standard deviation, $n>3$ biological replicates. Column E, p-value based on a pairwise comparison of the raw percentages of internalized bacteria for RNAi treated cells versus untreated control cells using the Student's t-test, with $p<0.05$ considered statistically significant. Column F, percentage of internalized *R. parkeri* normalized to the mean value for untreated control cells (n=2) in the same day's experiment, expressed as mean ± standard deviation. Column F, p-value based on a pairwise comparison of the normalized percentages of internalized bacteria for RNAi treated cells versus normalized untreated control cells using the Student's t-test, with $p<0.05$ considered statistically significant. Red signifies those targets for which values were significantly reduced compared with controls, while green signifies those targets for which values were significantly increased when compared with controls. Functional classification derived from: http://www.ihop-net.org; http://flybase.org; Siripala and Welch 2007, Cell 128:626; Siripala and Welch 2007 Cell 128:1014

APPENDIX 2

Welch Lab's Favorite Carrot Cake

Shawna's Carrot-Ginger Cake

Adapted from: Lagasse E., Gigi's Carrot Cake, (2002). Food Network (USA)
http://www.foodnetwork.com/recipes/emeril-lagasse/gigis-carrot-cake-recipe/index.html

Ingredients

Cake:
3 sticks (1 ½ cups) Organic Valley Cultured unsalted butter, softened
1 cup white sugar
¾ cup brown sugar
1 ½ cups all-purpose flour
½ cup white whole wheat flour
2 teaspoons baking soda
2 teaspoons ground cinnamon
½ teaspoon ground ginger
⅛ teaspoon freshly grated nutmeg
pinch allspice
pinch cloves
1 teaspoon salt
4 large eggs (preferably organic)
1 teaspoon pure vanilla extract
3-4 cups grated carrots
1.5 inch piece fresh ginger, peeled and grated with carrots
1 cup chopped toasted pecans (or walnuts)

Cream Cheese Icing:
16 ounces (2 packages) Philadelphia cream cheese, softened
1 ½ sticks (12 Tb) Organic Valley Cultured Sweet Cream Butter, softened
1 (1-pound) box confectioners' sugar
1 teaspoon pure vanilla extract
pinch dried ginger
pinch cinnamon

Instructions

Soften butter and cream cheese at room temperature for up to three hours.
Preheat the oven to 350 degrees F.

Butter, or use cake spray (oil+flour), to coat 2 (9-inch) cake pans, and line with circles of parchment paper. Grate carrots and ginger using a food processor. You may use pre-grated carrots, but should then blend up to ½ of them in food processor or blender to soften, as they tend to be dry. Chop nuts and toast them on a cookie sheet in the oven for 5-8 minutes until fragrant but not burnt. Remove from cookie sheet so they don't burn.

In a mixing bowl or stand mixer, cream the butter (mix until fluffy). Add the brown and white sugar, and beat until fluffy and well incorporated. In a sifter over a medium bowl or on a piece of parchment, combine the flours, baking soda, spices, and salt, and mix well.

Add the vanilla extract, then a part of the flour mixture to the butter/sugar in the mixing bowl, alternating with each egg, beating well after the addition of each and finishing with the dry ingredients. Add the grated carrots and ginger and beat on medium speed until carrots start to break down and are well incorporated, about 2 minutes. Batter may look slightly curdled – that's fine. Add the nuts and mix or fold in to combine. Divide between 2 cake pans and smooth top of each cake. Bake in oven until cake slightly springs back and a toothpick inserted into the middle comes out clean, 35 to 40 minutes. Remove from the oven and let rest in the cake pans for 10 minutes. Invert onto wire racks and remove cake pans, leaving parchment on cakes as they cool. Cakes may cool overnight, covered with a kitchen towel, and will stay moist. Cake layers can be wrapped well and frozen for up to two months.

For the Icing: In a large bowl, beat together the cream cheese and butter until light and fluffy. Add powdered sugar gradually, beating constantly. Add the vanilla and spices and taste for sweetness and texture. Adjust with more cream cheese or icing if needed.

When cake layers are completely cool, remove parchment sheets. Place 1 cake layer on a cake plate or stand. Spread the top with cream cheese frosting and sprinkle on nuts or ginger, if desired. Top with a second layer. Spread the icing on top and sides of the cake.

Serves 10-14 people.

Variations

- Flour may be 2 cups all-purpose, or up to 1 cup whole wheat plus 1 cup all-purpose
- For a gluten-free flour cake, simply substitute any GF flour mix for the 2 c flour and mix for an extra 3-5 minutes before adding carrots to build structure.
- Vegetable oil may be substituted for the butter for a less tasty, but dairy-free cake.
- If you don't have fresh ginger, increase dried ginger (powder) to 1 tsp
- Toasted pecans or candied ginger pieces can be added to icing or between cake layers
- Proportions of cream cheese and sugar may be modified in icing to taste. If icing is too thin, add more sugar; too sweet, add more cream cheese or softened butter 1 Tb at a time. 1 package of low fat (Neufchatel) cream cheese may be substituted for half of the full-fat.
- Recipe can be baked in muffin or cupcake tins; make ½ of the icing recipe and bake 20-30 min.